THE CELLULAR AND MOLECULAR UNDERPINNINGS OF INTESTINAL EPITHELIAL REGENERATION

Maryam Yousefi

A DISSERTATION

in

Cell and Molecular Biology

Presented to the Faculties of the University of Pennsylvania

in

Partial Fulfillment of the Requirements for the

Degree of Doctor of Philosophy

2017

Supervisor of Dissertation

_____

Christopher J. Lengner, Ph.D.

Associate Professor of Biomedical Sciences

Graduate Group Chairperson

_____

Daniel S. Kessler

Associate Professor of Cell and Developmental Biology

Dissertation Committee

Klaus H. Kaestner, Ph.D., Thomas and Evelyn Suor Butterworth Professor in Genetics

Peter S. Klein, MD, Ph.D., Professor of Medicine

Benjamin Stanger, MD, Ph.D., Associate Professor of Medicine

M. Celeste Simon, Ph.D., Arthur H. Rubenstein, MBBCh Professor of Cell and Developmental Biology

ACKNOWLEDGMENTS

There are many people I would like to thank and many reasons to thank each. First, I would like to thank my Ph.D. advisor Chris Lengner, for letting me join his amazing team and supporting my professional and personal development from my early days in the US. Thanks for helping me to grow by trusting me, challenging me, and encouraging me to follow up on my ideas. You have been one of the most influential people in my life and I will carry what I learned from you for the rest of my life.

I also want to thank the current and previous Lengner lab members, with whom I spent most of the past 5 years: Ning Li, Angela Ddamba, Ryan Cedeno, Zhengquan Yu, Shan Wang, Kamen Simeonov, Jenna Schoenberger, Clarissa Rous, and Carla Hoge. Thanks for being such an amazing team, I learned a lot from you and had so much fun with you. Thanks for making my first years of being in a new country much easier. I will miss you and look forward to seeing you in future scientific and non-scientific events.

Thanks to the members of my thesis committee, Peter Klein, Ben Stanger, Klaus Kaestner, and Celeste Simon for their valuable inputs and support on my research and future career decisions. I also want to thank Anil Rustgi and Nancy Speck for all their unforgettable support, guidance, and encouragement during my Ph.D.

I would like to thank core facilities at the University of Pennsylvania: Molecular Pathology and Imaging Core, Cell and Developmental Biology Microscopy core, Flow-cytometry and Cell Sorting Facility, Penn Vet Imaging Core, and Center for Host-Microbial Interactions. I also want to thank Cell and Molecular Biology graduate group and Developmental, Stem Cell, and Regenerative Biology program, specially Daniel Kessler, Stephen DiNardo, and Meagan Schoefer for giving me the opportunity to attend the amazing Ph.D. program at the Perelman School of Medicine and their help and support in every step of the way in the graduate school.

I have several friends that I would like to recognize as well. Mohadese Mehrabian, Pegah Yakhchalian, Padideh Moghadam, Parvaneh Khosravi, Negar Foroughi, and Rozhin Penjweini: thanks for standing by my side in all my ups and downs, thank you for always being supportive and bringing so much fun to my life.

I would like to say a big thank you to my family, who have been endlessly supporting me and my decisions every single day of my life with their love. Thanks to my mom for all her effort to overcome the time zone differences to stay in touch regularly, for her positivity, and support. Thanks to my dad to whom I have always been able to turn to when I needed to be guided, to feel stronger, and to be patient. Thanks to my siblings Mehrnaz, Mandana, and Amir Mohammad, and their families: Thanks for your endless kindness! Thanks for always being there for me! And thanks for warming my heart. I would like to thank my nephews Roham, Radman, and Radin: I am so grateful for having you in my life, you bring a lot of joy to my every day, I love you so much and cannot wait to see your sweet faces.

ABSTRACT

THE CELLULAR AND MOLECULAR UNDERPINNINGS OF INTESTINAL EPITHELIAL REGENERATION

Maryam Yousefi

Christopher J. Lengner

Injury to the intestinal epithelium is a hallmark of numerous common clinical disorders, including radiation enteropathy, ischemia-reperfusion, and inflammatory bowel diseases. Disruption of the epithelial barrier in these conditions must be quickly restored to avoid dehydration and translocation of gut microbiota to the bloodstream. Short-term calorie restriction can enhance regenerative response of the intestinal epithelium following DNA damaging injury. However, the specific cell type responsible for this enhanced regenerative capacity and as a result the molecular determinants of this process remain unknown.

Regeneration of the intestinal epithelium is driven by multiple intestinal stem cell (ISC) types, including an active, radiosensitive Wnt^{high} ISC that fuels turnover during homeostasis and a reserve, radioresistant $Wnt^{low/off}$ ISC capable of generating active Wnt^{high} ISCs. In this study, I utilize mouse genetic approaches to mark, isolate, and ablate intestinal stem cell (ISC) populations in order to address, for the first time, the functional importance of reserve ISCs for optimal regeneration following DNA damaging injury in response to caloric restriction. I demonstrate that modulation of mTORC1 signaling in reserve ISCs is a key factor in the regenerative response to radiation injury. I show that mTORC1 is both necessary and sufficient for the activation reserve ISCs. Loss of mTORC1 activity in reserve ISCs following injury impairs tissue regeneration due to failure of reserve stem cell activation. Conversely, promiscuous mTORC1 activation prior to injury sensitizes the epithelium to radiation damage as premature activation of reserve ISCs renders them susceptible to the radiation-induced apoptosis.

I demonstrate that Musashi (Msi) family of RNA-binding proteins are potent upstream regulator of mTORC1 signaling and metabolic genes in reserve ISCs and, similar to mTORC1

signaling, Msi proteins are necessary for intestinal regeneration despite their dispensability for intestinal basal homeostasis. I could modulate mTORC1 activity *in vivo* through caloric restriction, nutrient stimulation with branched chain amino acids, and pharmacological intervention with Rapamycin to govern activation of reserve ISCs and their sensitivity to radiation. These findings delineate a critical role for Msi-mTORC1 axis in regulating reserve ISC activation and epithelial regeneration and inform clinical strategies to protect reserve ISCs from genotoxic insults based on nutrient modulation.

TABLE OF CONTENTS

LIST OF FIGURES

Chapter 1

Chapter 3

Chapter 4

LIST OF TABLES

Chapter 4

CHAPTER 1

Introduction

Hierarchy and Plasticity in the Intestinal Stem Cell Compartment

Introduction

High-turnover tissues including the blood, skin, testes, and intestinal epithelium lose millions of cells daily due to basal turnover associated with tissue function and environmental exposure. This tremendous turnover highlights the need for exquisite coordination of self-renewal of upstream stem and progenitor cells and downstream production of differentiated effector cells.

It is becoming increasingly clear that the highest turnover tissues (the intestinal epithelium and hematopoietic system) organize their stem cell compartments into a hierarchical structure with a slow cycling, long-term, injury-resistant stem cell residing at the top of the hierarchy giving rise to an actively cycling stem cell that bears the proliferative burden required for tissue function. The benefits of such an organizational structure include the capacity to maintain the proliferative output necessary to keep up with the demands of high-turnover tissues using a relatively small stem cell pool, the ability to efficiently regenerate the tissue after damage, and the maintenance of regenerative capacity throughout the lifetime of the organism through preservation of stem cell function. Recent studies have not only revealed the existence of this hierarchical stem cell organization, but have also demonstrated considerable plasticity within the hierarchy.

Stem cell dynamics in the hematopoietic system

Hematopoietic stem cells (HSCs) serve as a paradigm for studying adult stem cells. HSCs are defined as cells with the ability to self-renew and the potential to give rise to all the hematopoietic lineages (Weissman et al., 2001). HSCs are a heterogeneous population with subsets of long-term (LT) and short-term (ST) HSCs. LT-HSCs vs ST-HSCs is determined by their ability to support hematopoiesis post-transplantation into recipient mice for a lifetime (LT) or a few months (ST); however these definitions are arbitrary and subject to change as the field progresses. ST-HSCs further give rise to multipotent progenitor cells (MPPs) that have the potential to give rise to all hematopoietic lineages, but lack long-term self-renewal ability as

evidenced by their rather limited ability to support hematopoiesis for only a few weeks post-transplantation. MPPs can further give rise to common myeloid progenitors (CMPs), which produce mega-erythroid progenitors (MEPs) and granulocyte-macrophage progenitors (GMPs). The latter two are the resources of mature megakaryocytes, erythrocytes, granulocytes, and macrophages. On the axis of immune lineages, MPPs can give rise to common lymphoid progenitors (CLPs), and the latter further produce T, B, and NK cells (Kostetskii et al., 2005; Weissman, 2000). This 'clonal succession' model in which a very small number LT-HSCs sitting at the apex of the hematopoietic pedigree generate the entire hematopoietic system at any given time has been dominant in the field for decades. However, this model is based on the transplantation assay, a non-physiological condition that can be considered highly stressful and relies upon a cell's ability to survive in the circulation and home to the bone marrow. Thus, the transplantation assay may better represent a post-injury regenerative scenario rather than a readout of homeostatic HSC function. Whether basal (or native) hematopoiesis behaviors follow this model has recently been challenged.

The clonal succession model of hematopoiesis, which mainly describes the behavior of transplanted donor cells into highly stressed recipient mice, indicates that LT-HSCs rarely divide over a life time and mice can tolerate loss of LT-HSCs for up to 6-months without showing any lineage bias (Bernitz et al., 2016; Venkatraman et al., 2013; Wilson et al., 2008). These observations suggest that LT-HSCs function only as a back-up or reserve subpopulation on shorter-term (6-month) time frames (Haug et al., 2008; Li and Clevers, 2010). Taking an alternative approach by employing retrotransposition as a means to uniquely barcode individual cells and their lineage (as all cells within a lineage will bear the same transposon tag), researchers demonstrated that a pool of long-lived progenitors (at least 40 weeks), rather than classically defined LT-HSCs, are the main drivers of basal hematopoiesis during most of adulthood (Sun et al., 2014). While additional studies employing independent methodologies will be important for developing a clear understanding of native versus post-transplantation

hematopoiesis, our understanding of stem cell activity in the intestinal epithelium, is derived largely from *in vivo* lineage tracing in native (non-transplanted) tissue.

Active and reserve stem cells of the intestinal epithelium

As a result of constant exposure to pathogens and xenobiotics, intestinal epithelial cells have a short half-life, and have therefore evolved the ability to rapidly regenerate after damage. This ability to regenerate rapidly after injury makes the intestine an excellent model system to study tissue homeostasis, regeneration and tumorigenesis. In the intestinal epithelium, the most highly proliferative tissue in the body, the existence of a hierarchically organized stem cell compartment is becoming increasingly evident (Figure 1.1). Actively proliferating and relatively abundant crypt-base columnar (CBCs) stem cells exhibit high expression of the canonical Wnt pathway target gene *Lgr5* and were the first genetically marked intestinal stem cell (ISC) population functionally validated to give rise to all cell-types in the intestinal epithelium through lineage tracing experiments (Barker et al., 2007). The robust contribution of actively cycling $Lgr5^{+}$ CBCs to intestinal homeostasis has been clearly shown under basal conditions and may be conceptually analogous to the pool of active hematopoietic progenitors described above in native hematopoiesis (Sun et al., 2014). Remarkably, however, genetic ablation of $Lgr5^{+}$ cells with diphtheria toxin showed that they are dispensable for intestinal homeostasis under basal conditions (Tao et al., 2015; Tian et al., 2011). Consistent with this, $Lgr5^{+}$ cells, and particularly Wnt^{high} $Lgr5^{high}$ CBCs, like all proliferative cells are quantitatively ablated in response to DNA damage, such as high dose gamma-irradiation (Tao et al., 2015; Yan et al., 2012) (Figure 1.2). Interestingly, diphtheria toxin ablation of $Lgr5^{+}$ CBCs shortly after or concomitant with radiation injury revealed a requirement for these cells for a robust regenerative response, suggesting that post-injury *de novo* generated $Lgr5^{+}$ CBCs and/or the small fraction of $Lgr5^{+}$ cells that survive the radiation injury play an important role in epithelial regeneration (Metcalfe et al., 2014). The expendable nature of $Lgr5^{+}$ CBCs during intestinal homeostasis and the susceptibility of actively

cycling CBCs to DNA damaging injury imply the presence of additional epithelial cells capable of compensating for CBC loss.

Concomitant with the identification of Lgr5 as a marker of crypt base columnar stem cells, a second population of functionally distinct cells was identified through insertion of a *CreER* reporter into the endogenous *Bmi1* locus (Sangiorgi and Capecchi, 2008). These cells are slower cycling and less frequent than CBCs and, unlike the CBCs, appear indispensable for epithelial maintenance under basal conditions (Sangiorgi and Capecchi, 2008). Since this initial report, numerous additional studies have identified rare cells with shared characteristics of the *Bmi1-CreER*-marked cells, including those marked by *Hopx-CreER (Li et al., 2014; Takeda et al., 2011)*, *mTert-CreER* (Breault et al., 2008; Montgomery et al., 2011), and likely subpopulations of much larger groups of cells marked by more broadly expressed reporter alleles including *Krt19-CreER* (Asfaha et al., 2015), *Lrig1-CreER* (Powell et al., 2012), *Axin2-CreER* (Li et al., 2016a), and *Sox9-CreER* (Roche et al., 2015). These rare stem cells are often referred to as 'reserve ISCs' based on their slow cycling relative to CBCs, their resistance to DNA damaging injury, as well as their proliferative response and increase in lineage tracing in response to such injury (Figure 1.2) (Li et al., 2014, 2016b; Sangiorgi and Capecchi, 2008; Yan et al., 2012). They have similarly been referred to as 'quiescent' stem cells, although only recently has their residence in the quiescent state outside of the cell cycle (G0) been formally demonstrated (Li et al., 2016b; Yousefi et al., 2016). They have also been referred to as '+4' cells based on their position above the crypt base, although we now appreciate that numerous molecularly and functionally distinct cells reside around this position. Curiously, the endogenous *mTert, Hopx*, and *Bmi1* mRNAs are non-specifically distributed throughout all cells of the crypt base, and thus the presence of the transcripts cannot be taken as evidence of cell identity. Why *CreER* reporters in most of these instances mark a fairly specific subpopulation of reserve ISCs remains unclear; however it is tempting to speculate that because these *CreER* insertions disrupt native 3'UTR sequences, the *CreER* reporters may mark cells in which these loci are actively transcribed, while distribution of endogenous mRNAs may reflect message stabilization and inheritance to daughter cells through

activity of the long 3'UTR sequences transcribed from these loci and additional noncoding functions of protein coding genes, as has been observed in other stem cell compartments (Crist et al., 2012). There are considerable disconnects between cells marked by reporter transgenes, endogenous protein, and mRNA for many intestinal stem cell markers, and thus caution must be taken when assigning stem cell identity based on mRNA/protein/reporter expression as most demonstrations of stem cell activity rely solely on lineage tracing assays conducted with Cre recombinase.

Single cell expression profiling confirmed an overlap in the molecular identity of the majority of cells marked by *Hopx-CreER* and *Bmi1-CreER*, with the *Hopx-CreER*$^{+}$ reserve ISCs being as homogenous a population as that marked by *Lgr5-CreER,* but also one that is molecularly distinct from the *Lgr5-CreER*$^{+}$ CBCs (Li et al., 2014). The population marked by *Bmi1-CreER* largely overlaps with that marked by *Hopx-CreER,* although *Bmi1-CreER* marks a more heterogeneous population, including some presumably differentiated cells within the villi and rare CBCs (Li et al., 2014). Thus, caution should be exercised when interpreting molecular profiles taken from bulk populations, as population heterogeneity may prove misleading. In contrast to CBCs, the reserve ISCs have little to no detectable readouts of canonical Wnt pathway activity (e.g., expression of *Lgr5, Ascl2, Ccnd1*, etc.), little expression of genes associated with cellular metabolism and proliferation (e.g., *H6PD*, *Myc*, *Msi1),* and higher expression of genes encoding cell cycle inhibitors (*Cdkn1a*) (Li et al., 2014, 2016a; Takeda et al., 2011). In summary, these reserve ISCs, including those marked by *mTert-CreER*, share a number of unique functional properties: 1) they appear highly resistant to DNA damage (e.g., chemotherapeutics or 12-15Gy of gamma irradiation) (Li et al., 2016b; Montgomery et al., 2011; Tinkum et al., 2015), 2) they are slow cycling (Li et al., 2014; Yan et al., 2012), 3) they appear refractory to stimulation of the canonical Wnt pathway *in vivo* (Yan et al., 2012), 4) they routinely give rise to lineages (assessed by crypt-villus lineage tracing) containing all intestinal cell types, including CBCs (Li et al., 2014; Montgomery et al., 2011; Sangiorgi and Capecchi, 2008; Tian et al., 2011; Yan et al., 2012), and

5) they are necessary for both epithelial maintenance in the basal state as well as proper regeneration after injury (Sangiorgi and Capecchi, 2008).

Importantly, numerous groups have independently confirmed that the Wnt^{OFF} reserve stem cells give rise to Wnt^{High} CBCs relatively frequently during homeostasis, both through histological lineage tracing techniques and molecular profiling of progeny (Asfaha et al., 2015; Li et al., 2014; Montgomery et al., 2011; Sangiorgi and Capecchi, 2008; Tao et al., 2015; Yan et al., 2012). An assessment of daughter cell identity from reserve ISCs done by coupling a *Hopx-CreER-Lox-Stop-Lox-tdTomato* lineage tracing with a nuclear H2B-GFP pulse-chase as a measure of cell division suggests that upon division, these reserve stem cells produce CBCs (evidenced by high *Lgr5* and Wnt target gene expression) and additional reserve ISCs at similar frequencies, indicating that asymmetric self-renewal/commitment (to CBC identity) divisions may occur (Li et al., 2014). Consistent with this, quantification of clonal exhaustion reveals that CBCs undergo exhaustion much more rapidly in comparison to reserve ISCs, the latter exhibiting no clonal exhaustion after 6 months, while approximately 2/3 of CBC clones undergo exhaustion over this same period (Li et al., 2014). Thus, the culmination of data from numerous groups supports a model in which a long-lived, injury resistant reserve stem cell resides upstream of an active, shorter-lived, Wnt-driven crypt base columnar stem cell (Figures 1.1 and 1.2).

Plasticity within the hierarchy

In addition to these compelling data supporting the existence of a hierarchically structured ISC compartment, several recent studies have identified surprising plasticity in the tissue as well, in which more committed progeny of CBCs can re-acquire the CBC identity, albeit at very low frequency (Buczacki et al., 2013) and in the case of non-physiological injury models (such as genetic ablation of specific cell types) (Figure 1.2) (Tetteh et al., 2016). Nonetheless, these studies clearly demonstrate plasticity in cell identity exists within the crypt.

The first evidence of such plasticity arose from studies of label-retaining cells (LRCs). DNA label retention was originally posited to mark cells undergoing asymmetric partitioning of the nascent and parental genomes into distinct daughter cells (originally employing tritiated thymidine as the label). This 'immortal strand' hypothesis was posited over 40 years ago to act as a mechanism protecting long-lived stem cells (which, theoretically, retain the parental genome) against replication-induced mutation (Cairns, 1975; Potten et al., 1978, 2002, 2003). While this hypothesis is elegant, little evidence supports it, and significant evidence opposes it (Kiel et al., 2007). Nonetheless, the existence of LRCs within the intestine is clear, but what is less clear is the identity and function of intestinal LRCs. Since the original tritiated thymidine pulse-chase experiments, fusion proteins between fluorophores and histone H2B have become the favored tool for identifying LRCs, as H2B fusions enable prospective identification and isolation of living cells for molecular profiling and functional assays. The LRC assay is now used as a means to identify non-dividing cells, with the caveat that truly non-dividing cells would be unable to incorporate the label because the label can only be incorporated during S-phase. Thus LRC labeling is usually performed by pulsing after injury or early during development, when a presumptive dormant stem cell is actively dividing prior to reentering/entering dormancy (Potten et al., 2002).

Curiously, the first study to test the functionality of LRCs in the intestine incorporated the label not after injury or in an immature animal, but during a relatively short pulse in a mature animal (Buczacki et al., 2013). This suggests that the LRCs identified by this method represent cells undergoing cell cycle exit downstream of a proliferative cell rather than a dormant stem cell population. Indeed, it is now broadly appreciated that long-term (one month chase or longer) LRCs of the intestine are in fact a homogenous population of terminally differentiated Paneth cells downstream of the CBCs (Buczacki et al., 2013; Li et al., 2016c; Potten et al., 2002; Roth et al., 2012). These long-term LRCs are restricted to the small intestine, consistent with the absence of Paneth cells in the colon. Perhaps more interesting was the population of LRCs found after shorter-term (8-12 days) chase. These cells reside at or near the crypt base, and unlike long-

term LRCs, single cell profiling reveals this population to be highly heterogeneous, including cells with gene expression signatures consistent with Paneth cells, enteroendocrine cells, as well as rare cells with reserve ISC molecular identity (Buczacki et al., 2013; Li et al., 2016c). Indeed, compound reporter mice, where *Hopx-CreER* marks reserve ISCs and H2B-GFP marks label retaining cells, reveals only a very small fraction of double-positive cells (i.e. label retaining reserve ISCs) (Li et al., 2016b). Employing an inducible H2B-Split-Cre system to enable *in vivo* lineage tracing from LRCs demonstrated extremely rare tracing events, particularly in response to injury, consistent with the presence of very rare cells with reserve ISC identity within this short-term LRC population (Buczacki et al., 2013; Li et al., 2016b). Interestingly, short-term LRCs that exhibit hallmarks of Paneth or enteroendocrine cell identity retain the ability to form small intestinal organoids *in vitro*, albeit at significantly lower efficiencies than purified populations of reserve ISCs (Buczacki et al., 2013; Li et al., 2016c). When the label retention chase is extended to one month, LRCs are no longer able to form organoids.

Interestingly, the functional and molecular properties of short-term label-retaining secretory progenitor cells are shared with cells marked by a *Dll1-CreER* allele (van Es et al., 2012a). These *Dll1-CreER*-marked cells are the progeny of CBCs, normally generate cells of the secretory lineage, form organoids *in vitro* in the presence of Wnt3a (which is not required for organoid formation from CBCs or reserve ISCs), and exhibit very rare lineage tracing activity in response to mid-dose radiation injury (6Gy gamma-IR). Taken together, these findings support a model where CBCs activate Dll1 as they enter the secretory lineage (in opposition to the transit-amplifying enterocyte lineage, Figure 1.3) and shortly thereafter exit the cell cycle. These now post-mitotic LRCs retain developmental plasticity for some time, enabling them to re-acquire stem cell activity given a favorable environment (Figures 1.2 and 1.3).

The LRCs of the intestine and other non-dividing cells are often referred to as being quiescent (Buczacki et al., 2013), however the distinction between true quiescence and differentiation/G1 arrest are unclear. For example, LRCs are referred to as being quiescent, yet the vast majority of these cells are arrested in the G1 phase of cell cycle, typical of a terminally

differentiated cell (Li et al., 2016b). The definition of quiescence, to be "in a state or period of inactivity or dormancy" implies that 1) quiescent cells have a dormant genome (and thus reside in G0 not G1, usually distinguished by global levels of transcription and cellular metabolism) and that 2) quiescent cells can re-enter the cycle and act as a stem/progenitor cell. By this definition, the vast majority of non-dividing cells are not quiescent, and thus drawing this distinction becomes important for creating clear framework for understanding the intestinal stem cell compartment.

Developmental plasticity downstream of the CBC state can also be observed in transit-amplifying (TA) cells committing to the enterocyte lineage (Figure 1.2). These cells, marked with *Alpi-CreER,* give rise to full crypt-villus lineage tracing events at low frequency in response to genetic ablation of CBCs using an *Lgr5-DTR* allele (Tetteh et al., 2016). Similarly, generation of small intestinal organoids followed by *Lgr5-DTR* CBC ablation results in organoid maintenance from an *Alpi-CreER*-marked population. While this provides some evidence for plasticity downstream of the CBC state, whether this mechanism functionally contributes to intestinal regeneration in any physiological injury setting is unclear. It would be expected that an injury which kills cycling cells such as DNA damage would ablate both the CBC compartment as well as these *Alpi-CreER*-marked transit-amplifying cells (Tao et al., 2015).

Ultimately, the ability of short-term LRCs and transit-amplifying cells displaying hallmarks of lineage commitment downstream of the CBC state to acquire stem cell properties, either forming organoids *in vitro* or giving rise to clonal lineage tracing events *in vivo* is a clear demonstration of the plasticity of cellular identity within the intestinal crypt.

Signaling pathways regulating intestinal stem cells' activity and differentiation

The self-renewal and differentiation activities of intestinal stem cells are precisely regulated by signaling molecules such as cytokines and growth factors, which are secreted from

epithelial cells and from non-epithelial cells surrounding the intestinal epithelium. These include fibroblasts, immune cells, and enteric neurons. Genetic studies have shown that various signaling pathways, including Wnt, Notch, Bmp, and EGF signaling pathways regulate the balance between proliferation and differentiation in the intestinal epithelium (Moore and Lemischka, 2006).

Wnt signaling

In the gastrointestinal (GI) tract the Wnt pathway is required for crypt base proliferation, differentiation to the secretory lineage, and migration along the crypt-villus axis (Gregorieff et al., 2005; Haramis et al., 2004; He et al., 2004). Many human diseases, including cancer and diabetes, are associated with mutation in the Wnt signaling pathway (Clevers and Nusse, 2012). The Wnt signaling pathway mostly acts over short distances through binding of Wnt ligands to a heterodimeric receptor consisting of Frizzled (Fz) and Lrp5/6 proteins. The output of Wnt ligand binding to its receptor is inhibition of β-catenin degradation through the multiprotein destruction complex consisting of Axin, Apc, WTX, CK1α/δ and Gsk3α/β (Aberle et al., 1997).

In the absence of Wnt ligand, phosphorylation of β-catenin by CK1α/δ and Gsk3α/β leads to its degradation by E3 ubiquitin ligase complex. Binding of Wnt ligand to its receptor recruits the destruction complex to the plasma membrane through interaction between Lrp and Axin, which acts as the scaffold of the destruction complex. Localization of destruction complex to the cell membrane and inhibition of Gsk3α/β by Lrp prevents degradation of β-catenin leading to saturation of the destruction complex. Thus, newly translated β-catenin is not degraded by the destruction complex and can translocate to the nucleus, leading to transcriptional activation of β-catenin target genes (Li et al., 2012; Stamos et al., 2014).

In one of the first functional studies of the role of Wnt signaling in intestinal crypt biology, germline disruption of Tcf4, the transcriptional activation partner of β-catenin, led to loss of proliferative compartments in the intestinal epithelium of neonatal mice (Korinek et al., 1998). In

the adult intestine, ubiquitous deletion of Tcf4 using a *Villin-CreERT2* expressing transgenic mouse model caused rapid loss of CBCs (van Es et al., 2012b) and intestinal overexpression of the secreted Wnt inhibitor *Dickkopf 1* (*Dkk1*) led to loss of crypts and decreased epithelial proliferation (Kuhnert et al., 2004).

Lgr5, one of the known targets of Wnt signaling pathway, marks the actively cycling CBCs (Barker et al., 2007). CBC-specific activation of the Wnt pathway by inactivating mutations in APC stabilizes β-catenin and confers stem cells with a competitive advantage over their wild-type counterparts resulting in rapid formation of adenomas (Barker et al., 2009; Snippert et al., 2014; Vermeulen et al., 2013).

The stem cell niche provides signaling cues that maintain stem cell self-renewal and dictate the balance of stem cell proliferation with differentiation. The importance of Wnt signaling for maintenance of intestinal epithelium, and specifically CBC function, raised the question about the cellular identity of the Wnt-secreting niche. Sato et al. originally hypothesized that Paneth cells form the CBC niche because they are intercalated at the crypt base between CBCs, secrete Wnt3, Egf, and the Notch ligand Dll4, their co-culture with CBCs enhances organoid formation efficiency from CBCs *in vitro*, and addition of Wnt3a can substitute co-culturing Paneth cells with CBCs (Sato et al., 2011).

Despite these findings, several recent studies have called into question the role of the Paneth cells in supporting CBCs. Paneth cell loss via deletion of *Atoh1/Math1* (the master secretory lineage specifying transcription factor) has no effect on CBCs and intestinal homeostasis under basal conditions, nor does it adversely affect regeneration following radiation injury (Durand et al., 2012; Kim et al., 2012). Moreover, epithelial-specific deletion of *Wnt3* or Wnt processing protein *Porcupine* (*Porcn*) using *Villin-CreER* has no effect on intestinal stem cell activity (Farin et al., 2012; Kabiri et al., 2014a), suggesting the presence of non-epithelial sources of Wnt and other niche factors.

Turning to potential non-epithelial Wnt sources, deletion of *Porcn* in myofibroblasts using *Myh11-CreER* alone or in combination with epithelial deletion using *Villin-CreER* did not affect intestinal stem cell proliferation or differentiation (San Roman et al., 2014). In contrast, a recent study showed that rare Foxl1^{+} cells, which are located just under the intestinal epithelium, have mesenchymal characteristics, highly express niche factors such as Wnt and Fgf2, and are distinct from myofibroblasts. Further, their ablation using diphtheria toxin halts proliferation and Wnt signaling activity in the intestinal stem cell compartment, leading to tissue failure. This is in contrast to what is observed upon Paneth cell ablation. This recent study, for the first time, shows the requirement for a single cell type in providing niche signals to CBCs(Aoki et al., 2016). However, whether the requirement for Foxl1^{+} cells is due to their production of Wnt ligands or other niche factors remains to be definitively demonstrated

Notch

Notch signaling pathway is an evolutionarily conserved pathway known to be involved in cell fate determination during development, and is dysregulated in different human cancers (Katoh and Katoh, 2007). Notch signaling is active in the stem and progenitor zone of gastrointestinal tract such as in the intestinal and colonic crypts (van Es et al., 2005; Jensen et al., 2000; Riccio et al., 2008; Schröder and Gossler, 2002). Activation of Notch signaling expands the proliferative zone in the intestinal epithelium, represses secretory cell differentiation, and increases the number of absorptive enterocytes (Fre et al., 2005; Stanger et al., 2005). Conversely, Notch inhibition leads to loss of proliferation, loss of CBCs, and enhanced differentiation to goblet cells and enteroendocrine cells in the intestine. Consistently, deletion of Atoh1, which is repressed downstream of active Notch, prevents differentiation toward the secretory cell types including goblet, Paneth, and enteroendocrine cells (van Es et al., 2005, 2010; Milano et al., 2004; Shroyer et al., 2007) while induction of Atoh1 promotes differentiation towards this lineage (Ueo et al., 2012). The suppression of differentiation to the secretory lineage is oncogenic in gastric cancer;

inhibition of this suppression by Notch signaling inhibitors could be a therapeutic strategy (Fischer et al., 2011; Hoey et al., 2009; Liu et al., 2011).

Notch signaling acts between two cells: one presents the Notch ligand, and the adjacent cell presents the Notch receptor. Activation of Notch signaling in the cell with the Notch receptor leads to release of the Notch intracellular domain (NICD) and its translocation to the nucleolus. In the nucleus, NICD along with Rbpj, one of the principle effectors of the Notch pathway, regulates transcription of Notch target genes (Logeat et al., 1998). Secretory progenitor cells, Paneth cells, and goblet cells express the Notch ligands Delta-like 1 and 4 (Dll1 and Dll4) and present these ligands to their adjacent cells in the intestinal epithelium (Fre et al., 2005; Sato et al., 2011; VanDussen et al., 2012; Vooijs et al., 2007).

Bmp

Juvenile polyposis syndrome (JPS), which is the development of multiple benign tumors in the gastrointestinal tract, is caused by loss-of-function mutations in the Bone morphogenetic protein (BMP) signaling pathway (Howe et al., 1998, 2001). BMP is also one of the major barriers to colorectal cancer development (Hardwick et al., 2008). Bmp signaling acts through binding of Bmp ligands (BMP2 and BMP4) to a type II receptor, recruiting a type I receptor (Bmpr1a or Bmpr1b) and finally activation of SMAD transcription factors. In the intestine, BMP ligands and their receptors are expressed both in mesenchymal and epithelial cells. Bmpr1a is expressed in the crypt base and in the intestinal villi, but not in the transit amplifying zone. Noggin, a BMP antagonist, is expressed in the mesenchyme adjacent to the crypt base and some cells located higher in the crypts (He et al., 2004). As a result of the interplay between BMP agonist, receptors, and antagonists, BMP signaling is only active in the villi and some cells around the +4 position of the intestine and in the in the intercrypt epithelial cells of the colon (Haramis et al., 2004; Hardwick et al., 2008; He et al., 2004). Inhibition of BMP signaling via overexpression of Noggin or deletion of BMP receptor leads to expansion of stem cell compartment and generation of the

ectopic crypts (Haramis et al., 2004; He et al., 2004). Consistently, absence of Noggin in organoid culture media causes stem cell differentiation (Sato et al., 2011). Interestingly, following Doxorubicin-induced tissue injury, when surviving stem cells become activated to repopulate the damaged intestinal epithelium, *chordin-like 2*, a BMP antagonist, is upregulated in the mesenchyme (Seiler et al., 2015) This result emphasizes the role of Bmp signaling in regulation of intestinal epithelial proliferation.

Hippo

The Hippo pathway is highly conserved from *Drosophila melanogaster* to mammals and it responds to a variety of signals, including stress (oxidative stress, hypoxia, unfolded proteins, and mechanical stress), hormones, and growth factors (Bossuyt et al., 2014; Ma et al., 2015; Meng et al., 2016; Shao et al., 2014; Wu et al., 2015). The primary components of the Hippo pathway are six kinases, including MST1 and MST2, and two homolog transcriptional co-activators, YAP and TAZ (Yu and Guan, 2013). The Hippo pathway is involved in regulating cell fate decision, cell survival, proliferation, and organ size. Dysregulation of the Hippo pathway can lead to malignant transformation and failure in tissue regeneration (Lee et al., 2010; Lei et al., 2008; Shen and Stanger, 2015; Yimlamai et al., 2014).

Activation of the kinase cascade leads to phosphorylation of YAP/TAZ transcriptional co-activators. This phosphorylation regulates the cellular localization and stability of these proteins. When the pathway is active, phosphorylated YAP/TAZ are sequestered to the cytoplasm and are destined for degradation. When the pathway is off, unphosphorylated YAP/TAZ moves to the nucleus and interacts with the TEAD family of DNA-binding proteins, which alone have low transcriptional activity. The interaction between YAP/TAZ and TEAD leads to formation of a transcriptionally active complex and transcription of genes important in cell survival and proliferation (Zhao et al., 2007, 2008, 2010). YAP and TAZ are dispensable for intestinal homeostasis under basal conditions (YAP/TAZ knockdown reduces the rate of proliferation of

CBCs and differentiation to goblet cells) but are necessary for intestinal regeneration following damage and for tumorigenesis in an *Apc* null mouse model of colorectal cancer (Azzolin et al., 2014; Barry et al., 2013; Cai et al., 2010; Zhou et al., 2011).

EGF

Epidermal growth factor (EGF) is one of the main components of organoid formation media from intestinal stem cells (Sato et al., 2009). EGF receptor (EGFR/ErbB/HER1) belongs to the ErbB receptor tyrosine kinase family that signals through Akt, MAPK, and many other pathways to regulate cell proliferation, migration, differentiation, apoptosis, and cell motility (Roskoski, 2014). Phosphorylated EGFR (activated receptor) is detected in all intestinal crypt cells but it is at its highest level at around +3 to +12 cell positions from the crypt base. Lrig1, a negative regulators of EGF signaling, is also expressed in the intestinal crypts and its loss causes crypt hyperplasia (Wong et al., 2012).

Activation of EGF signaling could lead to upregulation of the mechanistic target of Rapamycin (mTOR) signaling pathway. mTOR signaling integrates the intracellular and extracellular signals such as energy, stress, nutrients, growth factors, hormones and, it serves as one of the main regulator of cell metabolism, growth, and proliferation. mTOR signaling is highly upregulated in human cancers including colorectal cancer, however, the components of this signaling pathway are infrequently found to be mutated. This means that hyperactivation of mTOR signaling is mainly due to mutations in its upstream regulators such as components of EGF or Wnt signaling. For example, around 50% of colorectal cancers have been found to have increased copy numbers of EGFR gene (Cappuzzo et al., 2008). Mutations in phosphatidylinositol-3-kinase (PI3K), which is downstream of EGF receptor activation and upstream of mTOR, can also be identified in 32% of colorectal cancer patients (Samuels et al., 2004). Similarly, mutation in APC, one of the main component of Wnt signaling pathway, is found in 80% of sporadic colorectal tumors (Kwong and Dove, 2009).

mTOR, which is a serine threonine kinase, can be part of two different multiprotein complexes, mTOR complex 1 (mTORC1) and mTOR complex 2 (mTORC2). The mTORC1 signaling pathway is the master regulator of anabolic processes such as protein and lipid synthesis (Laplante and Sabatini, 2009) and, besides receiving input from signaling pathways such as EGF and Wnt signaling, availability of nutrients such as amino acids can directly regulate mTORC1 activity (Inoki et al., 2006; Valvezan et al., 2012, 2014; Zoncu et al., 2011). mTORC1 signaling is required for intestinal tumorigenesis and regeneration following injury (Ashton et al., 2010; Faller et al., 2015; Fujishita et al., 2008; Gulhati et al., 2009). Surprisingly, despite its clear role in cell growth and proliferation, mTORC1 signaling is dispensable for basal homeostasis of adult intestine (Faller et al., 2015), the most highly proliferative tissue in mammalian body. mTORC2 is believed to be involved in cell survival, proliferation, and cytoskeletal organization but, in contrast to mTORC1, very little is known about mTORC2 (Laplante and Sabatini, 2009).

Dysregulation of signaling in the intestinal stem cells

Homeostasis in adult tissues, particularly in the highly proliferative ones, is dependent on the appropriate function of resident stem cells: on their capacity to self-renew and differentiate and replace damaged or dying cells. Thus, perturbations in the function of stem cells could be excessively costly compared to perturbations in the function of terminally differentiated cells. Dysregulation in adult stem cells not only has consequences for the originally affected cells, but also for their progeny. Altered self-renewal of adult stem cells can result in oncogenic transformation if it is enhanced, or decline in tissue regeneration if it is impaired (Noah and Shroyer, 2013).

Dysregulation of stem cell self-renewal underlies most hematopoietic malignancies and has been implicated in cancers of the breast, gastrointestinal system, central nervous system, and many other solid tumors (Rossi et al., 2008). Colorectal cancer, one of the common cancer types of the gastrointestinal tract, is a leading cause of death in the world. Colorectal cancer

evolves clonally by acquiring a series of mutations that ultimately convert normal epithelial cells to metastatic carcinoma. The initiating mutation, which provides a selective growth advantage to a normal epithelial cell, is thought to be homozygous inactivation of the *APC* tumor suppressor gene. APC is a large protein with diverse cellular functions, including antagonism of canonical Wnt signaling, microtubule nucleation, and RNA binding (van Es et al., 2005, 2010; Milano et al., 2004; Shroyer et al., 2007). Acute and broad loss of *Apc* throughout the epithelium in mice results in crypt hyperplasia, differentiation block, and crypt fission (Sansom et al., 2004). Subsequent mutations in KRAS, TGF-B, P53, and PI3K pathways occur later and result in clone expansion and progression from small adenoma to malignant invasive carcinoma (Markowitz et al., 1995; Samuels and Waldman, 2010; Sansom et al., 2004; Vogelstein et al., 1988, 2013).

Inherited mutation, aging, and environmental factors such as diet may also result in reduced effectiveness of stem cells in tissue regeneration. The monolayer of the intestinal epithelial cells provides a selective barrier to microbiota, nutrient, water, and xenobiotics in the lumen. The rapid rate of epithelial cell proliferation in the small intestine makes gastrointestinal toxicity one of the most common off-target effects of a variety of radiation/chemo-therapy for cancer patients. Mucositis, ulceration, necrosis, and perforation are some of the off-target effects of radiation/chemo-therapy approaches partly as a result of crypt apoptosis and villous atrophy after receiving these treatments. Damage in the intestinal epithelium can lead to inflammation, electrolyte imbalance, dehydration, malnutrition, and many other unwanted complications for cancer patients (Carneiro-Filho et al., 2004; Keefe et al., 2000; Melichar and Zezulová, 2011; Nejdfors et al., 2000; Russo et al., 2013).

Disruption in the barrier function of the intestinal epithelium may also happen in inflammatory bowel diseases (IBD) or as a result of ischemia-reperfusion. Intestinal ischemia-reperfusion may occur during variety of surgeries including abdominal surgery, small bowel transplantation, and cardiopulmonary bypass. Disruption of barrier function can lead to high mortality rate due to translocation of bacteria into the body circulation and induction of systemic inflammation (Blikslager et al., 2007; Grootjans et al., 2010). Regeneration of the intestinal

epithelial layer is associated with a more favorable prognosis for IBD patients, including lower relapse and hospitalization rates (Shah et al., 2016). Thus, understanding the underlying molecular mechanisms of damage to the intestinal epithelium and regeneration following injuries caused by radiotherapy, chemotherapy, IBD, and ischemia-reperfusion may improve our ability to prevent damage and improve repair, and thus maintain the integrity of the epithelial barrier.

In this work, I describe the cellular and molecular underpinnings of intestinal regeneration in response to high dose radiation. I introduce methods to protect the tissue against injury, and to enhance the regenerative response to repair the damage.

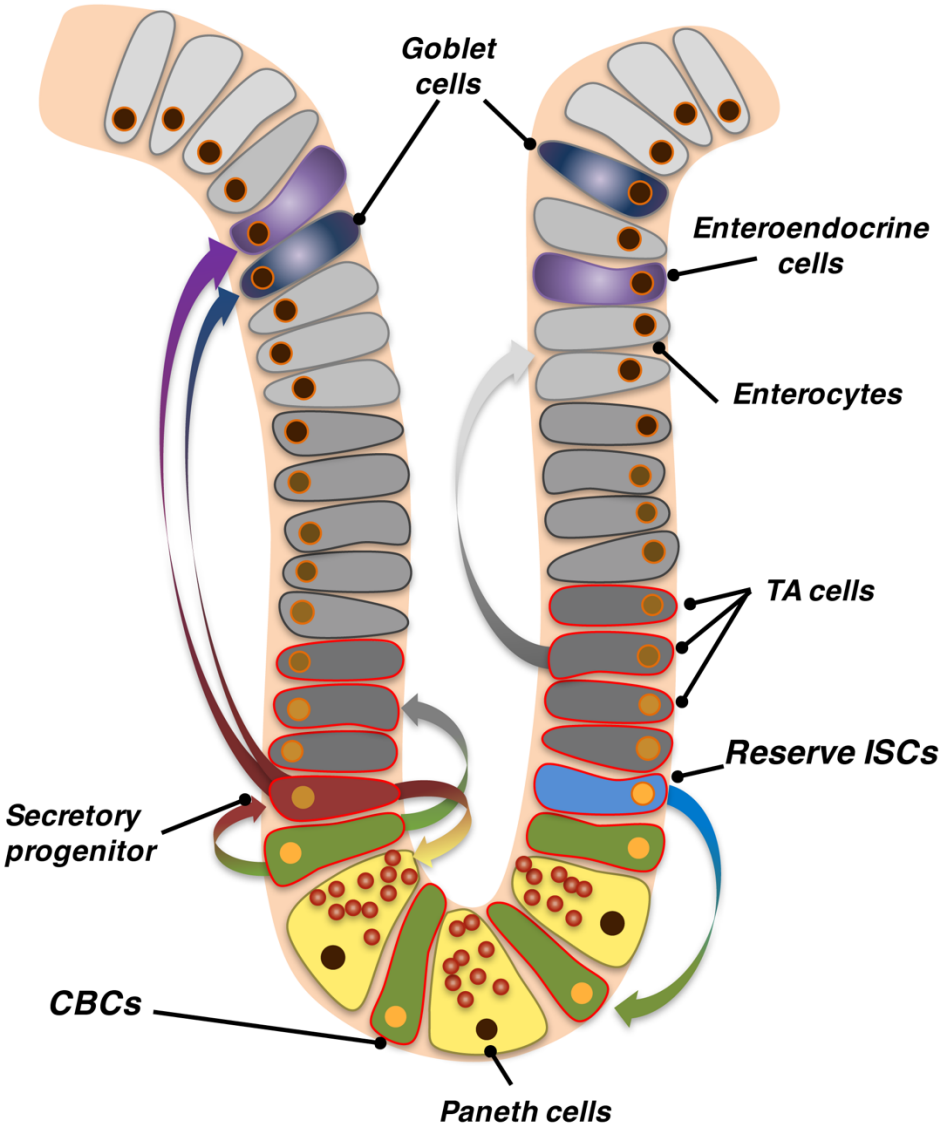

Figure 1. 1. Intestinal stem cell fate determination under basal conditions.

Figure 1.1. Intestinal stem cell fate determination under basal conditions

In the resting state, reserve ISCs (blue) periodically divide to give rise to the active crypt base columnar stem cells (CBCs, green). These active CBCs then either produce transit-amplify progeny (T/A cells, dark grey), which go on to divide very rapidly in order to produce large quantities of enterocytes (light grey), or can generate secretory progenitor cells (maroon). These secretory progenitor cells then commit to either Paneth, goblet, or enteroendocrine cell lineages (yellow, navy blue, or purple, respectively).

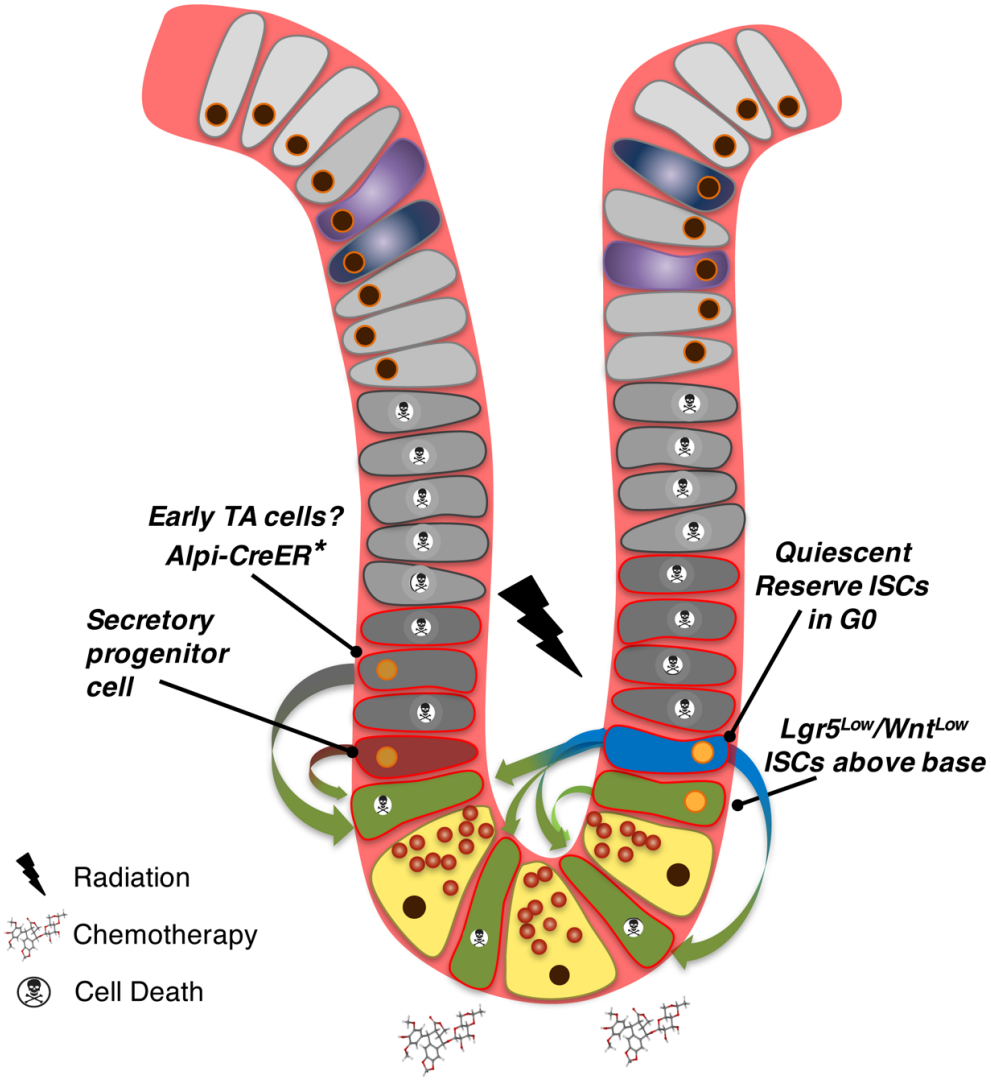

Figure 1. 2. Intestinal regeneration after injury

Figure 1.2. Intestinal regeneration after injury

Exposure to DNA damaging agents such as high-dose gamma radiation or chemotherapeutics ablates actively cycling cells, including CBCs and transit-amplifying cells. Some cells are able to survive DNA damage, and some of these cells can contribute to the post-injury regenerative process. In response to DNA damage, reserve ISCs enter the cell cycle to replenish the CBC compartment and epithelium. Additionally, some reports indicate that Wnt^{Low} CBCs above the crypt base as well as cells downstream of the CBC can resist DNA damage-induced cell death and contribute to repopulation, including a rare subpopulation of secretory progenitor cells. The quantitative contribution of these cells to regeneration based on lineage tracing is, however, minimal, and no evidence exists demonstrating its functional importance. Further, in non-physiological injury settings in which CBCs are genetically ablated with diphtheria toxin, transit-amplifying cells marked by *Alpi-CreER* can fall back into the CBC niche and re-establish stem cell identity.

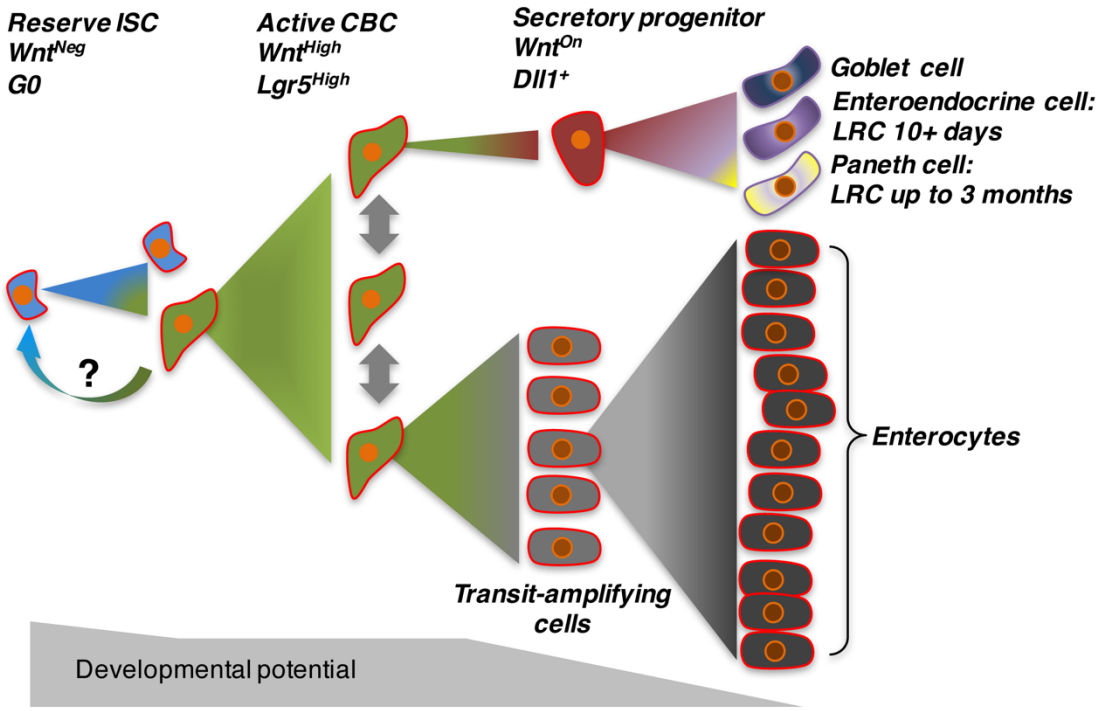

Figure 1. 3. Model of intestinal stem cell compartment organization

Figure 1.3. Model of intestinal stem cell compartment organization

Atop the hierarchy resides a population of rare stem cells that lack activity of the canonical Wnt pathway and reside in the quiescent G0 state. During homeostasis, these cells periodically divide to generate CBCs driven by high Wnt pathway activity and marked by Lgr5 expression. Whether CBCs can re-enter the Wnt^{off} reserve ISC state remains an outstanding question. CBCs divide symmetrically and stochastically and give rise to transit-amplifying cells, which begin to lose developmental potency as they undergo the massive proliferation required to generate large numbers of short-lived enterocytes. Conversely, CBCs can activate Dll1 expression and commit to the secretory lineage. These secretory progenitor cells retain some developmental potency, even after they exit the cell cycle and retain DNA label while they acquire hallmarks of enteroendocrine and Paneth cell lineages. The secretory progenitor cells can also give rise to goblet cells, a fate decision that is presumably coupled to additional cell divisions as no evidence for goblet cell identity is found in the short-term label retaining cell population. Long-term label retaining cells are terminally differentiated Paneth cells that have lost developmental potency.

CHAPTER 2

Materials and Methods

Mouse Strains

We obtained *Bmi1-CreER* (JAX strain 010531), *Lgr5-EGFP-IRES-CreER* (JAX strain 008875), *Tsc1* floxed (Jax mice strain 005680), *Raptor* floxed (Jax mice strain 013188), and *R26-CAG-LSL-tdTomato* (JAX mice strain 007914) from the Jackson Laboratory. *Hopx-CreER (*JAX strain 017606) mice were generated at the Perelman School of Medicine in the laboratory of Dr. Jonathan Epstein, University of Pennsylvania. Generation of the TRE-Msi1 doxycycline-inducible mouse model and Msi1 and Msi2 conditional alleles was previously described (Li et al., 2015; Park et al., 2014). All mice were maintained on a C57/BL6N background.

All experimental analyses were performed on three or more individual mice (male or female mice at 8–12 weeks of age). Controls and experimental groups were sex-matched littermates or age-matched, sex-matched non-littermates. To ablate *Tsc1*, *Raptor, and Msi* floxed *alleles* or to activate the *R26-LSL-tdTomato* or *R26-LSL-DTA* cassettes, Tamoxifen (Sigma) was dissolved in corn oil at 10mg/ml and 1mg was injected intraperitoneally per 20 gram of mouse body weight for each dose. To induce Msi1 gene expression, TRE-Msi1 and control (M2rtTA alone) mice received 1 mg/ml doxycycline hyclate (Sigma-Aldrich) in drinking water, supplemented with 1% (w/v) sucrose.

To activate mTORC1 signaling *in vivo* using nutrient modulation 1.5% (w/v) Leucine was dissolved in the drinking water and was given to mice during the time mentioned specifically for each experiment. To inhibit mTORC1 signaling non-genetically, Rapamycin (Selleck Chemical) was first reconstituted in absolute ethanol at 10 mg/ml and diluted in 5% Tween 80 (Sigma) and 5% PEG-400 (Hampton Research) before injection. 5 mg Rapamycin per 1000 grams of mouse body weight was administered by daily intraperitoneal injection for the time indicated for each experiments. For assessing regenerative efficiency, mice were exposed to 12 Gy whole body γ-irradiation and euthanized 3 days following radiation.

To calorie restrict mice, the food consumption was first measured for a period of 1-2 weeks and 60% of the food intake was given to calorie restricted mice daily for 4-6 weeks. All

mice in *ad libitum* group were fed irradiated rodent chow diet (Prolab RMH 3000, 5P00) and calorie restricted mice received irradiated chow diet fortified with vitamins and minerals (LabDiet, 5B6V) to prevent nutrient deficiency in calorie restricted mice (Kalaany and Sabatini, 2009). During the period of calorie restriction, the food intake of the calorie-restricted mice was readjusted based on their control counterparts' food consumption. Fasting experiments were done by removing the food for 16 hours from the mouse cages.

All mouse protocols were approved by the Institutional Animal Care and Use Committee at the University of Pennsylvania under protocol 803415 to Dr. Christopher Lengner.

Histology and Immunofluorescence

Tissues were fixed in buffered formalin phosphate or Zinc formalin (Fisher Scientific) overnight at 4°C and then, were washed in PBS for 30 minutes and moved to 70% ethanol until the time of paraffin embedding. Staining was done on 5 um tissue sections from the jejunum. Tissue regeneration assays were don on sections stained with Hematoxylin and Eosin in the Morphology Core of the Penn Center for Molecular Studies in Digestive and Liver Diseases according to standard procedures. For immunostaining, antigen-retrieval was performed by heating slides in 10 mM Tris base, 1mM EDTA solution, 0.05% Tween 20, pH 9 with a pressure cooker.

The following primary antibodies were used for immunostaining: Living Colors DsRed Monoclonal Antibody (1:200, Clontech, 632392), Phospho-S6 Ribosomal Protein Antibody (1:200, Cell Signaling, 4858), Anti-Ki67 Antibody (1:1000, leica novocastra, NCL-Ki67p), anti-Musashi1 antibody (1:200, D270-3; MBL International), anti-Musashi2 antibody (1:200, NBP1-42029; Novus Biologicals), anti–β-catenin antibody (1:1,000, C7207; Sigma-Aldrich), anti– E-cadherin (1:200, 13-1900; Invitrogen), Anti-PIP3 Antibody (1:50, echelon, Z-P345), and anti–lysozyme C antibody (C-19, 1:200, sc-27958; Santa Cruz Biotechnology, Inc.). Cy2-, Cy3- and Cy5- conjugated

secondary antibodies were obtained from the Jackson Immunoresearch Laboratories. Biotinylated secondary antibodies and DAB substrate kit for immunohistochemistry were purchased from Vector Laboratories.

All quantifications were done on 20 to 40 randomly selected areas in jejunum on indicated number of mice for each experiment. Regenerative foci were defined as 10 or more adjacent chromophilic cells and a lumen in hematoxylin and eosin stained sections of intestinal jejunum of mice that were exposed to 12 Gy whole body γ-irradiation 3 days before the harvest time.

For quantification of pS6, PIP3, and Msi1 fluorescence intensity in reserve ISCs of mice under ad libitum and calorie restricted diets, tdTomato+ populations were sorted by FACS, smeared over coverslips coated with CELL-TAK (354240; Corning), and allowed to settle at 37^0C for 10 min. The cells were subsequently fixed in 4% PFA and permeabilized in 0.5% Triton X-100 before staining. Quantification of fluorescence intensity was done using MetaMorph Microscopy Automation and Image Analysis Software.

Intestinal epithelial cell isolation and sorting

Small intestine was dissected out of mouse of the appropriate genotype, opened longitudinally, and washed twice with cold HBSS. The tissue was incubated in 5mM EDTA/HBSS for 10 min at 4^0C on a rotating platform and then the villi were scraped off gently using glass cover slip. The intestine was cut into 0.5 cm fragments and placed into 5mM EDTA/HBSS for 30 minutes on ice. Then the tissue fragments were transferred to fresh EDTA/HBSS buffer and vigorously pipetted until the tissue fragments floated. The supernatant was centrifuged at 1500 rpm for 5 minutes to collect crypts. The isolated crypts were incubated in 0.8 mg/ml dispase (gibco) for ten minutes at room temperature and filtered through 100 um and 40 um filters to acquire single cell population of intestinal epithelial cells. For isolating live reserve ISCs for further

analysis using RNA-sequencing, immunoblotting, or immunofluorescence staining, we utilized Fluorescence activated cell sorting(FACS) sorting on BD FACS Aria II or BD FACS Jazz.

Flow cytometry

Single cell suspension was obtained as described above. Frequency of $Lgr5^+$ stem cells was quantified by flow cytometry on cells isolated from *Lgr5-eGFP-IRES-CreER* mice. Frequency of reserve ISCs was quantified by flow cytometry on cells isolated from *Bim1-CreER/Hopx-CreER::Lox-Stop-Lox-tdTomato* mice, 18 hours after tamoxifen injection. 1 µg/ml DAPI was used to exclude dead cells from the quantification of ISCs. EdU incorporation was assessed by intraperitoneal injection of mice with 30 mg/kg EdU 4 hours before tissue harvest, and incorporation was analyzed with Click-it EdU assay kit (Life technologies, C10634) and flow-cytometry. To assess apoptotic cell death, single cell suspension was stained for cleaved Caspase3 using BD Cytofix/Cytoperm kit and cleaved Caspase 3 monoclonal antibody (1:50, Cell Signaling Technology 8788S).

For quiescence (G0) analysis, $tdTomato^+$ cells were sorted by FACS from experimental and control mice into 100% ethanol and placed at 4°C overnight. The cells were then stained with pyronin Y (1 µg/ml) and DAPI (10 µg/ ml) for 30 min before flow cytometric analysis.

Quantitative RT-PCR

1 µg total RNA was used in a 20-µl first-strand cDNA synthesis reaction (Thermo Fisher Scientific). SYBR green quantitative RT-PCR was performed under standard conditions using a QuantStudio 6 Flex (Thermo Fisher Scientific), and data were analyzed using QuantStudio RT-PCR software. Custom primers were validated with standard SYBR green qRT-PCR. Data were normalized to housekeeping gene Gapdh. The following sets of primers were used to assess Msi1 and Msi mRNA expression levels: Msi1, 5′-GCCATG CTGATGTTCGACAA-3′ and 5′-

CTACGATGTCCTCGCTCT CAA-3′; Msi2, 5′-GCGATGCTGATGTTCGACAA-3′ and 5′-TCT CCACAACGTCTTCATTCTCA-3′.

Determination of recombination of Msi1 and Msi2 genes

DNA was extracted from eGFP^{+} dtTomato^{+} sorted cells from *Msi1$^{flox/flox}$- ::Msi2$^{flox/flox}$::Lgr5-EGFP-IRES-CreER::LSl-tdTomato* mice. DNA was resuspended in Tris/EDTA, and the concentration was normalized before PCR. The following sets of forward and reverse primers were used: Msi1 floxed and wild-type, 5′-CGGACTGGGAGAGGTTTCTT-3′ and 5′-AGCTCCCCTGATTCCTGGT-3′; Msi2 floxed and wild-type, 5′- GCTCGGCTGACAAAGAAAGT-3′ and 5′-TCTCCTTGTTGCGCT CAGTA-3′; Msi2 null, 5′-CCTGTCTGGTTGCTTCCTCG-3′ and 5′-GAGCCAACTCGCTAGCTTG-3′. These primers were used to detect wild-type, floxed, and null alleles using Hot Start DNA polymerase (CB4040; Denville Scientific).

RNA-Sequencing

Reserve ISCs were FACS sorted form *Hopx-CreER::LSL-tdTomato* mice under ad libitum or calorie restricted diet, 18 hours after one single dose of Tamoxifen, into TRIzol LS (ThermoFisher). After phase separation using the standard TRIzol LS protocol, the aqueous phase containing RNA was mixed with 70% ethanol and transferred to RNeasy MinElute spin columns (QIAGEN). The cleanup and further concentration of the RNA was done using the standard procedure of RNeasy MinElute Cleanup Kit. The cDNA synthesis was done using SMART-Seq v4 Ultra Low Input RNA Kit for Sequencing (Clontech) and the library was prepared using Nextera XT DNA Library Prep kit (Illumina) and sequenced using Illumina NextSeq 500. Sequencing of mRNA libraries generated 20-40 million high-quality 75-bp reads/sample. Raw sample data were mapped to the mouse reference transcriptome using kallisto and data were analyzed in the statistical computing environment R. RUVseq and edgeR

bioconductor R packages were used for differential gene expression analysis. The effect of calorie restriction was estimated using a paired analysis (ad libitum-calorie restriction) in order to account for isolation, time, and litter dependent differences.

Microarray analysis

Total RNA was isolated from crypts of mouse small intestinal epithelium cells from three control and three *MsiDKO* mice that received five doses of Tamoxifen for five consecutive days 1 week before tissue harvest. Total RNA was isolated using TRIzol Reagent (Thermo Fisher Scientific) according to the manufacturer's instructions. Total RNA was DNase treated with an RNase-free DNase kit (Zymo Research). Purified RNA was submitted to the University of Pennsylvania Molecular Profiling Core, where samples were labeled and hybridized to Affymetrix Mouse Gene 1.0ST arrays. Microarray data were analyzed using Partek Genomics Suite software. After RMA background subtraction and normalization, one-way analysis of variance between controls and MsiDKO was run to compute p-values of significance and F statistic for each probe set. The q value, a measure of false discovery rate (FDR), was computed within the significance analysis of microarrays software for each probe set by running an unpaired t test. The FDR values were integrated with the one-way analysis of variance results. The set of differentially expressed genes were selected as those that were significant at an FDR cutoff of 5% and a p-value of 0.1 and that changed at least 1.5-fold in either direction in the *MsiDKO* group compared with the control group.

Immunoblotting

Isolated crypt cells or FACS sorted reserve ISCs were lysed in ice-cold RIPA buffer (50mM Tris pH8.0, 150mM NaCl, 1% NP40, 0.5% deoxycholate, 0.1% SDS) and one tablet of protease inhibitors (Roche, 11697498001) per 50 ml. The soluble fractions of cell lysates were isolated by centrifugation at 12,000 r.p.m. for 15 min. Proteins extracts were denatured by the

addition of sample buffer, boiled for 5min, resolved by 12% SDS–PAGE, and transferred to PVDF membranes (GE Healthcare). Membranes were blocked in 5% BSA (Sigma) and then incubated with anti- Phospho-S6 Ribosomal Protein primary antibody (1:1000, Cell Signaling, 4858), and beta Actin antibody [AC-15](1:5000, Abcam, Ab6276), followed by incubation with a horseradish peroxidase (HRP) conjugated secondary anti-rabbit (1:2,000, Cell Signaling, 7074) or anti-mouse antibody (1:1000, cell signaling, 7076). Immunoreactive proteins were visualized using LumiGLO chemiluminescent substrate (Pierce).

Organoid culture

For crypt culture, 50 isolated crypts were mixed with 50 µl Matrigel (BD) and plated in 24-well plates. For single cell organoid formation assays, a total of 1,000 *tdTomato*$^{+}$ cells from *Hopx-CreER::tdTomato* mice were sorted into each well of 96-well-plate coated with Matrigel (BD Bioscience) and containing crypt culture medium (Advanced DMEM/F12 containing growth factors (50 ng/ml EGF (Invitrogen), 0.5 µg/ml R-spondin 1 (Wistar Institute protein production facility), 100 ng/ml Noggin (Peprotech) and 3 µM GSK-3 inhibitor (CHIR99021, Stemgent)). Final concentration of 10uM Leucine and Rapamycin was added to culture media for 3 days.

Fluidigm single-cell gene expression

The two-step single-cell gene-expression protocol (advanced development protocol) from Fluidigm was adopted for this study. Briefly, 5 µl of RT Mix Solution which includes 1.2 µl 5× VILO Reaction Mix (Life Technologies; 11754-250), 0.3 µl SUPERase-In (Life Technologies; AM2696), and 0.25 µl 10% NP40 (Thermo Scientific; 28324) was dispensed into each well of 96-well plate. Single cells were sorted into the well directly. The plate was vortexed and immediately frozen on dry ice. For room temperature cycling, the plate was thawed on ice and RNA denatured by incubating at 65°C for 90 s and then chilled on ice for 5 min. Each well was supplemented with 1 µl mixture of 10x SuperScript Enzyme Mix (Life Technologies; 11754-250) and T4 Gene 32

Protein (New England BioLabs; PN M0300S). mRNA was reverse transcribed into cDNA following the thermal cycling conditions below: 25°C, 5 min/50°C, 30 min/55°C, 25 min/60°C, 5 min/70°C, and 10 min. Resulting cDNA was preamplified with 50 nM primer mix for 23 PCR cycles (96°C for 5 s and 60°C for 4 min) and then treated with ExoI for 30 min to remove unincorporated primers. The final product was diluted 1:3 with Tris-EDTA (TE) buffer. For each chip sample inlet, 2.25 µl diluted cDNA, 2.5 µl 2× Sso Fast EvaGreen supermix with low ROX, and 0.25 µl of Fluidigm sample loading agent were added. Individual gene-specific DELTAgene assays were diluted at 1:10 ratios with TE buffer. Two and a half microliters of each primer was then mixed with 2.5 µl assay loading agent inserted into chip "assay" inlets. Chip loading and PCR was performed according to the manufacturer's protocol. The data were analyzed by Fluidigm Gene Expression Analysis Package.

Genes analyzed include: Areg, Ascl2, Atoh1, Axin2, Bmi1, Bmpr1a, Ccnd1, Cdkn1a, Cdx1, Chga, Cubn, Dll4, Dvl2, Efnb1, Epas1, Ephb2, Ereg, Fut2, Gapdh, Gsk3b, Gusb, H6pd, Hes1, Hes5, Hif1a, Hopx, Jag1, Lgr5, Lrig1, Lyz2, Msi1, Msi2, Myb, Myc, Notch1, Numb, Olfm4, Pcna, Ppargc1b, Rhoa, Saa2, Sirt3, Sox9, Tat, Tcf4, Tert, Wnt3, and Wnt6.

Statistical analysis

We performed Shapiro-Wilk test to assess normality and calculated statistical significance using Mann–Whitney for non-normal and student t-test for normal data sets. Error bars reflect standard deviation. For animal studies, samples were only excluded from experiments if animals were considered unhealthy.

CHAPTER 3

Calorie restriction governs intestinal epithelial regeneration through cell autonomous regulation of mTORC1 in reserve stem cells

Introduction

Calorie restriction (CR-receiving fewer calories while maintaining adequate essential nutrients) is one of the most well-established interventions that prolongs life span and retards aging across numerous species, possibly by preserving stem and progenitor cell function, which normally declines with age (Colman et al., 2009; Guarente, 2005; Houthoofd and Vanfleteren, 2006; McCay et al., 1989). Short-term calorie restriction in healthy young animals enhances the recovery from injury in several tissues including skeletal muscle and small intestine (Cerletti et al., 2012; Yilmaz et al., 2012).

In the intestinal epithelium, the most highly proliferative tissue in the body, the existence of both quiescent (residing in outside the cell cycle in G0) and actively cycling intestinal stem cells (ISCs) in the crypts is becoming increasingly clear. Actively proliferating stem cells are located at the base of the crypts (crypt-base columnar stem cells, CBCs), contribute robustly to tissue homeostasis under basal conditions, and exhibit high expression of canonical Wnt pathway target genes including *Lgr5* ($Lgr5^{high}$) (Barker et al., 2007). Extensive research on the effect of calorie restriction on $Lgr5^{high}$ CBCs has demonstrated that CR increases the number of actively cycling $Lgr5^{high}$ CBCs in response to signals sent from adjacent Paneth cells that sense nutrient availability (Igarashi and Guarente, 2016; Yilmaz et al., 2012). However, high Wnt activity in cycling $Lgr5^{high}$ CBCs sensitizes them to DNA damaging injury where they are quantitatively ablated, and the functional contribution of CBCs to the enhanced regenerative response to injury after calorie restriction has never been tested (Tao et al., 2015; Tian et al., 2011). In addition, genetic ablation of Paneth cells has no effect on the regenerative capacity of the epithelium after high-dose radiation injury (Durand et al., 2012). Thus, the specific cell type, and by extension the underlying molecular mechanism, responsible for the enhanced regenerative capacity of the calorie restricted epithelium, remains unknown.

In addition to the $Lgr5^{high}$ CBCs, another population of more radioresistant, slower cycling ISCs has been described in the intestinal crypts, generally referred to as reserve ISCs. Reserve ISCs are located higher in the crypts outside of the Wnt^{High} zone and are highly enriched in

populations marked by *Bmi1-CreER* and *Hopx-CreER* knockin alleles and an *mTERT-CreER* transgene (Montgomery et al., 2011; Takeda et al., 2011; Tian et al., 2011). These cells are also likely represented in populations of cells marked by more broadly expressed reporter alleles (Asfaha et al., 2015; Li et al., 2016a; Powell et al., 2012). Reserve ISCs are more resistant to DNA damage than active CBCs, possibly due to their slower cycling rate, residence in G0, and lack of canonical Wnt pathway activity (Li et al., 2014, 2016c; Yousefi et al., 2016). It is well-established that these cells undergo a robust proliferative response and contribute broadly to regeneration of the intestinal epithelium following DNA damage, particularly high dose (>12Gy) ionizing radiation (Montgomery et al., 2011; Tao et al., 2015; Yan et al., 2012; Yousefi et al., 2016). It is also worth noting here that these reserve ISCs appear to be a distinct population from non-cycling (G1 arrested), label-retaining secretory progenitor cells (Buczacki et al., 2013; Li et al., 2016c)

We investigated the response of reserve ISCs to CR and subsequent DNA damaging injury. We find that the reserve intestinal stem cell compartment expands in response to calorie restriction, contributes robustly to the CR-enhanced regenerative capacity of the epithelium, and is functionally important for optimal regeneration following radiation injury. We demonstrate that tight, cell-autonomous regulation of mechanistic target of Rapamycin complex 1 (mTORC1) signaling in the reserve ISCs of CR mice governs the regenerative response of the epithelium in the face of DNA damage. Our findings provide novel insight into the cell-type specificity of the beneficial effects of calorie restriction and have immediate implications for application of dietary modulation in patients exposed to DNA damaging agents.

Results

Calorie restriction increases reserve ISC availability and tissue regeneration efficiency

To assess the effects of CR on reserve intestinal stem cells, we reduced the caloric intake of mice harboring *Hopx-CreER::Rosa26*$^{LSL\text{-}tdTomato}$ reporter alleles (HT mice) by 40% for a

period of four to six weeks starting at two months of age. Consistent with previous reports (Li et al., 2014; Takeda et al., 2011), we observed that 18 hours following induction of *Hopx-CreER* by Tamoxifen (Tam) injection in HT mice, single reserve ISCs were marked at around +4 position from the crypt base of ad libitum (AL) fed mice. Interestingly, CR dramatically (514%) increased the number of cells marked by *Hopx-CreER* activity in HT mice (Figure 3.1A and 3.1B). To investigate whether the increased number of tdTomato^{+} cells was a result of expanded pool of reserve ISCs or promiscuous activation of the *Hopx* locus, we examined the effect of CR on frequency of reserve ISCs marked with an independent allele, *Bmi1-CreER::Rosa26*$^{LSL\text{-}tdTomato}$ (BT) mice 18 hours after Tam induction. *Bmi1-CreER* and *Hopx-CreER* mark a largely overlapping (60%) population of reserve ISCs, however *Hopx-CreER* marks a more homogenous population relative to *Bmi1-CreER* (Li et al., 2014; Takeda et al., 2011; Tian et al., 2011; Yan et al., 2012). Consistent with this notion, we observed a robust but smaller increase (165%) in the number of cells marked in BT mice indicating that CR expanded the pool of reserve ISCs (Figure 3.1B). Next, we measured proliferation of reserve ISCs following calorie restriction using EdU incorporation assays. Surprisingly, we observed a reduction in proliferation of *Hopx-CreER*$^{+}$ and *Bmi1-CreER*$^{+}$ reserve ISCs, as well as the expected decreased proliferation in bulk intestinal epithelial cells (Figure 3.1C). This indicates that the relative increase in reserve ISCs may be in part due to the decreased overall cellular mass of the calorie restricted tissue (Yilmaz et al., 2012), along with a potential increase in self-renewal versus commitment of these cells under CR conditions.

To assess stem cell activity within the expanded pool of reserve ISCs, we performed lineage tracing experiments in HT mice. Under basal conditions in ad libitum fed mice about 25% of reserve ISCs are in cycle at any given time and give rise to all the cell types in the intestinal epithelium, including CBCs, while the remainder reside in G0 (Figure 3.1D and Li et al., 2014; Sangiorgi and Capecchi, 2008; Takeda et al., 2011; Tian et al., 2011). Considering the 6.14-fold (514% increase) in frequency of *Hopx-CreER*$^{+}$ ISCs and the 75% decrease in their proliferation following a period of CR, we would predict a roughly 1.5 folds increase in lineage tracing events

from these cells. Experimentally, we observed a 1.6-fold increase in tracing events emanating from reserve ISCs (defined as contiguous tdTomotao^{+} ribbons emanating from crypts and passing through the crypt-villus junction into villi) in CR mice relative to AL fed counterparts (Figure 3.1D), confirming the stem cell capacity of the expanded pool of *Hopx-CreER*$^{+}$ cells.

Next, we aimed to assess the functional contribution of CR-induced expansion of reserve ISC pool to the reported enhanced regeneration of the intestinal epithelium upon caloric restriction. We bred the *Rosa26*$^{LSL\text{-}DTA}$ allele (Voehringer et al., 2008) into the *Hopx-CreER* mice (HD mice). In HD mice, a floxed stop cassette prevents expression of the diphtheria toxin fragment A (DTA) such that Tamoxifen injection results in selective ablation of *Hopx-CreER*$^{+}$ cells. After 6 weeks of calorie restriction, we injected 3 doses of Tamoxifen to HD mice and their control counterparts (lacking *Hopx-CreER*), then exposed them to 12 Gy γ-irradiation (γ-IR) 3 days after the last dose of Tamoxifen. We assessed regeneration efficiency by scoring the number of clonal regenerative foci per unit length of the intestine on histological sections. As previously reported (Yilmaz et al., 2012), we observed that calorie restriction enhanced regenerative capacity of the intestinal epithelium following injury relative to AL fed mice. Approximately 40% of this enhanced regenerative capacity was dependent on the presence *Hopx-CreER*$^{+}$ reserve ISCs, emphasizing the functional importance of these cells in mediating beneficial effects of CR (Figure 3.1E). The lack of complete abrogation of CR-enhanced regeneration may be due to effects on CBCs (Igarashi and Guarente, 2016; Yilmaz et al., 2012) as well as incomplete ablation of reserve ISCs due to inefficiencies of the tamoxifen-diphtheria toxin system, or a combination of these.

Calorie restriction downregulates mTORC1 signaling in reserve ISCs

To better understand the mechanisms underlying enhanced tissue regeneration from reserve ISCs following calorie restriction, we performed RNA sequencing on FACS-purified populations of reserve ISCs from control (AL) and CR mice. Gene set enrichment analysis (GSEA) of these transcriptome profiles revealed that genes encoding ribosomal proteins and

involved in translation were contained in the most highly depleted gene sets in reserve ISCs of calorie restricted mice relative to ad libitum fed control counterparts (Figure 3.2A). Ribosome biogenesis is a primary determinant of cellular translational capacity and accordingly has an essential role in the control of cell growth. The mechanistic target of rapamycin complex 1 (mTORC1) is one of the major pathways coupling nutrient availability to the regulation of ribosome biogenesis and has been reported to regulate effects of calorie restriction in a number of somatic tissues (Dibble and Manning, 2013; Igarashi and Guarente, 2016; Powers and Walter, 1999; Yilmaz et al., 2012). Thus, we aimed to assess mTORC1 activity in reserve ISCs following calorie restriction.

We used phosphorylation of ribosomal protein S6 (pS6) by the mTORC1 target S6 Kinase as a readout for mTORC1 activity and, as previously reported (Morley and Traugh, 1990), calorie restriction repressed mTORC1 signaling under basal conditions (Figure 3.2B). A recent study reported that mTORC1 signaling is required during regeneration of the intestinal epithelium after DNA damaging injury, as repression of this pathway leads to failed tissue regeneration (Faller et al., 2015). Interestingly, despite their lower mTORC1 activity under basal conditions, calorie restricted mice were fully capable of robust mTORC1 activation in regenerative foci in response to radiation injury to an extent greater than their ad libitum-fed counterparts (Figure 3.2C). We next confirmed that CR specifically represses mTORC1 in reserve ISCs by quantifying pS6 levels in FACS-sorted *Hopx-CreER*$^{+}$ ISCs from HT mice (Figure 3.2D). We also tested the ability of radiation damage to induce mTORC1 activity in reserve ISCs and, consistent with immunostaining results, found very low levels of pS6 in these cells in their resting, basal state. S6 phosphorylation was markedly induced in reserve ISCs 48 hours after radiation, a time where the first cell divisions are initiated in reserve ISCs after DNA damage-induced cell cycle arrest and repair is completed (Figure 3.2E and Yan et al., 2012). These data led us to hypothesize that dynamic regulation and expanded response range of mTORC1 activity in reserve ISCs in calorie restricted mice is a major contributing factor to the enhanced tissue regeneration observed after caloric restriction.

Precise control of mTORC1 activity is required for efficient tissue regeneration

To further functionally validate our hypothesis, we tested the ability of Leucine, a branched chain amino acid known to be among the most potent nutrient agonists of the mTORC1 complex *in vitro* (Fox et al., 1998), to activate mTORC1 *in vivo*. Western blotting of crypt extracts after 1.5% Leucine administration in the drinking water confirmed the ability of this amino acid to potentiate mTORC1 activity *in vivo* (Figure 3.3A). Next, we assessed the effect of mTORC1 activation by Leucine, as well as mTORC1 inhibition by Rapamycin treatment, on lineage tracing from reserve ISCs 2 weeks after reporter activation in HT mice. Leucine stimulation increased the number of tracing events from reserve ISCs and Rapamycin had the opposite effect, demonstrating the necessity and sufficiency of mTORC1 signaling for activation of reserve ISCs (Figure 3.3B). To assess whether the effect of mTORC1 modulation on reserve ISC activation was cell autonomous, we FACS-purified reserve ISCs and tested the outcome of adding Leucine or Rapamycin to the culture media on intestinal organoid formation from single cells. Consistent with our *in vivo* results, addition of Leucine increased the organoid formation efficiency, while Rapamycin had the opposite effect, indicating that mTORC1 activity regulates reserve ISC activation in a cell-autonomous manner (Figure 3.3C). Interestingly, the repressive effects of Rapamycin were significantly stronger that the inductive effects of Leucine, possibly due to the presence of high levels of potent ISC mitogens and known mTORC1 agonists in the culture media, including Wnt, Notch, and EGF ligands, as well as BMP antagonists, resulting in high basal levels of organoid formation in these cultures.

To further confirm the cell-autonomous effect of modulation of mTORC1 on activation of reserve ISCs *in vivo*, we utilized mouse models to genetically activate mTORC1 specifically in *Hopx-CreER*$^{+}$ reserve ISCs. We bred the *Hopx-CreER::Rosa26*$^{LSL\text{-}tdTomato}$ reporter alleles into mice harboring floxed alleles of *Tsc1* (*Tsc1*$^{flox/flox}$*::Hopx-CreER::Rosa26*$^{LSL\text{-}tdTomato}$, THT mice) (Kwiatkowski et al., 2002). Consistent with our results using Leucine, we observed increases in lineage tracing events from reserve ISCs of THT mice 2 weeks after *Hopx-CreER* induction of reporter activity/*Tsc1* deletion (Figure 3.3D). Conversely, inhibition of mTORC1 activity in reserve

ISCs via Raptor inactivation in *Raptor*$^{flox/flox}$*::Hopx-CreER::Rosa26*$^{LSL\text{-}tdTomato}$ (RHT) mice abrogated regeneration 3 days after radiation injury (Figure 3.3E) confirming the functional importance of mTORC1-mediated regulation of reserve ISC activity in tissue regeneration.

mTORC1 modulation regulates the intestinal response to high dose γ-IR Injury

Finally, we asked whether inhibition of mTORC1 in reserve ISCs, as we observed in CR mice, has a radioprotective role at the time of injury. We assessed apoptotic cell death in reserve ISCs of mice that were treated with either Leucine or Rapamycin beginning 3 days prior to radiation exposure. Interestingly, inhibition of mTORC1 signaling prior to injury protected reserve ISCs against apoptosis, while stimulation of mTORC1 during this same period sensitized reserve ISCs to ionizing radiation (Figure 3.4A). We then assessed the effect of modulation of mTORC1 prior to ionizing radiation exposure on the subsequent regenerative response. To this end, we activated mTORC1 signaling through administration of Leucine in drinking water starting 3 days prior to radiation injury and observed that premature activation of mTORC1 signaling impaired the epithelial regenerative response (Figure 3.4B).

Taken together, our findings demonstrate that reserve intestinal stem cell-autonomous activity of mTORC1 plays a significant functional role in governing the regenerative response of the epithelium to DNA damaging injury and contributes to the beneficial effects of calorie restriction.

Discussion

There has been considerable interest in gaining a better understanding of the cellular basis underlying regeneration of the intestinal epithelium following DNA damage by radiation exposure, chemotherapy, microbiome dysbiosis, and ischemia-reperfusion injury, not only to enable strategies to targeting these cells to enhance regeneration, but also because of the apparent parallels between intestinal regeneration and oncogenic transformation.

Previous studies reported that calorie restriction improves regeneration of the intestinal epithelium following high dose γ-IR through a non-cell autonomous effect on actively cycling CBCs mediated by Paneth cells intercalated between CBCs (Yilmaz et al., 2012). Given that $Wnt^{High}/Lgr5^{High}$ CBCs are quantitatively ablated by high dose γ-irradiation and that regeneration following radiation injury is mostly driven by surviving $Wnt^{Low/Off}$ cells, the beneficial effects of calorie restriction are likely not limited to active Lgr5 CBCs and may rather reflect the activity of additional stem cell populations (Asfaha et al., 2015; Tao et al., 2015; Yan et al., 2012). This notion is further supported by recent data that Paneth cells, purported to be the niche for CBCs responsible for governing their activity, are actually dispensable for CBC function and for epithelial regeneration in response to high dose radiation injury(Durand et al., 2012; Kabiri et al., 2014b; Kim et al., 2012; San Roman et al., 2014).

Here, we show that radioresistant ISCs within *Hopx-CreER*-marked populations functionally contribute to the enhanced regenerative outcome following DNA damaging injury in CR mice. We demonstrate that calorie restriction suppresses mTORC1 signaling in these reserve ISCs and this, in turn, protects reserve ISCs against radiation injury. However, we and others have shown that potent activation of mTORC1 signaling and metabolic pathways are also required during regeneration following injury. Interestingly, despite the repression of mTORC1 in calorie restricted mice, the epithelium maintained the ability not only to activate mTORC1 in response to injury, but did so to an extent greater than that seen with ad libitum-fed animals. Curiously a similar phenomenon has been observed in the context of fasting, where Pten inactivation through phosphorylation poises reserve ISCs to contribute to epithelial regeneration upon feeding(Richmond et al., 2015).

Ultimately, our findings emphasize the significance of precisely governed mTORC1 activity in protecting stem cells against injury and driving them to expand and repopulate the tissue when called upon. The discovery of the role of mTORC1 signaling in controlling reserve intestinal stem cell activity provides a framework for future studies aimed at the development of pharmacological or dietary interventions that delay ISC activation in an effort to protect patients

against acute side effects of radiation therapy and radiation-induced acute gastrointestinal syndrome.

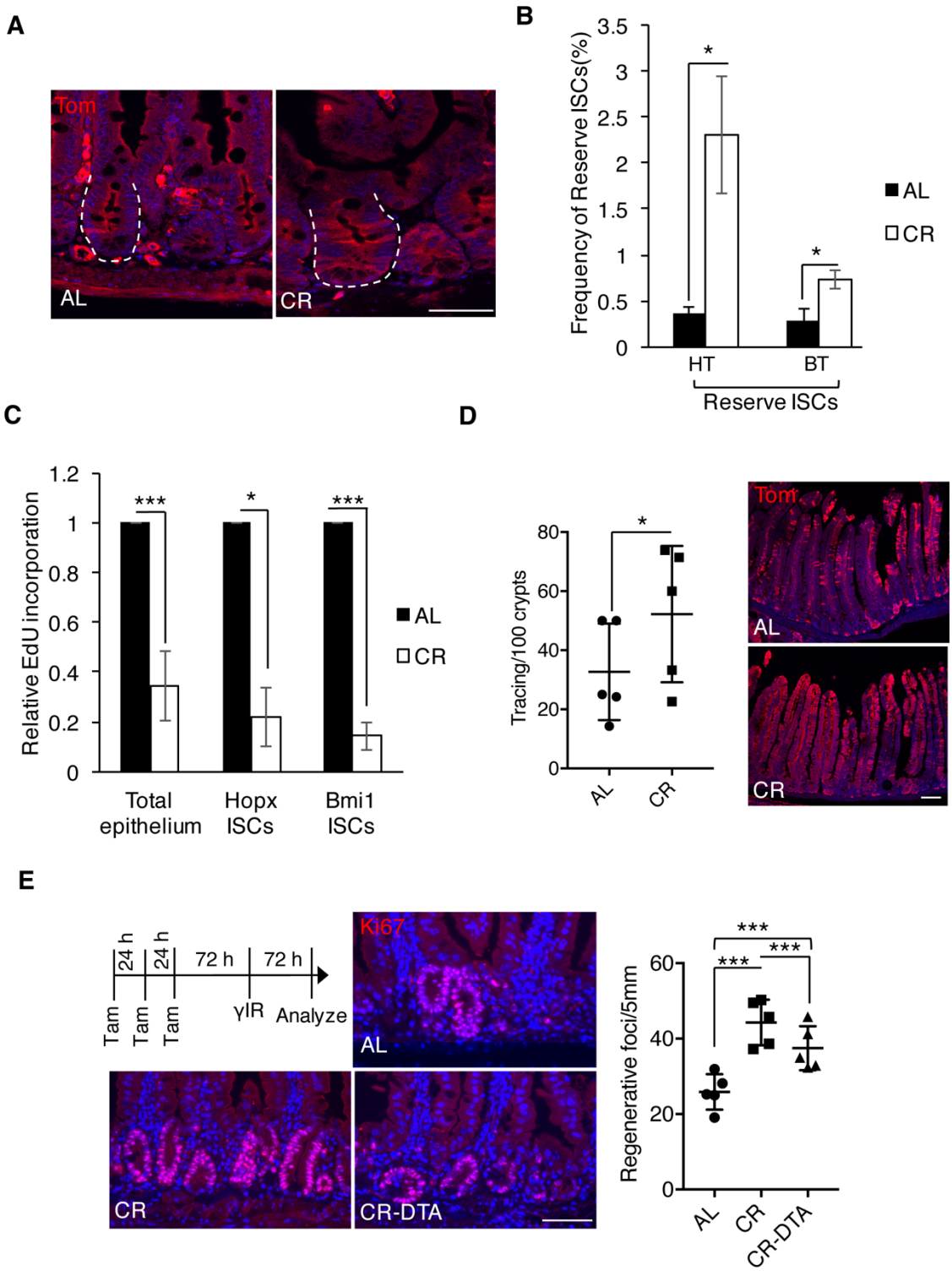

Figure 3. 1. Calorie restriction expands the pool of radioresistant reserve intestinal stem cells

Figure 3.1. Calorie restriction expands the pool of radioresistant reserve intestinal stem cells

(A) Immunofluorescence staining for tdTomato (red) on jejunal sections from *Hopx-CreER::LSL-tdTomato* ad libitum(AL) and calorie restricted(CR) mice 18 hours after a single Tamoxifen injection. Epithelial crypts are outlined by a white dash line. Scale bar=50 μm

(B) Analysis of frequency of reserve ISCs in CR and AL *Hopx-CreER::LSL-tdTomato* and *Bmi1-CreER::LSL-tdTomato* mice using flow-cytometry, 18 hours after Tamoxifen injection (n=4-6 for each condition, * $p<0.05$).

(C) Analysis of EdU incorporation in reserve ISCs and crypt cells of AL and CR *Hopx-CreER::LSL-tdTomato* and *Bmi1-CreER::LSL-tdTomato* mice using flow-cytometry, 18 hours after Tamoxifen and 4 hours after EdU injections. The proliferation of CR groups is normalized to their control AL counterparts (n=4-6 for each condition, * $p<0.05$ and *** $p<0.0005$).

(D) Immunofluorescence staining for tdTomato (red) and quantification of lineage tracing events (ribbons of tdTomato$^+$ cells with contiguous tracing from crypts, through crypt-villus junction, and into villi) from *Hopx-CreER*$^+$ ISCs 14 days after marking reserve ISCs with a single Tamoxifen injection to *Hopx-CreER::LSL-tdTomato* mice under AL and CR diets (n=4-6 for each condition, *$p<0.05$, scale bar= 100 μm).

(E) Representative Ki67(red)-stained sections from jejunum of irradiated *Hopx-CreER::LSL-DTA* and their control counterparts *(LSL-DTA)* mice after 6 weeks of receiving CR or AL diet and quantification of number of proliferative crypt foci per unit length of small intestine. All groups of mice were given 3 daily consecutive doses of Tamoxifen and were exposed to 12Gy γ-IR 3 days after the last dose of Tamoxifen. Tissue was harvested 3 days after γ-IR (n=5 for each condition, ***$p<0.0005$, scale bar=100 μm).

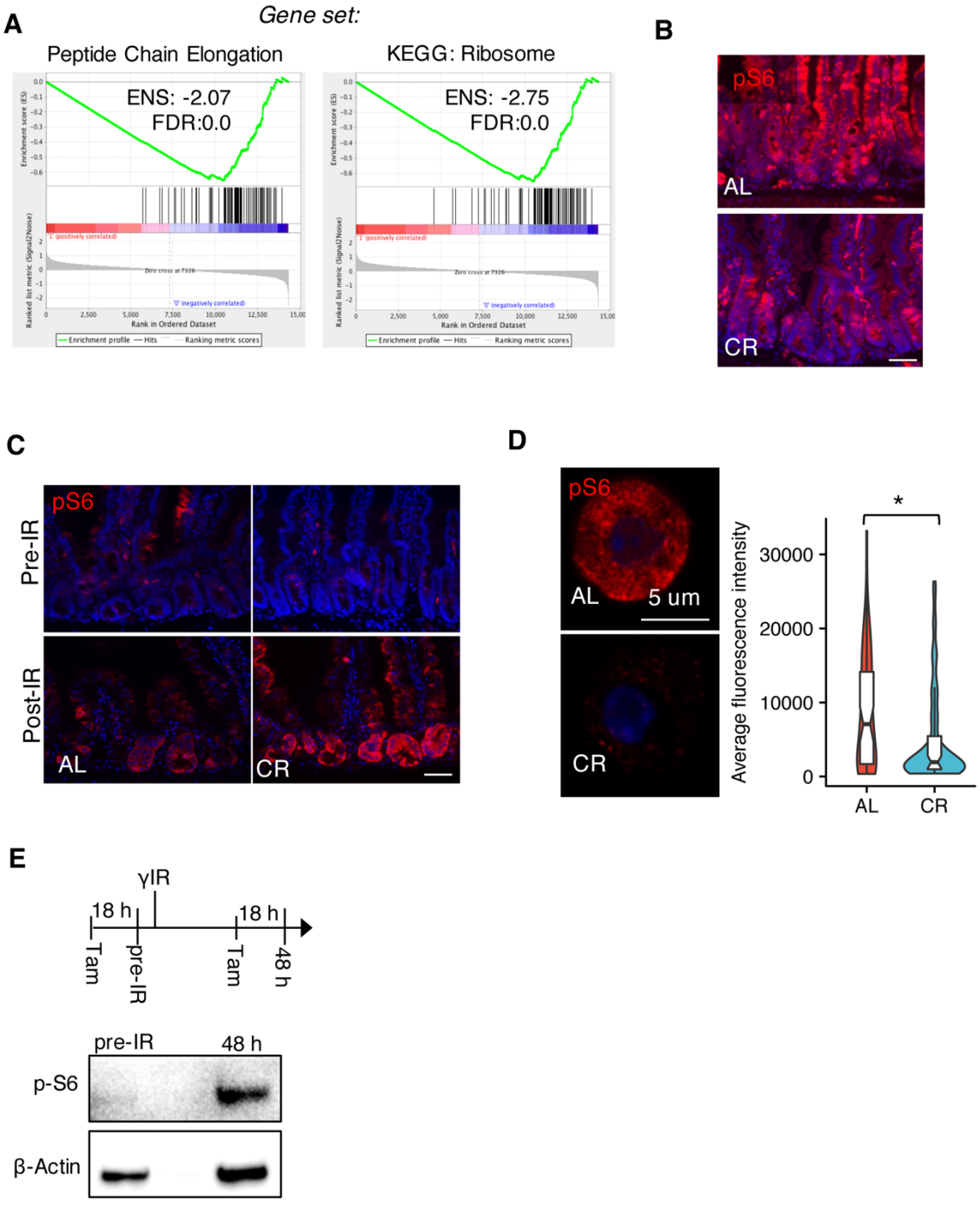

Figure 3. 2. mTORC1 activity is precisely regulated during the regenerative response of the intestinal epithelium following radiation injury

Figure 3.2. mTORC1 activity is precisely regulated during the regenerative response of the intestinal epithelium following radiation injury

(A) Gene set enrichment analysis (GSEA) of the *Hopx-CreER*$^{+}$ ISCs isolated from CR mice and AL mice.

(B and C) Immunofluorescence staining for pS6 (red) in the jejunum of CR and AL mice under basal conditions (pre-IR) and 3 days after radiation injury. The exposure time in figure 3.2 B is higher (5 seconds) that those in 3.2 C (1 second) in order to clearly highlight differences in pS6 levels under basal conditions. scale bar=50 μm

(D) Immunofluorescence staining for pS6 and quantification of pS6 fluorescence intensity in reserve ISCs from *Hopx-CreER::LSL-tdTomato* AL and CR mice, 18 hours after Tamoxifen induction. (n=30-40 ISCs from each of 2 mice in each group, **$p<0.05$, scale bar=5 μM).

(E) Western blot analysis for pS6 in 21,000 FACS-purified reserve stem cells from *Hopx-CreER::LSL-tdTomato* mice under basal conditions and 48 hours after irradiation injury. Both groups were given Tamoxifen 18 hours before tissue harvest.

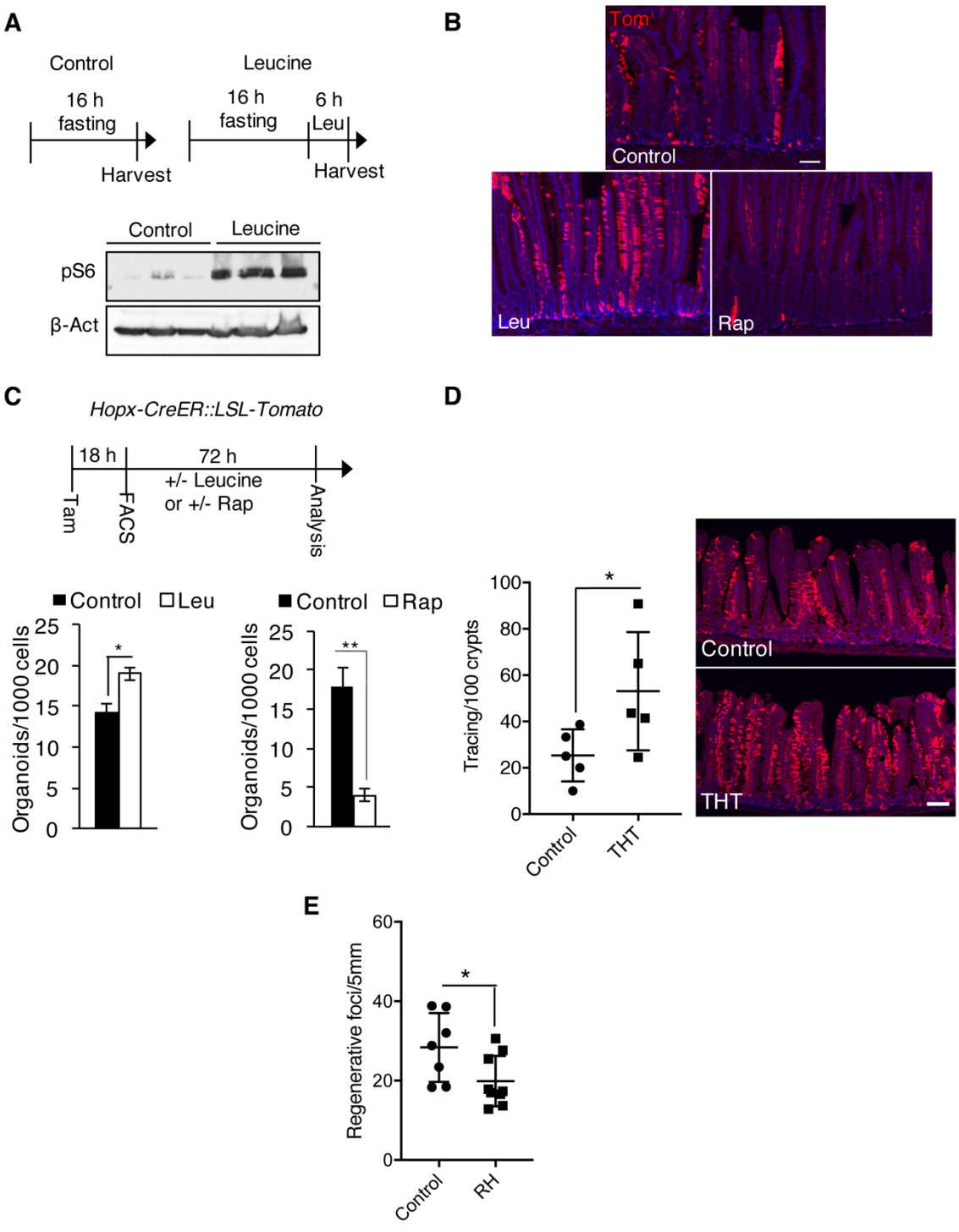

Figure 3. 3. mTORC1 modulates activation of reserve ISCs in a cell-autonomous manner

Figure 3.3. mTORC1 modulates activation of reserve ISCs in a cell-autonomous manner

(A) Western blot analysis for pS6 in protein extracted from the intestinal epithelium of a cohort of mice that were fasted for 16 hours and then divided into two groups. One group was harvested after fasting and the other group received 1.5% Leucine in the drinking water for 6 hours following fasting (n=3).

(B) Lineage tracing from *Hopx-CreER*$^{+}$ ISCs using immunofluorescence staining for tdTomato in sections from *Hopx-CreER::LSL-tdTomato and* control mice 2 weeks after Tamoxifen treatment (Scale bar =50μM). Rapamycin and Leucine treatments started 3 days before Tamoxifen injection and continued until time of harvest (n=2, scale bar= 100 um).

(C) Organoid formation assays from single FACS-purified *Hopx-CreER*$^{+}$ ISCs from *Hopx-CreER::LSL-tdTomato* mice that received one dose of Tamoxifen 18 hours before tissue harvest. Sorted cells were treated with 10 uM Leucine or Rapamycin for 72 hours in culture (n=2, * $p<0.05$ and ** $p<0.005$).

(D) Lineage tracing from reserve ISCs in *Hopx-CreER::Tsc1*$^{flox/flox}$*::LSL-tdTomato (THT)* mice visualized with immunofluorescence staining for tdTomato in jejunal sections 2 weeks after Tamoxifen treatment (n= 5, *$p<0.05$, scale bar =100μm).

(E) Quantification of regeneration efficiency of *Raptor*$^{flox/flox}$*::Hopx-CreER (RH)* and control mice following 12 Gy γ-IR. All groups received 3 consecutive doses of Tamoxifen and were irradiated 3 days after the last dose. Tissue was harvested 3 days after γ-IR (n=7, *$p<0.05$).

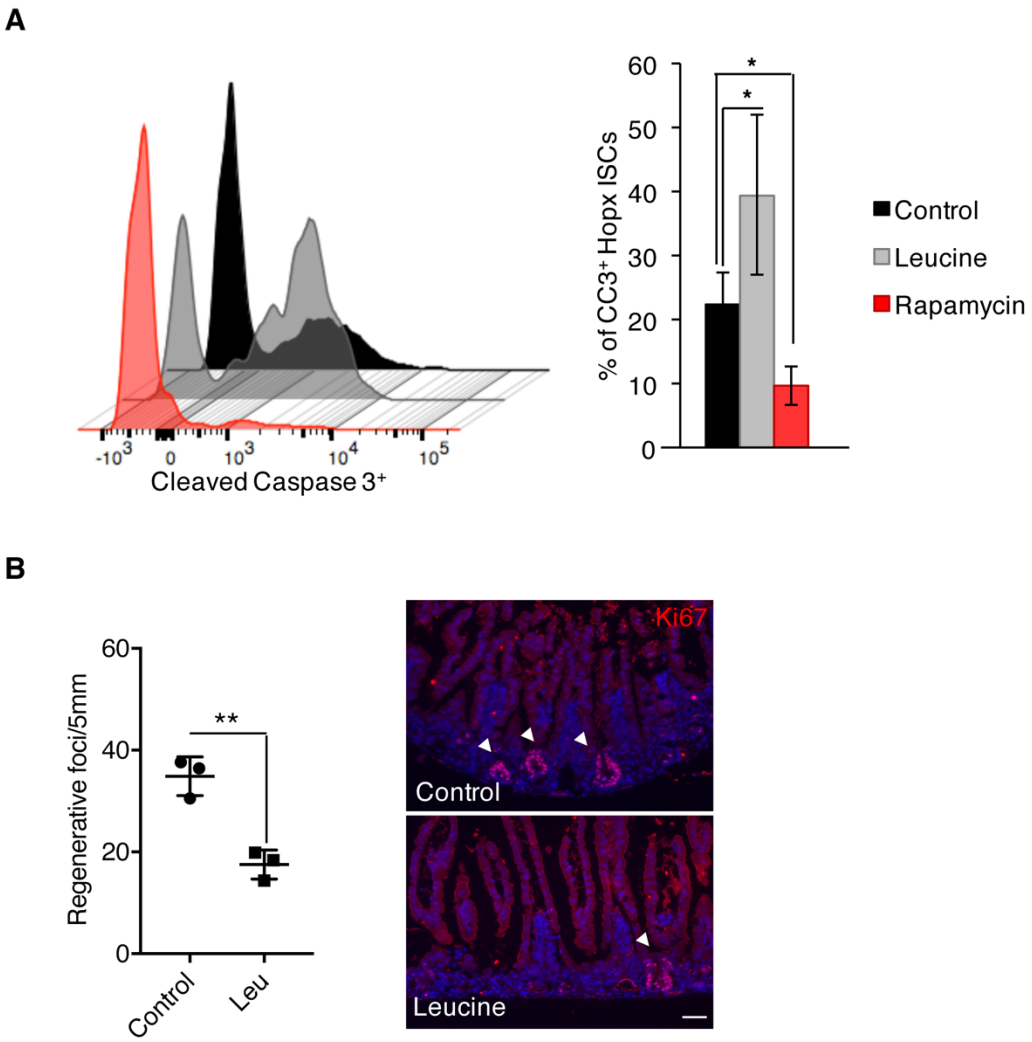

Figure 3. 4. Premature activation of mTORC1 sensitizes reserve ISCs to radiation injury and results in regeneration failure

Figure 3.4. Premature activation of mTORC1 sensitizes reserve ISCs to radiation injury and results in regeneration failure

(A) Flow-cytometric analysis of apoptosis in reserve ISCs from *Hopx-CreER::LSL-tdTomato* mice by staining for cleaved Caspase 3, two hours after 12 Gy γ-IR. Rapamycin and Leucine treatments were started 3 days before the time of harvest, and all group were given a single Tamoxifen dose 18 hours prior to tissue harvest (n=2-7, *p<0.05).

(B) Ki67 (red) staining and quantification of the regeneration efficiency after irradiation injury in mice receiving 1.5% Leucine in their drinking water 3 days before γ-IR and control groups. Arrowheads indicate regenerative crypt foci (n=3, **p<0.005, scale bar= 50 um).

CHAPTER 4

Msi RNA binding proteins control reserve intestinal stem cell quiescence

Introduction

Radiation-induced acute gastrointestinal syndrome is caused when the body is exposed to high doses of penetrating radiation (usually 10Gy or higher). Mortality rates are high in these instances, as destructive damage in the gastrointestinal (GI) tract results in electrolyte imbalance and rapid dehydration. The molecular determinants of intestinal radiosensitivity and GI syndrome are poorly understood. Intestinal stem cells (ISCs), which are crucial for physiological tissue homeostasis and regeneration after injury, are thought to play a critical role in this process (Ch'ang et al., 2005; Potten, 2004).

Crypt base columnar (CBC) cells are highly proliferative stem cells that reside at the base of intestinal crypts. CBCs are characterized by high activity of the canonical Wnt pathway, and activity of the Wnt target gene *Lgr5* is commonly used for their identification and prospective isolation (Barker et al., 2009; Cheng and Leblond, 1974). While CBCs are widely believed to maintain the daily proliferative burden of the high-turnover epithelium, they are sensitive to DNA damage-causing agents such as high dose gamma-irradiation (γ-IR), and several independent studies demonstrated that CBCs are largely ablated following γ-IR (Asfaha et al., 2015; Metcalfe et al., 2014; Yan et al., 2012). Recently, Tao et al. showed that high Wnt pathway activity and basal crypt positioning sensitize CBCs to DNA damage, leading to their preferential depletion (Tao et al., 2015). Interestingly, this study also characterized a population of $Wnt^{low}/Lgr5^{low}$ cells above the crypt base that appear more radioresistant, raising the possibility that the Lgr5-marked population is heterogeneous, and that $Lgr5^{low}$ cells may contribute to regeneration following irradiation. Another study showed that ablation of Lgr5-expressing cells by virtue of a diphtheria toxin receptor inserted into the endogenous *Lgr5* locus activated shortly before (or after) administration of high dose radiation impairs the regeneration efficiency of the epithelium, suggesting a contribution from $Lgr5^{+}$ cells to regeneration after radiation injury, although the timing of diphtheria toxin administration make it difficult to dissect the contribution of radio-resistant versus *de novo*-generated $Lgr5^{+}$ cells to the regenerative process (Metcalfe et al., 2014).

Despite the loss of the vast majority of Wnt^{high} CBCs after high-dose γ-IR, regenerative crypt foci begin appearing approximately 2-3 days after γ-IR exposure and fully repair the epithelium within approximately 5 days. This regeneration is driven by a population of radioresistant stem cells with little to no canonical Wnt pathway activity (referred to hereafter as "reserve ISCs"). At least some of these reserve ISCs can be marked by *CreER* reporter genes targeted to the endogenous *Bmi1* and *Hopx* loci(Li et al., 2014; Sangiorgi and Capecchi, 2008; Takeda et al., 2011; Yan et al., 2012), however recent evidence also suggests that more differentiated cells may also act as facultative stem cells upon ablation of CBCs (Tetteh et al., 2016). Despite the lack of consensus on the precise population(s) contributing to regeneration after injury, clear evidence demonstrates that under basal conditions in the absence of injury *Bmi1-/Hopx-CreER*-marked reserve ISCs give rise to CBCs. Lineage tracing coupled with single cell gene expression profiling reveals that *Bmi1-/Hopx-CreER* alleles mark a largely overlapping population of Wnt^{off} reserve ISCs that give rise to active, Wnt^{high} $Lgr5^{+}$ CBCs upon division, and consequently all functional cell types of the epithelium over long periods of time (Li et al., 2014; Takeda et al., 2011; Tian et al., 2011; Yan et al., 2012). Unlike $Lgr5^{+}$ CBCs, the population of reserve ISCs is largely quiescent (in G0 and metabolically inactive) rather than activated (metabolically active and within the cell cycle) (Li et al., 2016c). It has been postulated that the low metabolic activity of quiescent stem cells discourages genetic lesions induced by reactive oxygen species (Pazhanisamy, 2009). However, knowledge of the molecular mechanisms governing their radioresistance and subsequent exit from the quiescent state in response to γ-IR injury is lacking.

Musashi (Msi) RNA-binding proteins are expressed in the stem cell compartments of several tissues including the brain, intestine, and blood, and are upregulated in cancers arising from these tissues (Li et al., 2015; Park et al., 2014; Wang et al., 2015). Msi proteins act primarily as translational regulators binding to messenger RNAs, and known target transcripts are involved in the regulation of cell cycle progression, metabolism, and stem cell self-renewal (Li et al., 2015; Park et al., 2014; Wang et al., 2015). In the hematopoietic system, Msi2 is an important

modulator of long-term hematopoietic stem cell (LT-HSC) proliferation and self-renewal (Hope et al., 2010; Ito et al., 2010; Kharas et al., 2010; Park et al., 2014). Ectopic induction of Msi2 increases LT-HSC numbers, which is associated with a reduction in stem cell quiescence and a concomitant increase in the percentage of actively cycling LT-HSCs (Kharas et al., 2010). Conversely, *Msi2* deletion results in loss of engraftment potential of LT-HSCs in transplantation assays, demonstrating the importance of Msi2 in this largely dormant stem cell population (Park et al., 2014).

In the intestinal epithelium, Msi proteins are expressed throughout the crypt, including in the active CBC stem cell compartment (Itzkovitz et al., 2011; Li et al., 2014, 2015; Wang et al., 2015). We have previously established that Msi proteins are obligate and functionally redundant intestinal oncoproteins that drive epithelial transformation in large part through inhibition of intestinal tumor suppressors including Pten resulting in downstream mTORC1 complex activation (Li et al., 2015; Wang et al., 2015); however, their role in intestinal homeostasis, regeneration, and stem cell self-renewal *in vivo* is entirely unknown.

Here, we establish that Msi proteins are dispensable for the Wnt-driven self-renewal of CBCs, but are required for cell cycle entry of quiescent reserve ISCs. Msi upregulation in reserve ISCs is sufficient to induce expression of metabolic genes including *Myc*, *H6pd*, and *Hif1α* and drive exit of reserve ISCs from G0 and into the cell cycle. Conversely, genetic ablation of *Msi* genes abrogates cell cycle entry. This manifests phenotypically in the failure of epithelial regeneration in response to injury. Further, we demonstrate that Msi expression must be tightly regulated in quiescent ISCs, as premature Msi induction prior to γ-irradiation injury sensitizes the intestinal epithelium to injury and impairs regenerative capacity. This emphasizes the importance of maintaining a pool of quiescent stem cells in order for the tissue to mount an effective injury response.

Results

Msi activity is dispensable for intestinal homeostasis, Wnt pathway activity, and CBC function under basal conditions

We initially confirmed published reports of Msi expression in the intestinal crypt, where Msi1 and Msi2 are expressed in CBCs and in the transit-amplifying zone (Figure 4.1A and (Li et al., 2015)). To unequivocally test the functional contribution of Msi proteins to intestinal homeostasis and stem cell self-renewal, we intercrossed *Msi1* and *Msi2* conditional knockout alleles previously generated in our laboratory (Katz et al., 2014; Li et al., 2015; Park et al., 2014; Wang et al., 2015) with mice harboring a *Villin-CreER* transgene that drives robust, inducible recombination throughout all epithelial cells in the small intestine and colon (Li et al., 2015; el Marjou et al., 2004). Ablation of either *Msi1* or *Msi2* individually throughout the intestinal epithelium and colon had no effect on tissue homeostasis, proliferation, or differentiation (not shown), consistent with published studies demonstrating their functional redundancy (Li et al., 2015; Sakakibara et al., 2002).

We therefore examined the consequences of concomitant ablation of both *Msi1* and *Msi2* in *Msi1*$^{flox/flox}$*::Msi2*$^{flox/flox}$*::Villin-CreER* double knockout (*MsiDKO*) mice. We followed *MsiDKO* mice for one week and up to 6 months after deletion and, surprisingly, observed no overt phenotypic changes to intestinal crypt-villus architecture (Figure 4.1B) or alteration in proliferation (Figure 4.1C, 4.2A) or differentiation based on the frequency of Paneth and Goblet cells (Figure 4.2B, C). We also examined the colon in *MsiDKO* and control mice and similarly observed no phenotypic changes (Figure 4.3A, B) or alteration in proliferation (Figure 4.3C).

Transcriptome profiles from the crypts of control and *MsiDKO* mice 1 week after *Msi* deletion with *Villin-CreER* showed little differential gene expression, consistent with the phenotypic analysis. The few genes with significant changes in expression (fold change ≥1.5, p-value ≤ 0.1) were not enriched for any specific functional ontology (Table 4.1). Importantly, loss of Msi activity had no deleterious consequences for expression of Wnt pathway target genes, which

are critical for proper intestinal homeostasis and CBC proliferation (Figure 4.1D). In addition, ablation of *Msi1*, *Msi2,* or both had no effect on nuclear localization of the Wnt transcriptional effector β-catenin in cells at the crypt base (Figure 4.3D). Further, we were able to generate *Msi*-null crypt organoids *in vitro* and passage them serially with no decrease in organoid forming efficiency or detectable increase in *Msi* expression expected to result from selective pressure if rare cells escaping recombination had a growth advantage (Figure4.1E and 4.3E). There was also no difference in organoid formation efficiency between *MsiDKO* and control crypts at any R-spondin concentration tested in the absence of GSK-3 inhibitor (Figure 4.1E). These findings demonstrate that Msi does not support activity of the canonical Wnt pathway, and this is in contrast to *in vitro* studies and *in vivo* gain of function assays suggesting that Msi potentiates activity of this pathway.

Ultimately, we tested the effects of Msi loss on the activity of CBCs marked by an *Lgr5-eGFP-CreER* reporter allele (Barker et al., 2007). Msi loss had no effect on the frequency or proliferation of CBCs (Figure 4.3F, G). In addition, lineage tracing in *Lgr5-eGFP-CreER::Msi1*$^{flox/flox}$*::Msi2*$^{flox/flox}$*::R26-Lox-Stop-Lox-tdTomato* or control (*Lgr5-eGFP-CreER::R26-Lox-Stop-Lox-tdTomato)* mice demonstrates that Msi loss has no detrimental consequences for CBC stem cell activity *in vivo*, either in the small intestine or colon (Figure 4.1F, 4.3H). We confirmed efficient deletion of *Msi1/2* in Lgr5^{+} ISCs and their progeny (Figure 4.3I, J).

Taken together, these findings demonstrate that Msi loss has no effect on the activity of the canonical Wnt pathway or the proliferative self-renewal of crypt base columnar stem cells.

Msi proteins are required for intestinal regeneration following radiation injury

Given prior findings demonstrating that Msi1/2 activity potentiates the activity of the mTORC1 complex in colorectal cancer (Li et al., 2015; Wang et al., 2015) and that mTORC1 is similarly dispensable for intestinal homeostasis, but is required for epithelial regeneration in response to injury (Ashton et al., 2010; Faller et al., 2015), we next sought to determine how Msi

loss affects intestinal regeneration in response to radiation injury. *Msi1*$^{flox/flox}$*::Msi2*$^{flox/flox}$*::Villin-CreER* or control *Msi1*$^{flox/flox}$*::Msi2*$^{flox/flox}$ mice were treated with 5 daily doses of Tamoxifen, and subjected to 12 Gy of ionizing gamma-irradiation (γ-IR) one week later to ablate proliferative cells including CBCs (Tao et al., 2015; Tian et al., 2011). In this context, intestinal regeneration (quantified by the number of clonal regenerative crypt foci per unit length, 72 hours after injury) was severely compromised in the absence of Msi activity (Figure 4.4A, 4.5A). No differences in the distribution of residual differentiated cell types were observed (Figure 4.5B, C). Any regenerative crypt foci observed in *Msi1*$^{flox/flox}$*::Msi2*$^{flox/flox}$*::Villin-CreER* mice were found to have escaped recombination at one or more of the floxed *Msi* alleles (Figure 4.4B). These data demonstrate that Msi activity is necessary for regeneration of the epithelium

Recent studies indicate that the regenerative capacity of the epithelium in response to such high-dose γ-IR resides in a population of reserve intestinal ISCs that are marked, at least in part, by *Hopx-CreER* or *Bmi1-CreER* alleles (and possibly by other proxy reporter alleles) (Asfaha et al., 2015; Metcalfe et al., 2014; Montgomery et al., 2011; Takeda et al., 2011; Yan et al., 2012). *Bmi1-* or *Hopx-CreER* reporters are known to mark a largely overlapping population of rare reserve ISCs (although the *Hopx-CreER* population is more homogenous) (Li et al., 2014). We next asked, therefore, whether *Msi* ablation *specifically* in this rare reserve ISC population could account for the failed regenerative response we observed after *Msi* ablation throughout the epithelium using *Villin-CreER.* To address this, we crossed the *Hopx-CreER* allele into the *Msi1*$^{flox/flox}$*::Msi2*$^{flox/flox}$ mice and assessed regeneration of intestinal epithelium after deletion of Msi using *Villin-CreER, Hopx-CreER* or *Lgr5-CreER* and exposure to 12Gy γ-IR. Msi ablation with *Lgr5-CreER* had no significant effect on regeneration, although a modest, non-significant decrease in regeneration was observed, possibly reflecting the function of an *Lgr5*^{Low} cell previously described as radioresistant (Tao et al., 2015). In contrast, *Msi* loss in rare *Hopx-CreER* reserve ISCs (making up less than 0.5% of the crypt epithelium (Li et al., 2014; Takeda et al., 2011)), and some of their immediate progeny (as some reserve ISCs must divide during the time required for multiple Tamoxifen injections prior to irradiation) resulted in failed epithelial

regeneration to an extent indistinguishable from that observed with pan-epithelial *Villin-CreER* deletion, highlighting the importance of these rare reserve ISCs in the regenerative response of the intestinal epithelium (Figure 4.4C).

Msi activity selectively governs reserve stem cell proliferation

While these findings demonstrate that *Hopx-/Bmi1-CreER* reserve ISCs are important for epithelial regeneration after injury, recent data also suggests that the more differentiated progeny of *Lgr5*$^{+}$ CBCs can revert to the CBC state and reacquire stem cell activity after CBC ablation with diphtheria toxin (Tetteh et al., 2016). Under basal, non-injury conditions, *Hopx-/Bmi1-CreER* ISCs are known to give rise to *Lgr5*$^{+}$ CBCs upon division (Li et al., 2014; Takeda et al., 2011; Tian et al., 2011). We thus sought to examine if Msi plays an important role in the activation of these reserve ISCs during basal homeostasis. We initially performed single cell gene expression analysis in *Lgr5*$^{+}$ CBCs, in reserve ISCs, and in the progeny of reserve ISCs after 4 days of lineage tracing. As predicted, in the resting state reserve ISCs marked by *Hopx-/Bmi-CreER::R26-Lox-Stop-Lox-tdTomato* reporter activity 18 hours after a single Tamoxifen dose (Li et al., 2014; Takeda et al., 2011) express low levels of *Msi* genes and exist in a Wnt$^{Off/Low}$ state, with little to no expression of canonical Wnt targets such as *Lgr5*, *Ascl2* and *Ccnd1* along with high levels of the cell cycle inhibitor *Cdkn1a*, in stark contrast to CBCs (Figure 4.6A, B). Four days after initiation of lineage tracing (a time point at which about half of reserve ISCs have divided to form clusters of 2 or more daughter cells (Li et al., 2014; Takeda et al., 2011)), reserve ISC progeny began activating *Msi* genes and canonical Wnt target genes (Figure 4.6B). These data further suggest that Msi activity plays a role in promoting reserve ISC cell cycle entry.

To test this definitively, we examined lineage tracing from control mice (*Hopx-/Bmi1-CreER::R26-Lox-Stop-Lox-tdTomato)* or mice in which Msi activity is ablated specifically in reserve ISCs (*Msi1*$^{flox/flox}$*::Msi2*$^{flox/flox}$*::Hopx-/Bmi1-CreER::R26-Lox-Stop-Lox-tdTomato*). As predicted based on previous reports and single cell gene expression analysis (Figure 4.6B),

reserve ISCs in control mice gave rise to clonal lineage tracing events that encompassed the entire crypt-villus axis after 14 days. In contrast, Msi loss abrogated lineage tracing from reserve ISCs, and these cells remained as single labeled cells within intestinal crypts 14 days after initiation of tracing (Figure 4.6C, arrowheads). Thus, these findings demonstrate that Msi activity is required for reserve ISC activation under basal homeostatic conditions where these cells normally generate CBCs.

Reserve ISCs represent a quiescent stem cell pool residing in G0 and require Msi activity for S-phase entry

Recent findings that high Wnt pathway activity and cell cycling render CBCs susceptible to DNA damage (Tao et al., 2015) support a model in which a more dormant pool of reserve stem cells remains injury-resistant to regenerate the epithelium after damage. These reserve stem cells are often referred to as quiescent (i.e., residing in the G0 state outside of the cell cycle). We therefore sought to characterize quiescence in reserve ISCs. In stem cell biology, quiescence usually refers to cells with a dormant genome and low metabolic activity, reflected by low RNA levels in a diploid cell (G0), rather than simply the absence of cycling, which can also result from G1 arrest (Fukada et al., 2007; Hüttmann et al., 2001). We first examined reserve ISC populations marked by *Hopx-/Bmi1-CreER::R26-Lox-Stop-Lox-tdTomato* and found that the majority of these populations reside in G0 (Figure 4.7A). Exposure of these mice to 12 Gy γ-IR resulted in an exit of reserve ISCs from G0 and into the cell cycle concomitant to an increase in Msi (Figure 4.7B, C and 4.8A, B), consistent with the previous functional demonstration that Msi activity in these cells is important for effective regeneration. We next asked how Msi loss affected the quiescent status of the reserve ISC compartment. Interestingly, ablation of Msi in reserve ISCs resulted in a G1, not G0 arrest (Figure 4.7D). Further, these cells were no longer able to enter S-phase and incorporate EdU in response to 12 Gy γ-IR (Figure 4.7D, E). Interestingly, these findings are consistent with previous studies on the mTORC1 complex, inactivation of

which similarly results in a G1 arrest (Kalaitzidis et al., 2012) as well as a failure of the intestinal epithelium to regenerate in response to high dose γ-IR injury (Ashton et al., 2010; Faller et al., 2015).

Taken together, the findings thus far demonstrate that reserve ISCs represent a pool of quiescent stem cells that require induction of Msi activity for proper exit from quiescence and cell cycle entry which, in turn, is necessary for regeneration of the epithelium in response to injury.

Msi activity is sufficient to drive reserve ISCs out of G0 and into the cell cycle

We next asked whether Msi activity alone was sufficient to drive reserve ISC exit from G0 and into the cell cycle. For this we employed a mouse model in which a single copy of Msi1 is targeted into safe-haven chromatin and is under control of the doxycycline (Dox)-inducible tetracycline responsive element (*TRE-Msi1*) (Li et al., 2015). Administration of Dox to *Hopx-/Bmi1-CreER::R26-Lox-Stop-Lox-tdTomato::TRE-Msi1* mice for as little as 36 hours resulted in robust exit of reserve ISCs from G0 and subsequent entry into the cell cycle (Figure 4.9A). This ectopic Msi induction drove increased proliferation and lineage tracing from reserve ISCs (Figure 4.9B-D). At the molecular level, Msi induction activated expression of metabolic and proliferative genes such as *H6pd*, *Hif1α*, and *c-Myc* in reserve ISCs (Figure 4.9E and 4.10A). In contrast, ectopic Msi induction did not induce expression of canonical Wnt target genes such as *Lgr5* and *Ascl2* in reserve ISCs (Figure 4.9 E). Further, ectopic Msi induction had no effect on the molecular identity of CBCs, further confirming the cell type specificity of Msi function (Figure 4.9E, F). These findings indicate that Msi drives reserve stem cells out of quiescence in a Wnt-independent manner.

Premature exit of reserve ISCs from G0 sensitizes the intestinal epithelium to radiation injury

Ultimately, the data presented thus far lead to a model in which reserve ISCs maintain radioresistance by virtue of their residence in the quiescent G0 state outside of the cell cycle in the absence of Msi activity. Under basal conditions, Msi is periodically activated in reserve ISCs, enabling their exit from quiescence. Upon Msi ablation these cells can no longer enter the cell cycle, and the activity of CBCs (which do not require Msi activity) masks any phenotypic consequences of failed reserve ISC activation. Only upon radiation injury and CBC ablation do the phenotypic consequences of Msi loss and failed reserve ISC activation manifest themselves as failed epithelial regeneration.

If this model were correct, we would predict that premature exit of reserve ISCs from G0 and into the cell cycle should sensitize these cells and the intestinal epithelium to radiation damage, resulting in failed regeneration. To test this, we drove reserve ISCs out of G0 with a 24-hour pulse of ectopic Msi1 induction in *TRE-Msi1* mice followed by exposure to 12 Gy γ-IR injury and quantified the frequency of clonal regenerative crypt foci. Indeed, in this context the regenerative capacity of the epithelium was severely compromised (Figure 4.12A), providing support to the notion that maintenance of a pool of reserve ISCs in G0 acts as protective mechanisms for the tissue in the event of DNA damage. In contrast, *Dox* administration and Msi induction 48 hours after γ-IR had no deleterious effects on regeneration of *TRE-Msi1* mice (Figure 4.10B).

mTORC1 activation is sufficient to rescue the impaired in *Msi-DKO* mice after high-dose irradiation

We have recently shown that mTORC1 activity is strongly potentiated in the intestinal epithelium in response to forced *Msi* expression *in vivo*, and that endogenous Msi directly binds to several transcripts encoding known negative regulators of mTORC1, including Pten, Lrig1, and Bmpr1a (Li et al., 2015; Wang et al., 2015). Interestingly, the lack of phenotype in *MsiDKO* mice is consistent with that of mTORC1 inactivation during intestinal homeostasis (Ashton et al., 2010;

Faller et al., 2015), and the G1 arrest we observed in reserve ISCs has previously been observed in response to mTORC1 inactivation in the hematopoietic system (Kalaitzidis et al., 2012). We therefore set out to assess potential regulation of mTORC1 by Msi proteins in reserve ISC.

Dox-induction of *Msi1* in the *TRE-Msi1* mouse for 36 hours followed by purification of *Bmi1* or *Hopx*- ISCs revealed that Msi1 was sufficient to activate mTORC1 activity in these cells (Figure 4.11A). Next, we tested whether the previously observed interaction of Msi to transcripts encoding negative regulators of mTORC1 occurs specifically in reserve ISCs. We observed a significant increase of Msi1 binding to Pten mRNA upon Msi1 induction (Figure 4.11 B). We also observed Msi1 binding to Lrig1 and Bmpr1a mRNA (data not shown), however this binding did not increase in a statistically significant manner upon Msi1 induction. This further suggests that mTORC1 activation downstream of Msi-Pten mRNA interaction might promote ISC activation.

In response to 12 Gy γ-IR, Msi and mTORC1 activity were markedly increased in regenerative crypt foci (Figure 4.8 C and Figure 3.2E). To assess whether Pten links Msi upregulation following radiation to mTORC1 activation, we assessed level of Phosphatidylinositol (3,4,5)-trisphosphate (PIP3) after IR in reserve ISCs and observe an increase in the fluorescence intensity of PIP3 staining after IR, at the same time that Msi is upregulated (Figure 4.7 C and 4.11 C). PIP3 is the product of phosphatidylinositol-3 kinase (PI3K) and the main substrate for Pten phosphatase activity. Pten function antagonizes the PI3K signaling pathway by converting PIP3 to phosphtidylinositol 4,5-biphosphate (PIP2). Increased production of PIP3 or suppression of Pten leads to recruitment of Akt to the membrane and activation of Akt-mTORC1 signaling axis (Vazquez and Devreotes, 2006). Taken together, these data are consistent with a model in which Msi interaction with the Pten mRNA inhibits Pten, leading to PIP3 accumulation and downstream activation of the Akt-mTORC1 axis to drive reserve ISCs out of quiescence.

We have shown that Leucine stimulation activates mTORC1 signaling *in vivo* (Figure 3.3 A). Thus, we evaluated the effect of Leucine on regeneration in the absence of *Msi* throughout the epithelium using *Msi1/2*$^{flox/flox}$*::Villin-CreER* mice. We initially tested the effect of Leucine

administration (1.5% in drinking water) on regeneration efficiency following 12Gy γ-IR. Interestingly, Leucine administration 36 hours after γ-IR had no deleterious effects on regeneration of wild-type mice indicating that young healthy mice are capable of activating mTORC1 signaling at an optimal level during tissue regeneration (Figure 4.11 D). However, Leucine stimulation alone was sufficient to compensate for the loss of Msi activity and fully rescue the impaired regeneration of the intestinal epithelium (Figure 4.11 E). Taken together, these data provide compelling evidence that mTORC1 activation downstream of Msi1/2 activity is both necessary and sufficient for activation of quiescent reserve intestinal stem cells and their ability to regenerate the intestinal epithelium after high-dose γ-IR injury.

Discussion

It is becoming increasingly clear that several tissues in adult mammals, most notably the hematopoietic system, bifurcate their stem cell compartments into a slow cycling, quiescent stem cell capable of giving rise to a cycling, active stem cell (Li and Clevers, 2010). The benefit of such an organizational structure is the capacity to promote tissue regeneration after damage while maintaining the proliferative output necessary to keep up with the demands of high-turnover tissues using a relatively small stem cell pool.

In the intestinal epithelium, recent studies have begun to define a hierarchical stem cell organization similar to what has been observed in the hematopoietic system, with a radioresistant, slow cycling reserve ISC giving rise to an actively proliferating crypt base columnar cell, whose self-renewal is driven by high Wnt pathway activity (Asfaha et al., 2015; Li and Clevers, 2010; Li et al., 2014; Montgomery et al., 2011; Takeda et al., 2011; Tian et al., 2011). There has been considerable interest in gaining a better understanding of radioresistant intestinal cells that contribute to regeneration following damage by radiation/chemo- therapy because of its relevance in the context of traditional cancer therapies, and also because of the apparent parallels between regeneration after damage and intestinal oncogenic transformation.

Recently, we have demonstrated that the Msi2 RNA binding protein is capable of driving long-term hematopoietic stem cells out of quiescence and into the cell cycle (Kharas et al., 2010). In the intestinal epithelium Msi1 and Msi2 function redundantly by binding to a number of transcripts that encode known negative regulators of mTORC1, including Pten, Bmpr1a, and Lrig1, and aberrant Msi activation leads to Pten repression and induction of the Akt-mTORC1 axis (Li et al., 2015; Wang et al., 2015).

In the current study, we investigated the function of the Msi family of RNA-binding proteins in intestinal stem cell function under basal conditions and during regeneration in response to injury. The data demonstrate that Msi1 and Msi2 are upregulated during the exit of reserve ISCs from quiescence, both under basal conditions and during regeneration after ablation of Wnt^{High} CBCs in response to high dose radiation (Figure 4.12B). We therefore tested the sufficiency and necessity of Msi proteins for reserve stem cell activation and CBC self-renewal. Remarkably, genetic ablation of either *Msi* family member, as well as concomitant ablation of both *Msi1&2* throughout the intestinal epithelium and colon had no adverse effects on homeostasis, active CBC self-renewal, or Wnt pathway target gene expression, despite the high level of both Msi family members in the Wnt^{High} CBC stem cells (Li et al., 2015; Maria Cambuli et al., 2013; Potten, 2004; Wang et al., 2015).

In contrast to the lack of phenotype in crypt base columnar stem cells, *Msi* loss in of reserve ISCs (marked either by *Hopx-CreER* or *Bmi1-CreER)* resulted in the failure of these cells to become activated and contribute progeny to the epithelium. This failure of reserve ISC activation had no apparent detrimental consequences for the epithelium in the basal state, at least across the time period we investigated, likely due to the unaffected CBC compartment providing the proliferative output necessary for epithelial maintenance. However, when mice lacking Msi activity either in the entire epithelium, or specifically in the very rare reserve ISCs, were exposed to DNA damaging γ-IR injury at levels known to ablate the CBC compartment, intestinal regeneration failed. This finding highlights the importance of these rare reserve ISCs in mounting a regenerative response in the face of injury.

When considering how reserve ISCs resist DNA damage, we analyzed their cell cycle status. Reserve ISCs are often referred to as being quiescent, or residing in G0, as this state is thought of as being protective to stem cells in unfavorable environments (Cheung and Rando, 2013). Indeed, we observed that the majority of ISCs marked by *Hopx-CreER* or *Bmi1-CreER* reside in G0, while the remainder of the population cycles actively. We demonstrate that Msi activity controls the exit of reserve ISCs from the G0 state and their subsequent entry into the cell cycle. The importance of maintaining a pool of quiescent stem cells as a means to respond to injury can be observed in gain of function experiments in which ectopic activation of Msi1 drives reserve ISCs from quiescence. In this context, promiscuous exit of this population from G0 and into the cell cycle renders the epithelium susceptible to radiation injury, supporting the notion that residence in G0 protects ISCs from DNA damage.

Interestingly, the phenotype of Msi loss of function is reminiscent of inactivation of mTORC1- both result in failed intestinal regeneration after injury and in a G1 cell cycle arrest (Ashton et al., 2010; Faller et al., 2015; Kalaitzidis et al., 2012). We have previously established that in the context of colorectal cancer mTORC1 is a functionally important target of Msi activity, and both mTORC1 and Msi are required for transformation of the epithelium downstream of APC loss. Consistent with our current findings, a recent study found that the negative regulator of mTORC1 activity, Pten, regulates the proliferation of intestinal stem cells marked with proxy reporter alleles driven by the mTert promoter (a population that likely overlaps with the *Hopx-/Bmi1-CreER*-marked population in the current study based on their functional and molecular similarities) (Richmond et al., 2015). These findings are entirely consistent with observations in the hematopoietic and muscle tissues, where mTORC1 similarly governs stem cell quiescence (Kalaitzidis et al., 2012; Rodgers et al., 2014).

Taken together, our findings emphasize the significance of precise regulation of reserve stem cell quiescence in protecting the intestinal epithelium from genotoxic insults. The discovery that Msi proteins govern reserve intestinal stem cell activation provides a foundation for future studies aimed at the development of therapeutic interventions that delay ISC cell cycle entry in an

effort to protect patients against acute side effects of radiation therapy and radiation-induced acute gastrointestinal syndrome.

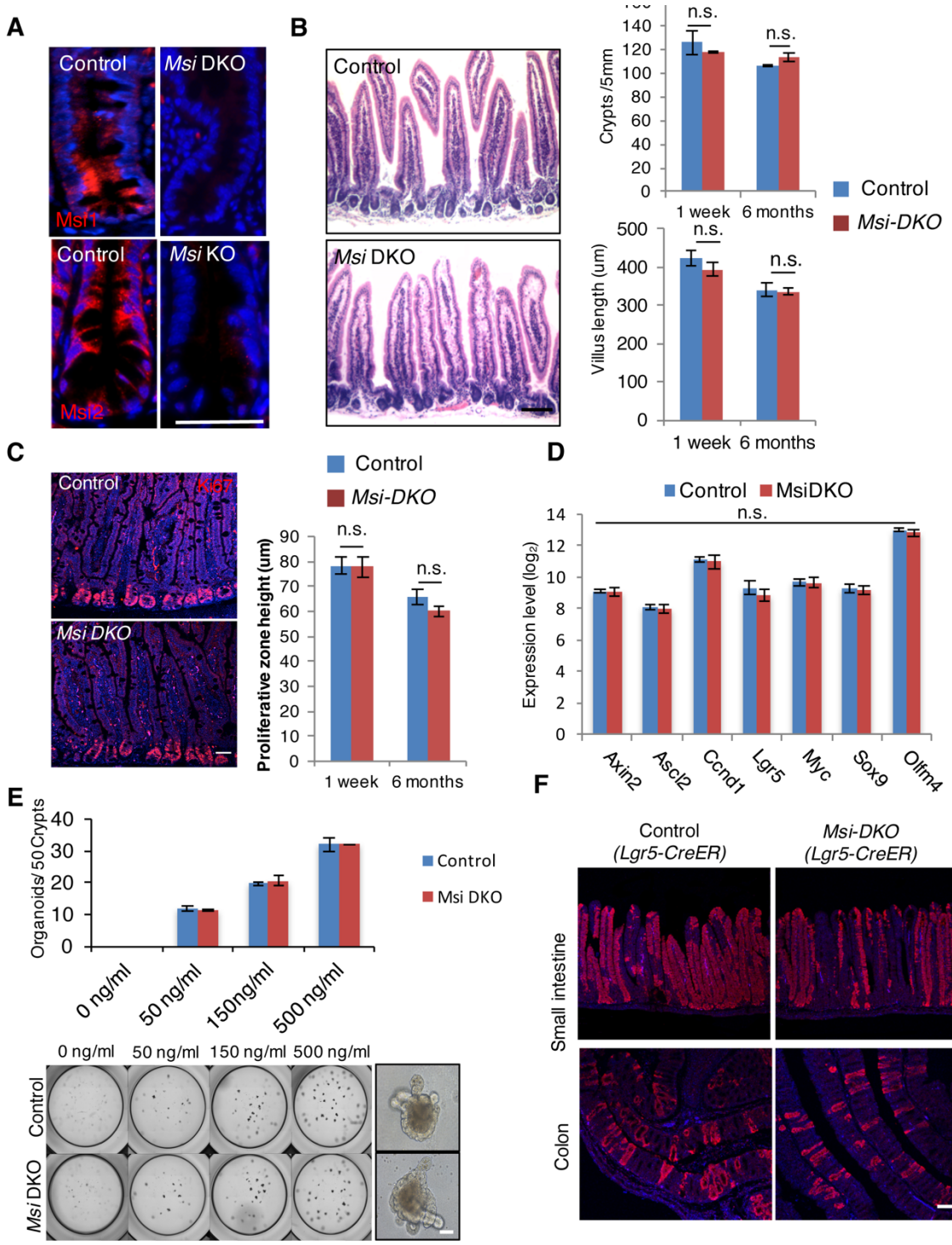

Figure 4. 1. Msi activity is dispensable for intestinal homeostasis, Wnt pathway activity, and CBC function under basal conditions

Figure 4.1. Msi activity is dispensable for intestinal homeostasis, Wnt pathway activity, and CBC function under basal conditions

Msi1/2$^{flox/flox}$*::Villin-CreERT2 (MsiDKO)* and control mice were given 5 consecutive daily doses of Tamoxifen and harvested either one week or 6 months later (n=3-5).

(A) Msi1 and Msi2 staining in normal intestinal crypts under basal conditions in control and *Msi-DKO* mice. Scale bar=50μM.

(B) Hematoxylin and eosin (H&E) stained sections from the jejunum of mice described above, 6 months after Tamoxifen injection and quantification of number of crypts per unit length of small intestine, and length of villi based on these H&E stained sections. Scale bar=100 μM.

(C) Ki67 staining of sections from jejunum of mice described above and measurement of length of proliferative zone based on these Ki67-stained sections. Scale bar=50μM

(D) Gene expression analysis of Wnt pathway target genes of crypts isolated from *Msi1/2*$^{flox/flox}$*::Villin-CreER* and control mice 1 week after Tamoxifen treatment (n=3).

(E) Organoid formation assay with crypts isolated from *Msi1/2*$^{flox/flox}$*::Villin-CreER* and control mice cultured with increasing doses of R-spondin in the absence of GSK-3 inhibitor. 50 crypts are initially plated per well (n=3). Scale bar=50μM

(F) Immunofluorescence staining for tdTomato in sections of small intestine and colon of *Lgr5-eGFP-IRES-CreER::LSL-tdTomato::Msi1/2*$^{flox/flox}$ mice and their control counterparts 14 days after activating the tdTomato reporter and deleting *Msi* genes with Tamoxifen. Scale bar =50um.

All data are expressed as mean +/- s.d. (* $p<0.05$, ** $p<0.005$, *** $p<0.0005$, Student's t test).

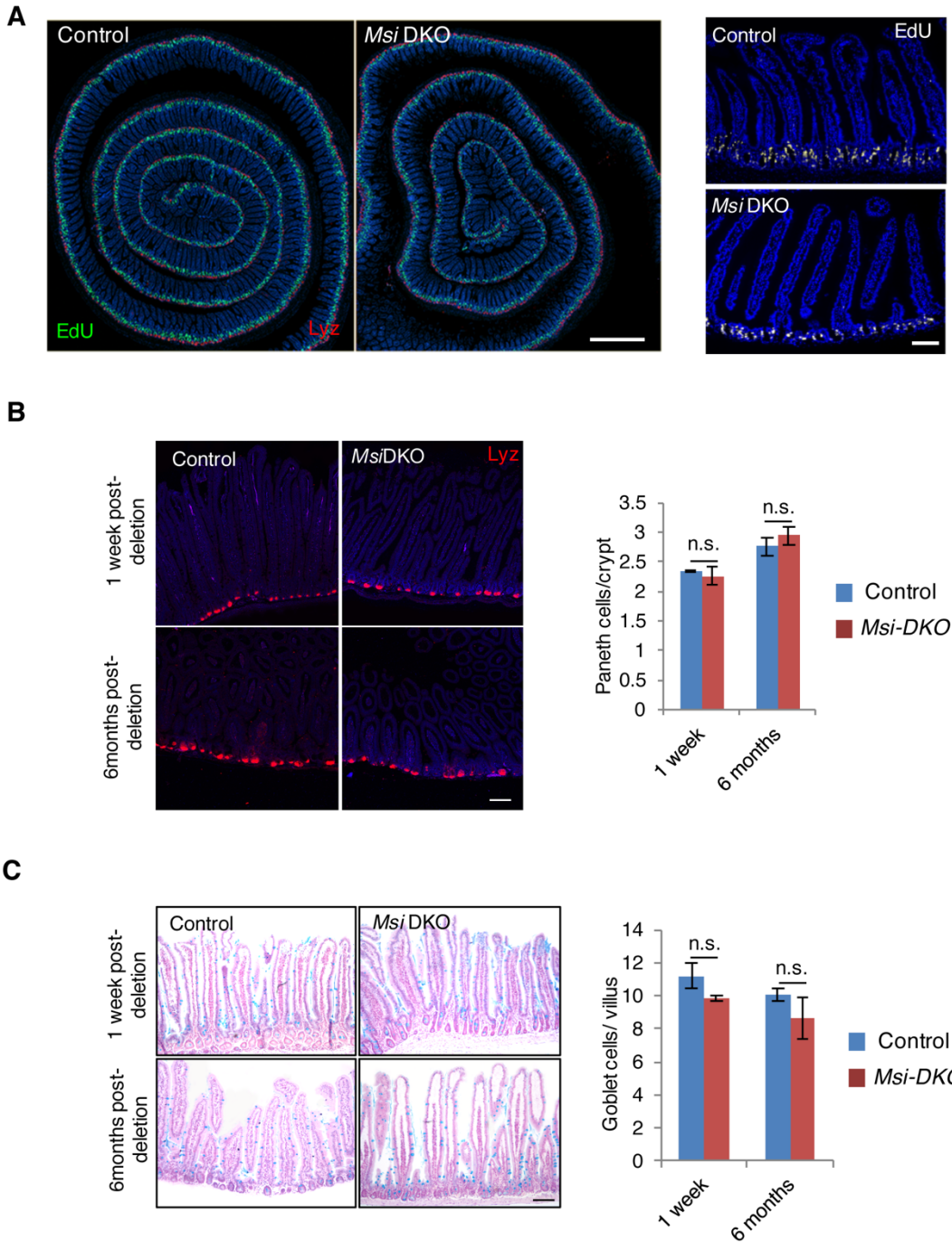

Figure 4. 2. Msi loss does not affect proliferation and differentiation of epithelial cells in the intestine under basal conditions

Figure 4.2. Msi loss does not affect proliferation and differentiation of of epithelial cells in the intestine under basal conditions.

Msi1/2$^{flox/flox}$*::Villin-CreER* and control mice were given 5 consecutive daily doses of Tamoxifen and harvested either one week or 6 months after the last dose (n=3-5). Scale bar=1000 μm

(A) EdU and Lyzozyme co-staining on Swiss rolls of the small intestines of mice described above (left) and higher magnification of EdU staining of the same sections (right). Scale bar =100μM.

(B) Lysozyme (Lyz) staining of sections from jejunum of mice described above and quantification of number of Paneth cells per crypt based on these sections. Scale bar=100 μm.

(C) Alcian blue staining of sections from small intestine of mice described above and quantification of number of goblet cells per Villus based on these sections. Scale bar=100 μm.

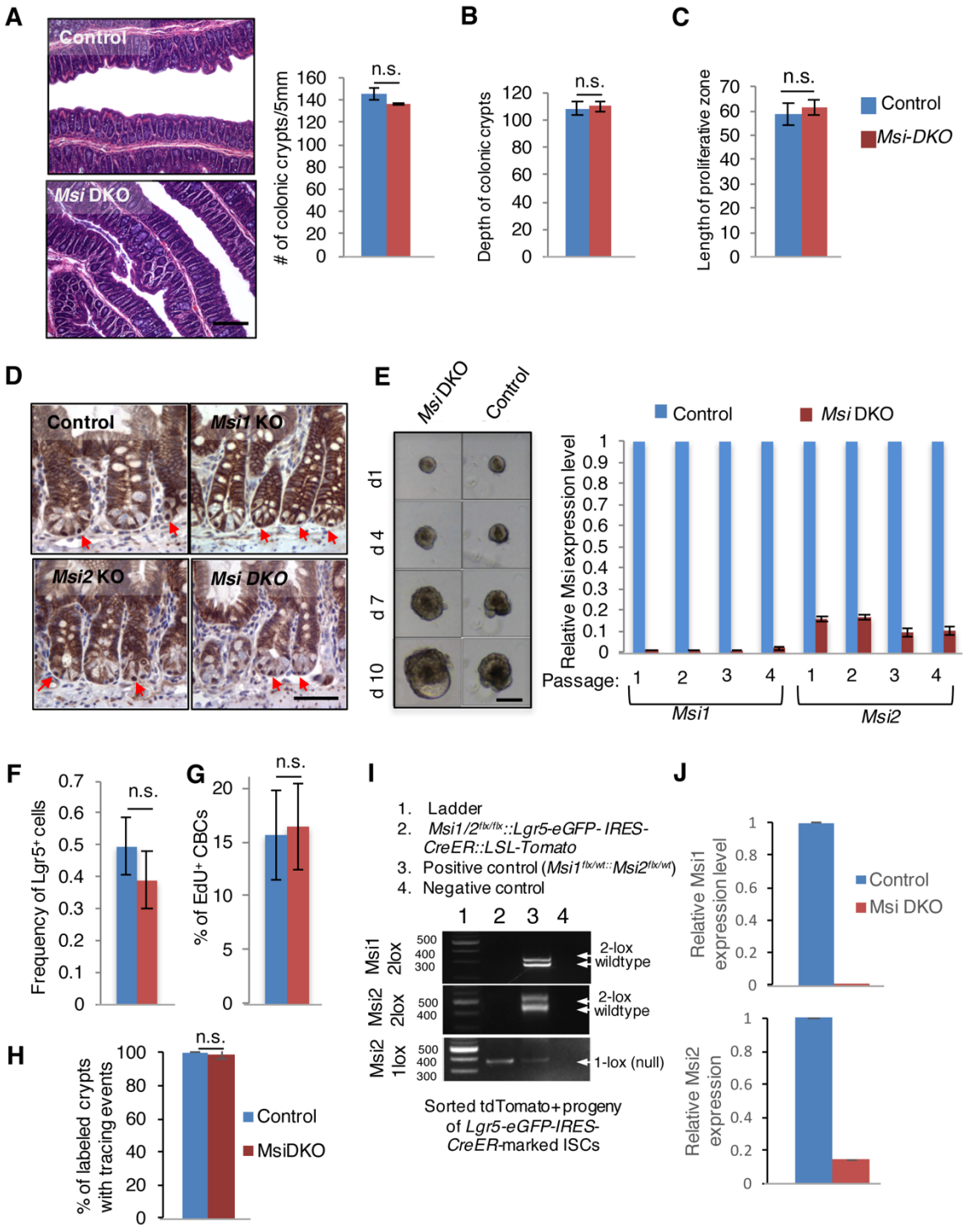

Figure 4. 3. Msi loss does not affect homeostasis of intestinal epithelium under basal conditions

Figure 4.3. Msi loss does not affect homeostasis of intestinal epithelium under basal conditions.

(A) H&E stained sections from colon of mice as described in Figure 4.2, one week after Tamoxifen treatment, and measurement of number of colonic crypts per unit length in these sections. Scale bar=200 μm.

(B) Measurement of depth of colonic crypts in sections described above.

(C) Proliferative zone length quantification based on Ki67-stained sections from colon of mice described above one week after 5 daily Tamoxifen treatments. Data are expressed as mean +/- s.d.

(D) Nuclear β-catenin staining of sections from jejunum of mice described above one week after 5 daily doses of Tamoxifen. Scale bar=100 μm.

(E) Organoid formation assays and gene expression analysis of *Msi1* and *Msi2* over 4 serial passages of organoids isolated from mice described in (A) (n=3). Residual Msi2 expression is likely from transcript read-through downstream of the deleted exons. This residual transcript is frame-shifted and non-functional. Scale bar=50 μm.

(F) Flow cytometric analysis of the frequency of Lgr5-eGFP^{+} CBCs in *Lgr5-eGFP-IRES-CreER::Msi1/2*$^{flox/flox}$ mice treated with 3 doses of Tamoxifen, 24 hours apart, and harvested 3 days after the last dose (n=3-4).

(G) Flow cytometric analysis of EdU incorporation of Lgr5^{+} CBCs in mice described in (F) (n=3-4).

(H) Quantification of lineage tracing from *Lgr5-eGFP-IRES-CreER*$^{+}$ CBCs. The percentage of crypts harboring marked cells upon Tamoxifen-induced *Lgr5-eGFP-IRES-CreER::LSL-tdTomato* recombination that also lead to lineage tracing events into the villi were quantified based on 13-20 random microscopic fields of jejunum of *Lgr5-eGFP-IRES-*

CreER::LSL-tdTomato::Msi1/2flox/flox mice and their control counterparts 14 days after activating the *tdTomato* reporter and deleting Msi genes with single dose of Tamoxifen. Confirmation of Msi deletion in subsequent panels I and J.

(I) Assessing Msi deletion in *Lgr5-eGFP-IRES-CreER::LSL-tdTomato::Msi1/2*$^{flox/flox}$ mice by PCR on DNA extracted from FACS-purified tdTomato^{+} cells. In the *Msi1-2lox* and *Msi2-2lox* PCR reactions, the positive control lane is derived from DNA from a *Msi* $^{flox/wt}$*::Msi*$^{flox/wt}$ animal, and thus the upper band indicates the 2lox (Floxed) allele and the lower band indicates the wild-type allele. In Msi2 1-lox PCR, the band indicates the null allele.

(J) Gene expression analysis of *Msi1* and *Msi2 in Lgr5-eGFP-IRES-CreER::LSL-tdTomato::Msi1/2*$^{flox/flox}$ CBCs 2 weeks after initiation of lineage tracing in mice described in (I). RNA was extracted from Tomato^{+}/eGFP^{+} cells. Residual Msi2 expression is likely from transcript read-through downstream of the deleted exons. This residual transcript is frame-shifted and non-functional.

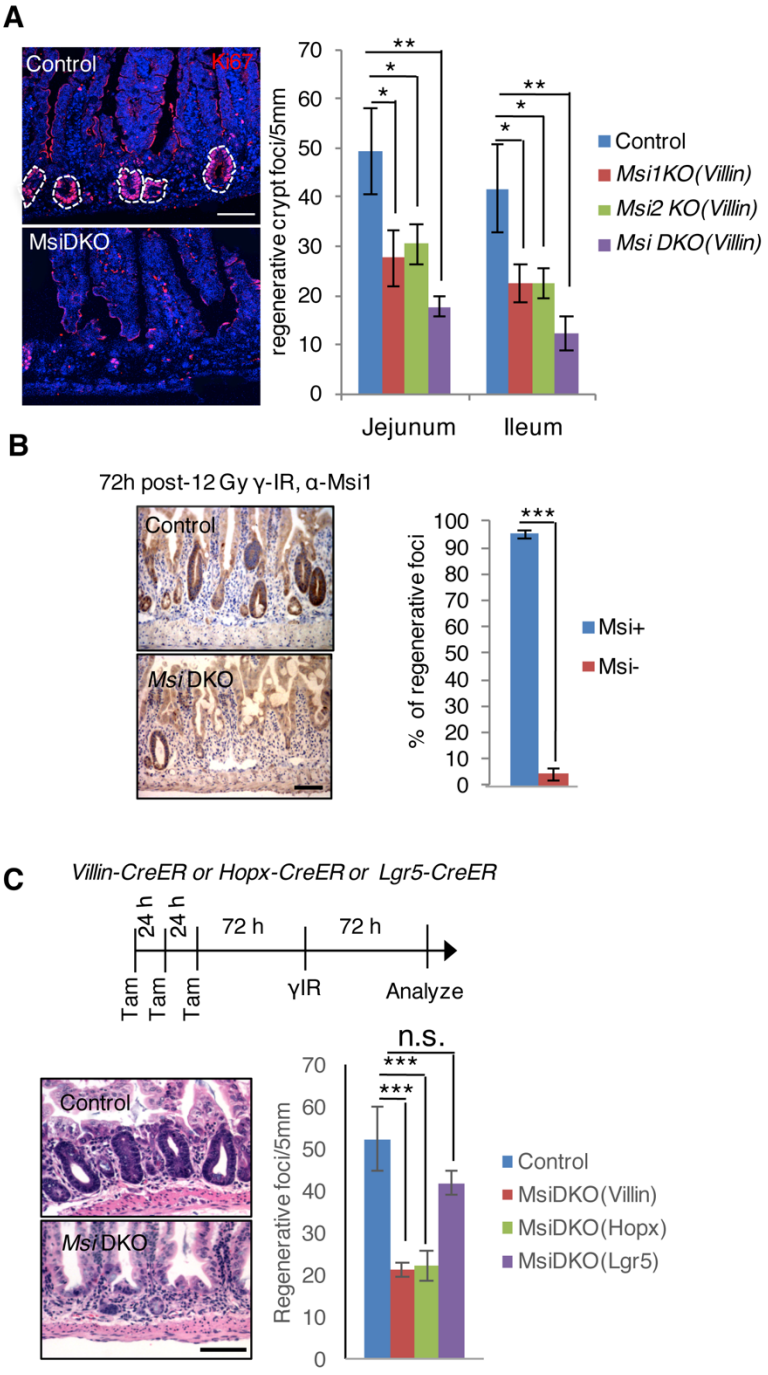

Figure 4. 4. Msi loss abrogates epithelial regeneration following γ-IR injury

Figure 4.4. Msi loss abrogates epithelial regeneration following γ-IR injury

(A) Representative Ki67-stained sections from jejunum of irradiated *Msi1/2$^{flox/flox}$::Villin-CreER* and control mice and quantification of number of proliferative crypt foci per unit length of small intestine. All groups of mice were given 5 daily consecutive doses of Tamoxifen and were exposed to 12Gy γ-IR one week later. Tissue was harvested 3 days after γ-IR (n=5-6). Scale bar=100μM

(B) Msi1 stained sections from jejunum of mice described in (A) and quantification of percentage regenerative crypts escaping recombination based on Ki67- and Msi- (Msi1/2) stained serial sections.

(C) *Msi1/2$^{flox/flox}$::Villin-CreER, Msi1/2$^{flox/flox}$::Hopx-CreER, and Msi1/2$^{flox/flox}$::Lgr5-CreER* and control mice were given 3 consecutive doses of Tamoxifen, 24 hours apart, and were exposed to 12 Gy γ-IR three days after the last dose. Tissue was harvested 3 days after γ-IR. H&E stained sections from the jejunum were used for quantification of regeneration efficiency (regenerative crypt foci per unit length of small intestine) (n=4-6). Scale bar=100μM

All data are expressed as mean +/- s.d. (* $p<0.05$, ** $p<0.005$, *** $p<0.0005$, Student's t test).

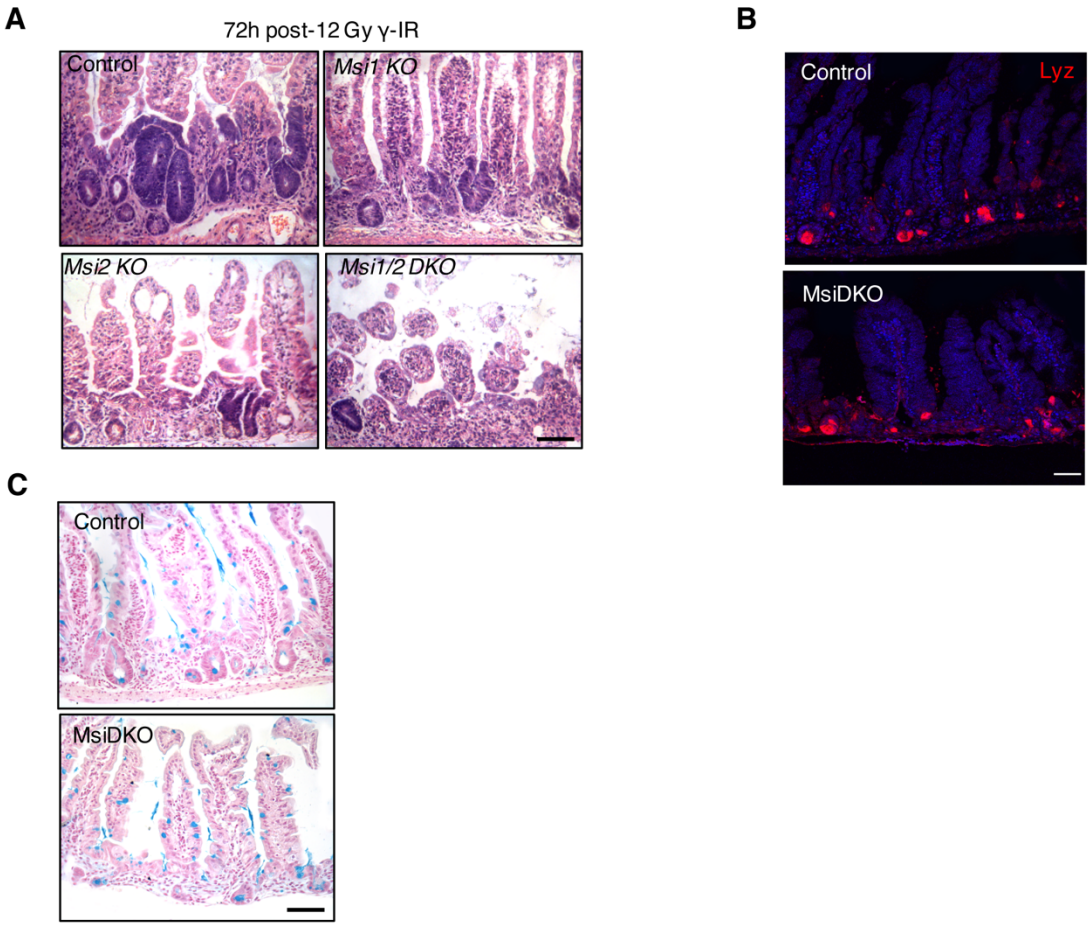

Figure 4. 5. Msi loss does not affect intestinal differentiation following radiation injury

Figure 4.5. Msi loss does not affect intestinal differentiation following radiation injury

(A) Representative hematoxylin and eosin (H&E) stained sections from jejunum of irradiated *Msi1*$^{flox/flox}$*::Villin-CreER, Msi2*$^{flox/flox}$*::Villin-CreER, Msi1/2*$^{flox/flox}$*::Villin-CreER*, and control mice. All groups of mice were given 5 daily consecutive doses of Tamoxifen and were exposed to 12Gy γ-IR one week later. Tissue was harvested 3 days after γ-IR (n=5-6). Scale bar=100μM

(B) Lysozyme staining of sections from jejunum of mice described above. Scale bar=100 μm

(C) Alcian blue staining of sections from jejunum of mice described above. Scale bar=100 μm

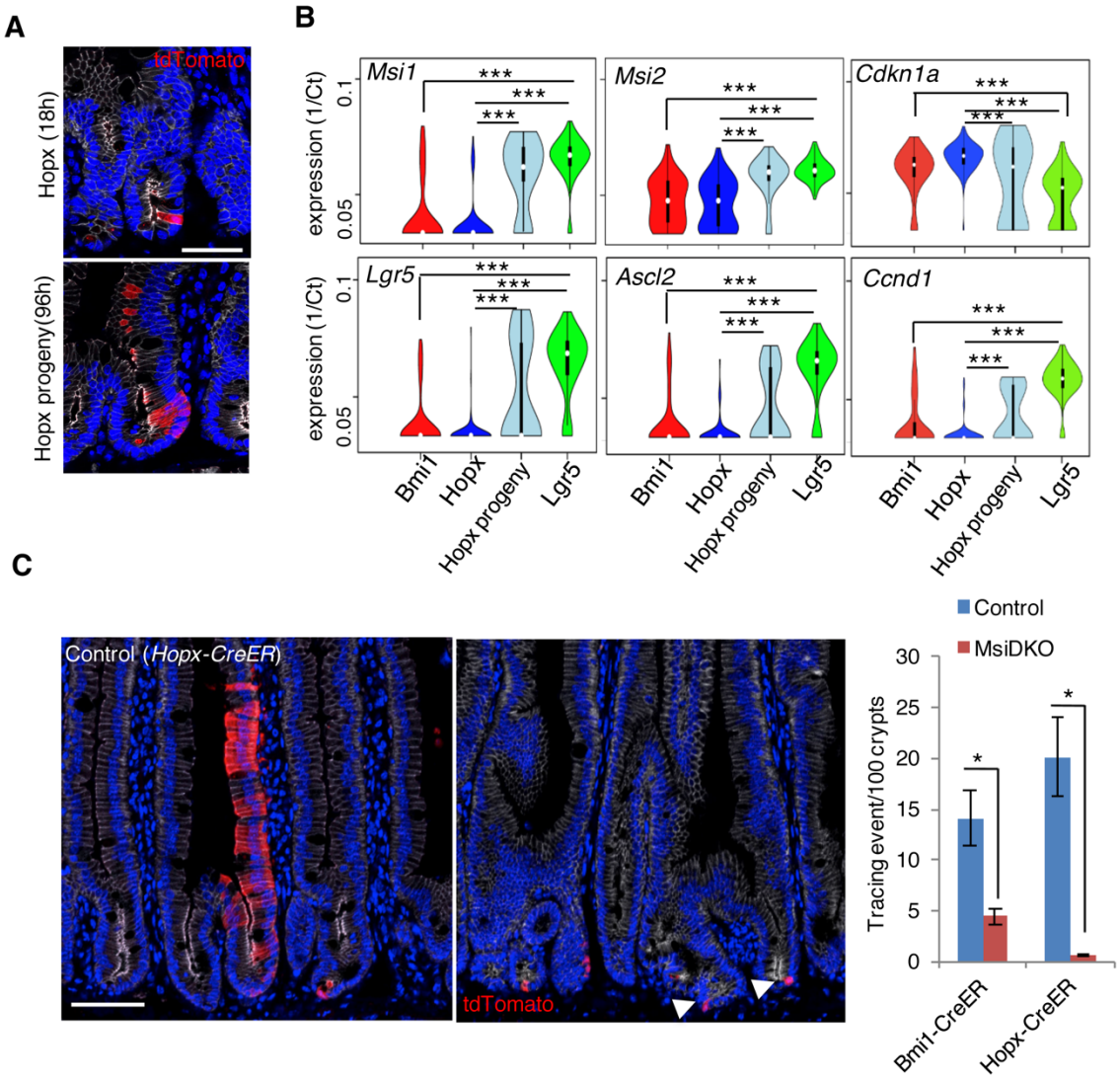

Figure 4. 6. Msi is upregulated during activation of reserve ISCs and is required for lineage tracing from these cells under basal conditions

Figure 4.6. Msi is upregulated during activation of reserve ISCs and is required for lineage tracing from these cells under basal conditions

(A) Representative immunofluorescence micrographs of *Hopx-CreER* reserve ISCs and their progeny in *Hopx-CreER::LSL-tdTomato* mice 18 hours (top) and 4 days (bottom) after a single Tamoxifen injection. TdTomato (red), E-Cadherin (white), and DAPI (blue). Scale bar=50 μM.

(B) Violin plots showing expression levels of *Msi1, Msi2, Lgr5, Ascl2, Cdkn1a, and Ccnd1* in single, FACS-purified *Bmi1-* and *Hopx-CreER* ISCs, their daughter cells (progeny), and *Lgr5-eGFP*$^{+}$ CBCs. *Bmi1-* and *Hopx-CreER*$^{+}$ ISCs were marked by a single dose of Tamoxifen in *Bmi1- or Hopx-CreER::LSL-tdTomato* mice and were purified by FACS 18 hours later. *Hopx-CreER* progeny were isolated by FACS purification of tdTomato^{+} cells 96 hours after activation of the *tdTomato* reporter. The width of the violin plot represents the number of single cells at the given expression level on the y-axis. The white dot within the violin plot represents the mean expression value for the group of cells.

(C) Immunofluorescence staining for tdTomato (red) and E-Cadherin (white) and quantification of lineage tracing events (ribbons of tdTomato^{+} cells with contiguous tracing from crypts, through crypt-villus junction, and into villi) from *Bmi1-* and *Hopx-CreER* ISCs 14 days after marking reserve ISCs with a single Tamoxifen injection to *Hopx-CreER::LSL-tdTomato::Msi1/2*$^{flox/flox}$ or *Bmi1-CreER::LSL-tdTomato::Msi1/2*$^{flox/flox}$ mice and their control counterparts (n=3, scale bar=50μM). Arrowheads point to single *MsiDKO* cells that are not able to contribute in lineage tracing.

All data are expressed as mean +/- s.d. (* $p<0.05$, ***$p<0.0005$, Student's t test).

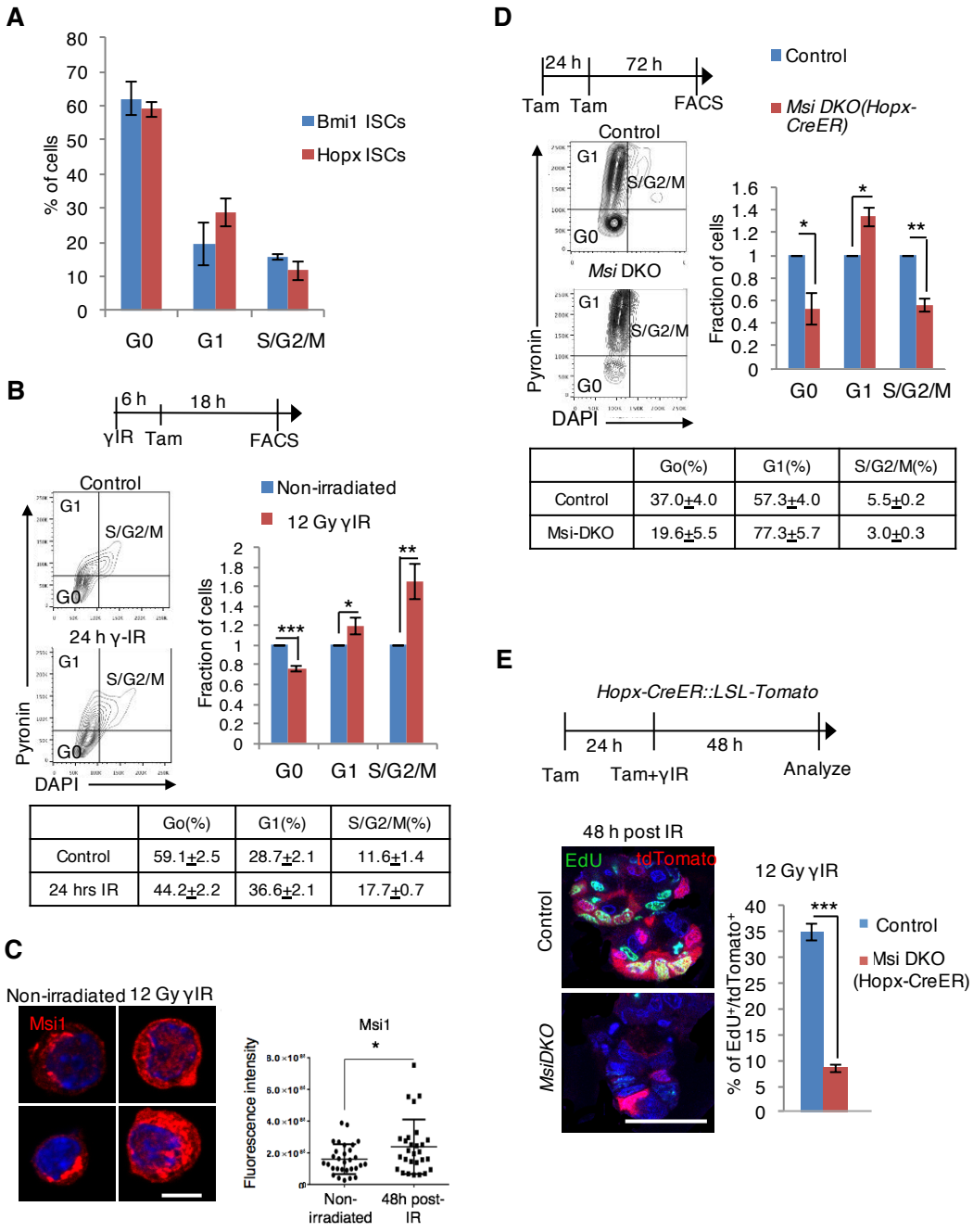

	Go(%)	G1(%)	S/G2/M(%)
Control	59.1±2.5	28.7±2.1	11.6±1.4
24 hrs IR	44.2±2.2	36.6±2.1	17.7±0.7

	Go(%)	G1(%)	S/G2/M(%)
Control	37.0±4.0	57.3±4.0	5.5±0.2
Msi-DKO	19.6±5.5	77.3±5.7	3.0±0.3

Figure 4. 7. Msi is upregulated following radiation injury coupled with exit of reserve ISCs from quiescence into cell cycle

Figure 4.7. Msi is upregulated following radiation injury coupled with exit of reserve ISCs from quiescence into cell cycle

(A) Analysis of cell cycle distribution of different reserve ISC populations using Pyronin Y and DAPI staining in *Bmi1-CreER::LSL-tdTomato* and *Hopx-CreER::LSL-tdTomato* mice, 18 hours after Tamoxifen injection. Cell cycle distribution was determined using Pyronin Y and DAPI staining during homeostasis. Pyronin Y^{low} $DAPI^{low}$ (2n) cells: G0; Pyronin Y^{high} $DAPI^{low}$ (2n) cells: G1; and Pyronin Y^{high} $DAPI^{high}$ cells (>2n DNA content): G2/M, (n=3).

(B) Analysis of quiescence in *Hopx-CreER*$^{+}$ ISCs using Pyronin Y and DAPI staining under basal conditions and 24 hours after 12Gy γ-IR. To mark *Hopx-CreER* ISCs, mice were injected with Tamoxifen 18 hours before harvest (n=4-5).

(C) Immunofluorescence staining for Msi1 and quantification of Msi1 fluorescence intensity in *Hopx-CreER*$^{+}$ ISCs, 48 hours after irradiation and 18 hours after Tamoxifen induction. Shown are micrographs of individual FACS-purified ISCs (n=3, scale bar=5 μM).

(D) Analysis of cell cycle distribution of FACS-purified tdTomato^{+} cells from *Hopx-CreER::LSL-tdTomato::Msi1/2*$^{flox/flox}$ or control mice 3 days after the second of two daily consecutive Tamoxifen doses given during homeostasis (n=3-4).

(E) EdU stained sections from the jejunum of *Msi1/2*$^{flox/flox}$*::LSL-tdTomato::Hopx-CreER* and control mice, treated with 2 daily doses of Tamoxifen. The mice were divided to two groups and one group received 12 Gy γ-IR immediately after the second dose of Tamoxifen. Tissue was harvested 2 days after the second dose of Tamoxifen. The graph shows EdU incorporation of tdTomato^{+} 48 hours after IR in either presence or absence of Msi (n=3, Scale bar=50μM).

All data are expressed as mean +/- s.d. (* $p<0.05$, ** $p<0.005$, *** $p<0.0005$, Student's t test).

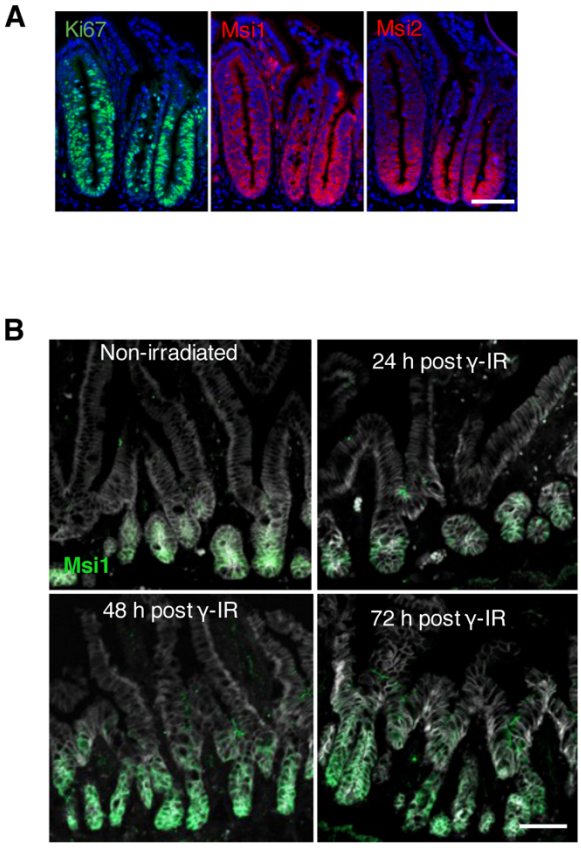

Figure 4. 8. Msi is upregulated in regenerative crypt foci following radiation injury

Figure 4.8. Msi is upregulated in regenerative crypt foci following radiation injury

(A) Sections from the jejunum of small intestine of wildtype mice, 4 days after exposure to 12Gy γ-IR, stained for Ki67, Msi1 and Msi2. Scale bar =25μM.

(B) Immunofluorescence staining of Msi1 at the indicated timepoints after 12Gy γ-IR. Scale bar=50 μm

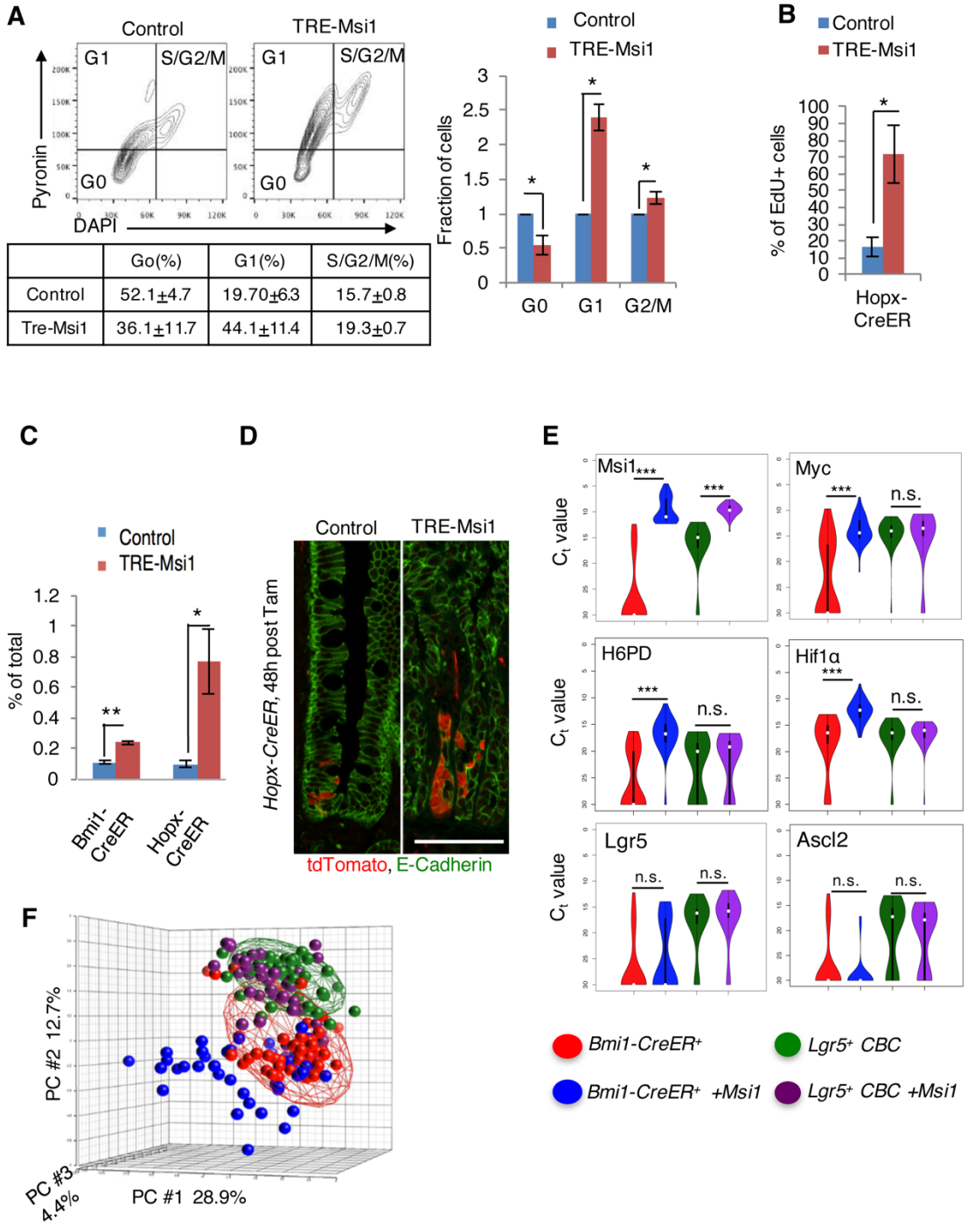

	Go(%)	G1(%)	S/G2/M(%)
Control	52.1±4.7	19.70±6.3	15.7±0.8
Tre-Msi1	36.1±11.7	44.1±11.4	19.3±0.7

Figure 4. 9. Msi upregulation is sufficient to activate metabolic genes in reserve ISCs and drive these cells out of quiescence into cell cycle

Figure 4.9. Msi upregulation is sufficient to activate metabolic genes in reserve ISCs and drive these cells out of quiescence into cell cycle

(A) Analysis of cell cycle distribution of *Bmi1-CreER* ISCs 36 hours after induction of Msi1 expression in *TRE-Msi1::Bmi1-CreER::tdTomato* and *Bmi1-CreER::tdTomato* control mice. Both *TRE-Msi1* and control (*R26-m2rtTA*) groups were treated with doxycycline in their drinking water for 18 hours then given 1 dose of Tamoxifen and maintained on dox for an additional 18 hours before tissue harvest (n=4).

(B) Assessment of EdU incorporation in *Hopx-CreER* ISCs from doxycycline and Tamoxifen treated *TRE-Msi1::Hopx-CreER::tdTomato* and control (*R26-m2rtTA* +dox) mice as described in (A) (n=4-5).

(C) Quantification of frequency of *Hopx-* and *Bmi1-CreER*$^{+}$ ISCs from doxycycline- (total 36 hours) and Tamoxifen- (18 hours before tissue harvest) treated *TRE-Msi1::Hopx-CreER::tdTomato, TRE-Msi1::Bmi1-CreER::tdTomato,* and control (*R26-m2rtTA* +dox) mice (n=3-4).

(D) Lineage tracing from *Hopx-CreER* ISCs staining for tdTomato in sections from *Tre-Msi1::Hopx-CreER::tdTomato* and control (*R26-m2rtTA* +dox) mice 48 hours after doxycycline and Tamoxifen treatment (Scale bar =50μM).

(E) Violin plots showing the expression level in populations of single ISCs. The white dot in the violin plot represents the median expression within the group of cells, the black box represents the interquartile range, and the width of the plot is directly correlated to the number of cells at the given expression level indicated on the y-axis.

(F) Principal component analysis of cellular identity in single *Lgr5-eGFP*^{High} CBCs and quiescent (*Bmi1-CreER*$^{+}$) ISCs with and without Msi1 induction based on the expression profiling of 48 transcripts representing the Wnt pathway, Notch pathway, proliferation, metabolism, and stem cell identity. Each sphere represents a single cell, and the percent of variation ascribed to each of

the principle components is delineated on the axes. The cages around the *Bmi1-CreER* (red) and *Lgr5-eGFP* (green) populations represent the domain contained within 2 standard deviations of the arithmetic centroid of the population. Color-coding of ISCs is indicated in panel. All data are expressed as mean +/- s.d. (*p<0.05, **p<0.005, ***p<0.0005, Student's t test).

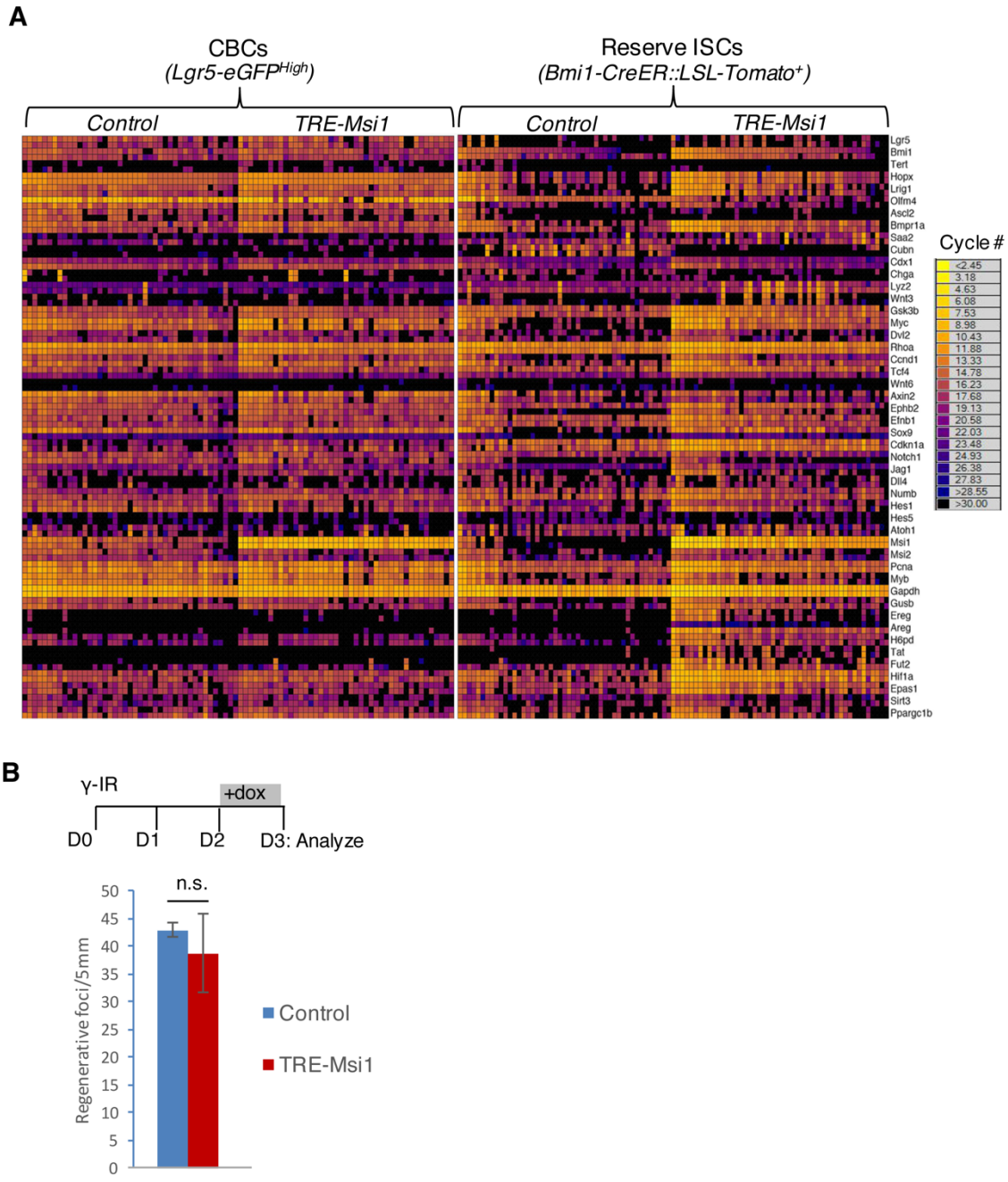

Figure 4. 10. Forced expression of Msi1 activates metabolic genes in reserve ISCs

Figure 4.10. Forced expression of Msi1 activates metabolic genes in reserve ISCs

(A) Heatmap showing Fluidigm Biomark profiling of *Lgr5-eGFP*^{High} CBCs and *Bmi1-CreER*$^{+}$ ISCs, both in the absence (control) and presence of Msi1 induction. Every column contains a single cell, and every row a single primer pair, with two distinct primer sets being used to interrogate each of the transcripts listed on the right. Colors correspond directly to Ct value, black being >30 (no detectable transcript).

(B) Quantification of regeneration based on H&E stained sections from the jejunum of irradiated *TRE-Msi1* and control (*R26-m2rtTA*) mice. Both groups received doxycycline for 24 hours starting 48 hours after irradiation and were harvested three days after γ-IR. Quantification of regeneration efficiency was done by counting regenerative crypt foci, defined as 10 or more adjacent chromophilic cells and a lumen in H&E stained sections (n=6).

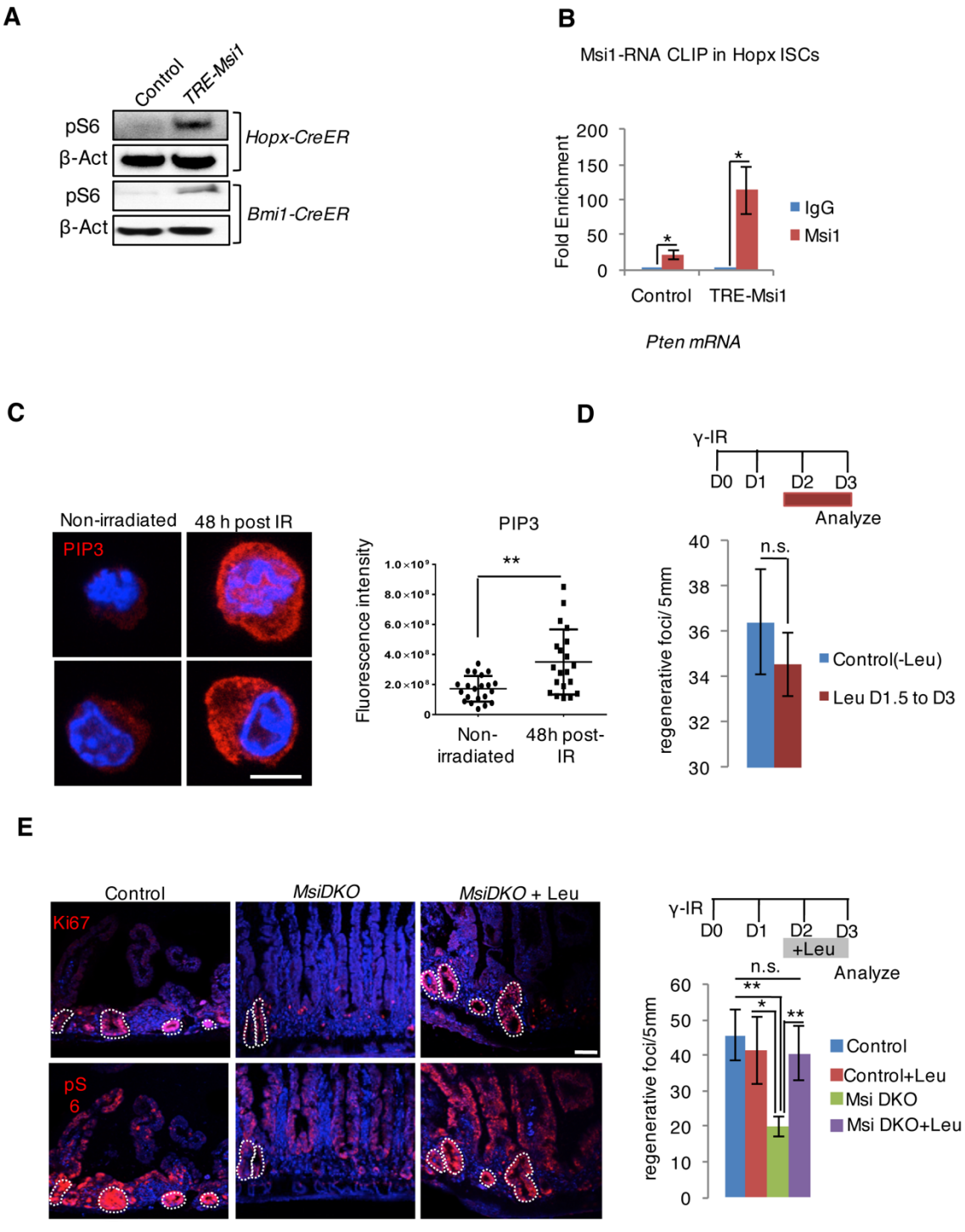

Figure 4. 11. mTORC1 activation is sufficient to rescue the impaired regeneration in *MsiDKO* mice after high-dose irradiation

Figure 4.11. mTORC1 activation is sufficient to rescue the impaired regeneration in *MsiDKO* mice after high-dose irradiation.

(A) Western blot analysis of phosphorylation of S6 as a proxy readout for mTORC1 activity, in ISC population 36 hours after induction of Msi1 expression in *TRE-Msi1::Bmi1-CreER::tdTomato and TRE-Msi1::Hopx-CreER::tdTomato* and control mice. Both *TRE-Msi1* and control groups were treated with doxycycline for 36 hours and 1 dose of Tamoxifen 18 hours before tissue harvest.

(B) Clip-qPCR assessing Msi1 binding to Pten mRNA in FACS-sorted *Hopx-CreER* ISCs. Both *TRE-Msi1* and *rtTA* (control) groups were treated with doxycycline for 36 hours and were given 1 dose of Tamoxifen to activate fluorescent marker 18 hours before tissue harvest.

(C) Immunofluorescence staining for PIP3 and quantification of PIP3 fluorescence intensity in *Hopx-CreER*$^{+}$ ISCs, 48 hours after irradiation and 18 hours after Tamoxifen induction. Control mice did not receive irradiation (n=2, scale bar=5 μM).

(D) Quantification of the regeneration efficiency after irradiation injury in mice receiving 1.5% Leucine in their drinking water 1.5 days after γ-IR and in control groups (n=3).

(E) Immunostaining for Ki67 and pS6 on sections from jejunum of control, *Msi-DKO* and Leucine-treated *Msi-DKO* mice 3 days following 12 Gy γ-IR (Scale bar=25μM) and Quantification of regeneration efficiency of *Msi1/2*$^{flox/flox}$*::Villin-CreER* and control mice following 12 Gy γ-IR. All groups received 5 consecutive doses of Tamoxifen and were irradiated one week after the last dose. 1.5% Leucine was given to + Leu groups 36 hours after γ-IR and tissue was harvested 3 days after γ-IR (n=8-9).

All data are expressed as mean +/- s.d. (* $p<0.05$, ** $p<0.005$, *** $p<0.0005$, Student's t test).

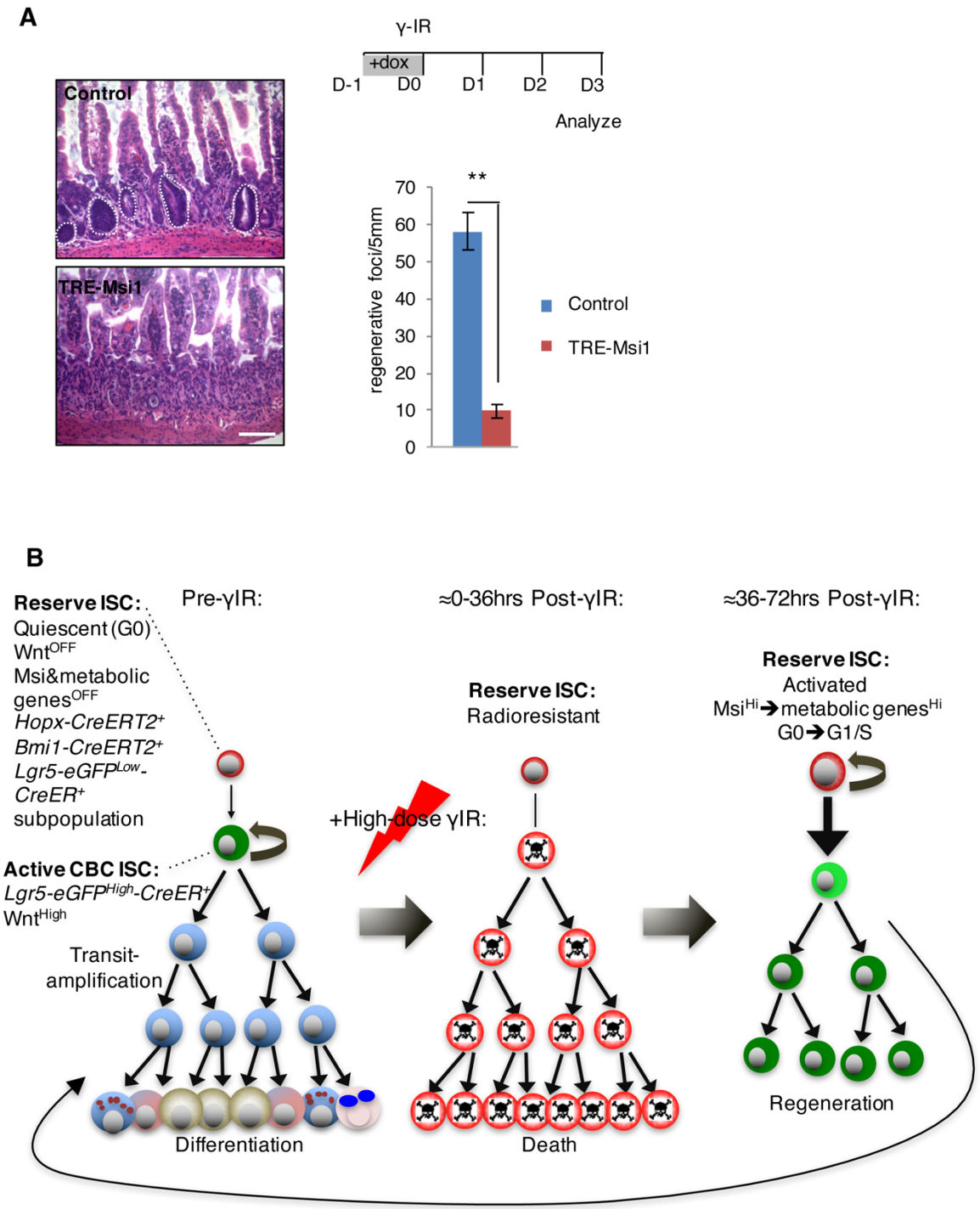

Figure 4. 12. Msi activity regulates radiosensitivity of intestinal epithelium

Figure 4.12. Msi activity regulates radiosensitivity of intestinal epithelium

(A) H&E stained sections from the jejunum of irradiated *TRE-Msi1* and control (*R26-m2rtTA*) mice. Both groups received doxycycline for 24 hours before irradiation and were harvested three days after γ-IR. During regeneration period mice received regular drinking water (no doxycycline). Quantification of regeneration efficiency following irradiation injury was done by counting regenerative crypt foci, defined as 10 or more adjacent chromophilic cells and a lumen in H&E stained sections (n=3-4).

(B) Model depicting behavior of reserve and active ISCs during homeostasis and regeneration following high-dose γ-IR.

All data are expressed as mean +/- s.d. (**p<0.005, Student's t test).

Table 4. 1. Differentially expressed genes between *MsiDKO (Villin-CreER)* intestinal crypts and their control counterparts identified by microarray

Gene Symbol	RefSeq	Fold-Change M12	p-value M12
5730507C01Rik	NM_001201330	2.66582	0.0950951
Grb10	NM_010345	2.60178	0.0895023
S1pr3	NM_010101	2.12768	0.0734615
Zfp125	AJ005350	2.05704	0.0536049
Snai2	NM_011415	1.99935	0.0720264
Fabp6	ENSMUST00000020672	1.95362	0.00564633
Sparcl1	NM_010097	1.91633	0.0851181
Pcdh18	NM_130448	1.8676	0.0613742
Rec8	ENSMUST00000002395	1.803	0.0793345
Hbb-y	ENSMUST00000033229	1.78254	0.0754809
Emcn	ENSMUST00000122064	1.77835	0.0906314
Tbx5	NM_011537	1.77116	0.0984079
Lix1l	NM_001163170	1.75491	0.0376084
Mmp2	NM_008610	1.75071	0.0532351
Pdgfra	NM_001083316	1.73018	0.0845211
1700024P16Rik	NM_001162980	1.71295	0.0138972
AF357355	NR_028433	1.66275	0.0769029
Gja1	NM_010288	1.63186	0.084757
Nrk	NM_013724	1.63038	0.0761408
Suox	NM_173733	1.63002	0.0971738
Fbn2	NM_010181	1.62848	0.0739999
Msn	NM_010833	1.6232	0.0482963
Nid1	NM_010917	1.61724	0.0476806
Epha7	NM_010141	1.60837	0.0980257
Slc25a4	ENSMUST00000034049	1.60303	0.0204463

AF357426	NR_046303	1.60253	0.0767984
Ddr2	NM_022563	1.59813	0.0159469
Hsd3b6	NM_013821	1.58659	0.0539781
Rgs5	ENSMUST00000027997	1.58512	0.0345155
Rcn3	NM_026555	1.5845	0.0108554
Rdx	NM_009041	1.58402	0.050361
Gucy1a3	NM_021896	1.57178	0.0410353
Gm14475	ENSMUST00000170569	1.55118	0.0360287
Gsta3	NM_001077353	1.53199	0.0310757
Robo1	NM_019413	1.52015	0.0798538
Actg1	NM_009609	-1.52	0.00633933
Gbp7	NM_145545	-1.54424	0.0957129
Iigp1	NM_001146275	-1.65319	0.0988337
ND6	ENSMUST00000082419	-1.69169	0.0197823
Tnfrsf23	NM_024290	-1.69404	0.0828604
Gm12250	NM_001135115	-1.8136	0.0948251
Gm3219	NR_027380	-1.88489	0.0345574
Gdpd3	NM_024228	-1.99316	0.0652661
Pnp2	ENSMUST00000095925	-2.81279	0.0386482

CHAPTER 5

Conclusion and Future Work

Summary and Conclusions

I have shown that calorie restriction increases the number of reserve stem cells and enhances the regenerative capacity of the intestinal epithelium. Ablation of reserve intestinal stem cells (ISCs) disrupts the enhanced tissue regenerative response of calorie-restricted mice following radiation injury. RNA-sequencing and histological analysis showed that mTORC1 signaling is downregulated in reserve ISCs in response to calorie restriction but calorie-restricted mice maintained an enhanced capacity to activate mTORC1 signaling following radiation injury. Downregulation of mTORC1 signaling utilizing mouse genetic approaches or Rapamycin decreases lineage tracing from reserve ISCs under basal conditions and proved to be protective of the reserve ISCs against radiation injury. However, if mTORC1 signaling is inhibited during the regeneration phase after injury, regenerative potential of the intestinal epithelium is strongly impaired. These findings support a model where low mTORC1 activity in reserve ISCs confers resistance to DNA damaging injury, while a robust ability to activate mTORC1 in these cells after DNA damaging injury is required for an efficient regenerative response.

The Musashi (Msi) family of RNA-binding proteins, which are expressed in the intestinal crypts and act as upstream activators of mTORC1 signaling in mouse models of colorectal cancer (Li et al., 2015; Wang et al., 2015), are dispensable for intestinal homeostasis. Consistently, loss of Msi does not affect frequency, proliferation, or stem cell capacity of actively cycling crypt base columnar cells (CBCs). Msi is upregulated during regeneration and its upregulation is sufficient to activate mTORC1 signaling and metabolic genes specifically in reserve ISCs. This results in the exit of reserve ISCs from quiescence and entry into the cell cycle. Conversely, Msi loss abrogates the ability of reserve ISCs to properly enter the cell-cycle, decreases lineage tracing events from reserve ISCs under basal conditions, and impairs the regeneration capacity of the intestinal epithelium following injury. Activity of the Msi-mTORC1 axis is absolutely required during the regeneration following DNA damaging injury, and, remarkably, stimulation of mTORC1 activity using Leucine can rescue the impaired regeneration in the absence of Msi. These results have implications for several fields of research, which I outline below.

Calorie restriction increases stem cell availability and regeneration efficiency

Long-term calorie restriction (CR) preserves the function of stem cells during aging and in some cases delays onset of age-related diseases, leading to longer life span (Lee et al., 2010; Mair and Dillin, 2008). Prior studies in the hematopoietic system suggested that lifelong calorie restriction preserves stem cell function, which normally declines with age (Ertl et al., 2008). Short-term calorie restriction in young and healthy animals can enhance the regenerative response following injury. However, the specific cell type responsible for this enhanced regenerative capacity and as a result, the molecular determinants of this process are poorly understood.

Cerletti et al showed that short-term calorie restriction, on both young and aged animals, leads to increase in frequency and *in vitro* myogenic capacity of satellite cells, a population of self-renewing skeletal muscle stem cells. The regenerative capacity of muscles after injury, is increased in calorie restricted mice, and calorie restricted satellite cells produce twice as many fibers as satellite cells from a freely fed mouse upon transplantation into a mouse model of Duchenne muscular dystrophy (Cerletti et al., 2012). Similarly, short-term calorie restriction prevents the age-related decline in frequency and reconstitution capacity of HSCs following transplantation (Chen et al., 2003). However, the extent of contribution of calorie-restricted stem cells to the increase in regenerative capacity and the response of these cells to injury in their native environment remain unknown.

In the intestinal epithelium, calorie restriction slightly increases the frequency of actively cycling CBCs and their *in vitro* organoid formation capacity. Calorie restriction instructs actively cycling CBCs through nutrient sensing and secretion of signaling molecules by their surrounding Paneth cells (Igarashi and Guarente, 2016; Yilmaz et al., 2012). Yilmaz et al. demonstrated an enhanced regenerative capacity of the intestinal epithelium after exposure to ionizing radiation in calorie-restricted mice (Yilmaz et al., 2012). However, whether this enhanced regeneration is a result of an increase in the frequency or function of actively cycling CBCs (which are highly sensitive to DNA damage), or whether Paneth cells are crucial in the enhanced regenerative

response following radiation injury in unclear. This is evident in experiments in which Paneth cells are genetically ablated and the tissue is subjected to radiation injury. These experiments suggest that the absence of Paneth cells does not negatively influence the regenerative response. Thus, the cellular basis for the enhanced regenerative response of the calorie restricted intestinal epithelium remains unknown.

My work demonstrated that calorie restriction increases the frequency of reserve intestinal stem cells, which are crucial for proper intestinal regeneration. To demonstrate the functional contribution of the reserve ISCs in regeneration following radiation injury, I ablated these cells using diphtheria toxin after a period of calorie restriction and showed that the reserve ISC ablation leads to about 40% reduction in the enhanced tissue regenerative capacity of calorie restricted mice. This piece of data clearly demonstrates that reserve intestinal stem cells respond to nutrient cues and play a major role in the enhanced regenerative capacity of the tissue after calorie restriction. However, the tissue regenerative capacity of calorie restricted mice in the absence of reserve ISCs was not fully reduced to regenerative capacity of freely fed control mice. This could be a result of inefficiency of our system in ablating reserve ISCs or the presence of other cell types playing a role in tissue regeneration. It is not clear whether actively cycling CBCs, which are highly radiosensitive, or Paneth cells, which are not required for intestinal regeneration following IR in freely fed mice, play different roles after calorie restriction and could possibly be crucial for the CR-induced enhanced tissue regeneration capacity. My findings provide the first evidence that reserve stem cells are functionally important for the enhanced regenerative response to injury in calorie restricted animals.

The studies mentioned above demonstrate that stem cells of different tissues are capable of responding to the metabolic state in the body, and nutrient intake can regulate their regenerative capacity in response to injury or upon transplantation. Answers to the questions surrounding the effect of calorie restriction on the response of tissue stem cells upon exposure to injury and understanding the functional contribution of specific cell types to the enhanced regenerative capacity in calorie restricted animals may help to improve the targeting and

transplantation of stem cells for therapy and illuminate metabolic regulators of tissue stem cell function.

My study and others show that mTORC1 signaling is inhibited in reserve ISCs and long-term HSCs in response to calorie restriction (Harrison et al., 2009; Yousefi et al., 2017). Hyperactivation of mTORC1 signaling leads to hyperproliferation and depletion of neural stem cells and HSCs (Groszer, 2001, 2001; Kalaitzidis et al., 2012; Yilmaz et al., 2006). Here, I show that downregulation of mTORC1 signaling in response to calorie restriction or Rapamycin treatment protects the reserve ISCs against radiation injury, and, conversely, mTORC1 stimulation with Leucine sensitizes the tissue to radiation injury (Yousefi et al., 2017).

Msi RNA binding proteins acts as upstream activators of mTORC1 in reserve intestinal stem cells under basal conditions and during oncogenic transformation(Li et al., 2015; Wang et al., 2015; Yousefi et al., 2016). However, it is not clear whether Msi regulates mTORC1 activity in reserve ISCs in response to calorie restriction as well. A clear understanding of a crosstalk between nutrient availability, Msi regulation, and modulation of mTORC1 signaling could provide novel targets for therapeutic intervention to protect patients against acute side effects of DNA damage associated with clinically relevant injuries such as radiation therapy, chemotherapy, ischemia-reperfusion, or chronic inflammation, with the ultimate goal of enhancing tissue regeneration and preventing oncogenesis.

An Msi-mTORC1 axis regulates activation of reserve stem cells

In most of the mammalian tissues, stem cells are responsible for proliferation and compensation for cell loss occurring during the normal tissue turnover or upon injury (Weissman, 2000). A fraction of stem cells resides in quiescence (G0), which is defined as a non-cycling state with the ability to enter cell cycle in response to normal physiological stimuli. Besides the cell cycle state, quiescent cells are believed to have low levels of global transcription and metabolic

activity, while retaining the ability to upregulate both processes upon receiving physiological stimuli (Cheung and Rando, 2013; Fukada et al., 2007; Hüttmann et al., 2001).

My study and others demonstrate that the majority of reserve ISCs (>60%) and LT-HSCs (≈90%) reside in G0. Interestingly, smaller fractions of populations of active stem cells in the intestinal epithelium and hematopoietic system (CBCs and ST-HSCs) are quiescent, and these cells also have shorter life-spans compared to their reserve ISC and LT-HSC compartments (Li et al., 2014, 2016b; Pietras et al., 2011; Yousefi et al., 2016). Consistently, dysregulation of quiescence could lead to depletion of stem cell populations due to inappropriate stem cell activation and production of downstream progenitor cells and as a result, this can impair tissue regeneration (Li and Clevers, 2010; Orford and Scadden, 2008). These observations imply a functional role for quiescence in preserving the tissue stem cell pool throughout the adult life by precisely regulating cell cycle entry and commitment to downstream cell types. However, whether quiescence and stem cell dormancy have varying roles under basal conditions, in response to injury, during regeneration, or in response to oncogenic transformation is poorly understood. While the molecular underpinnings of stem cell quiescence have been extensively studied in the HSCs and satellite cells of skeletal muscle (Kalaitzidis et al., 2012; Rodgers et al., 2014), very little is known about this phenomenon in intestinal stem cells. Answers to these questions may lead to new therapeutic strategies for preventing tissue damage, malignant transformation, and enhancing regenerative responses to injury.

Here, I show that activity of the Msi-mTORC1 axis is not required for intestinal homeostasis under basal conditions but absolutely essential during regeneration in response to radiation injury. The differential requirement for molecular pathways important for tissue maintenance versus those required in response to injury or oncogenic transformation is substantiated with an increasing body of literature (Biteau et al., 2011). My study and others demonstrate that the Msi-mTORC1 signaling axis is activated during regeneration after injury, as well as, in *Apc*^{min} mouse model of colorectal cancer. Loss of Msi or inhibition of mTORC1 signaling abrogates the regenerative response following damage and decreases the tumor

burden in *Apc*^{min} mouse model of colorectal cancer (Ashton et al., 2010; Faller et al., 2015; Li et al., 2015; Wang et al., 2015; Yousefi et al., 2016, 2017).

My work delineates a requirement for the activity of the Msi-mTORC1 axis in the rare population of reserve ISCs. In these cells, the Msi-mTORC1 is inactive in quiescent stem cells residing in G0, and activation of Msi-mTORC1 is sufficient to drive quiescent stem cells out of G0 and into cell cycle. Conversely, inactivation of this pathway leads to a G1 block in reserve ISCs (Yousefi et al., 2016). Interestingly, a nearly identical phenomenon is observed in LT-HSCs, where Msi2 is both necessary and sufficient for their proper exit from quiescence and cell cycle entry (Kharas et al., 2010; Park et al., 2014). The importance of this mechanism for tissue fidelity can be observed in the intestinal epithelium in the context of injury. I observed that premature upregulation of Msi-mTORC1 signaling drives reserve ISCs out of quiescence. If the tissue is then exposed to DNA damaging injury, these reserve ISCs now become sensitized to DNA damage, undergo cell death, and are no longer able to regenerate the tissue effectively. Thus, these findings show that besides the established effect of dysregulation of quiescence on stem cell exhaustion (Orford and Scadden, 2008), precise regulation of this process is also a determinant of a tissue's response to injury.

Future directions: mimicking calorie restriction, accelerating a cure for cancer, and reducing side effects of therapeutic approaches

Highly proliferative tissues provide a powerful platform to study adult stem cell behavior under basal, tumorigenic, and regenerative conditions. Injury (specifically DNA damage) to the intestinal epithelium is a hallmark of numerous common clinical disorders, including radiation enteropathy, chemotherapy, ischemia-reperfusion, and inflammatory bowel diseases. Disruption of the epithelial barrier in these conditions must be quickly restored to avoid dehydration and translocation of gut microbiota to the bloodstream. My results provide compelling evidence for nutrient sensing in regulation of intestinal stem cell resistance to radiation injury and

subsequently, the tissue's regeneration capacity. Further work is required to address whether the paradigm we established using radiation injury hold true in other injury models (e.g. chemotherapy, ischemia-reperfusion, and inflammation). It will also be critical to understand how nutrient modulation might affect tumor cells at the molecular level, since damage to highly proliferative tissues such as intestinal epithelium is one of the main side effects of cancer treatments by chemotherapy and radiotherapy with the aim of ablating tumor cells. For example, might the beneficial effects of calorie restriction on regeneration of the normal epithelium after chemo/radiation therapy also have unintended protective consequences for tumor initiating cells?

Calorie restriction regulates processes involved in cancer initiation and progression such as apoptosis, proliferation, angiogenesis, inflammation, hormone, and growth factor production. In addition, signaling pathways that are targeted in cancer treatment often overlap with those regulated by calorie restriction, such as Akt-mTORC1 signaling. These observations have led to investigations into CR as a potential treatment for cancer. In animal models, calorie restriction prevents tumor formation, progression, and metastasis (De Lorenzo et al., 2011; Michels and Ekbom, 2004; Phoenix et al., 2010). Rapamycin, a potent inhibitor of mTORC1 signaling, can also decrease the incidence, growth, and metastasis of cancer cells (Anisimov et al., 2011; Boffa et al., 2004; Guba et al., 2002).

Relative independence of cancer cells from external growth and anti-growth signals prevents their proper response to environmental cues (Hanahan and Weinberg, 2011; Lee et al., 2012). *In vitro* studies of cells in the culture have shown that activation of the Akt-mTORC1 signaling pathway, one of the highly upregulated signaling pathways in many tumor types, promotes oxidative stress and sensitizes the cells to oxidative damage partly through inhibition of FoxO transcription factors, which have a conserved role in regulation of detoxifying enzymes (Greer and Brunet, 2005; Nogueira et al., 2008). Following fasting, increased levels of Akt and S6 kinase phosphorylation in cancer cells relative to normal cells sensitize cancer cells to chemotherapeutic agents while protecting the normal cells (Lee et al., 2012; Raffaghello et al., 2008). Consistently, fasting prior to and/or following chemotherapy led to a reduction in fatigue,

weakness, and gastrointestinal side effects in patients with various malignancies including breast, esophageal, prostate, and lung cancers (Raffaghello et al., 2010; Safdie et al., 2009). Calorie restriction could also synergize with radiotherapy to increase the apoptosis of breast cancer cells (Saleh et al., 2013). These results suggest that a nutritional intervention not only can affect tumor initiation, progression, and metastasis, but it can also have additive effects when combined with radiation or chemotherapy.

Further investigation will be required to understand the molecular mechanisms underlying the differential effects of nutrient modulation on normal and cancerous tissues, and specifically tumor initiating and normal stem cells, which are the drivers of cancer and tissue regeneration following cancer treatments such as radiotherapy and chemotherapy. Dietary intervention might not be an optimal choice for cancer patients because of the weight loss associated with cachexia or the side effects of radiation/chemo-therapeutic approaches. However, my work shows that presence of a single amino acid, Leucine, in drinking water prior to the time of radiation can sensitize reserve intestinal stem cells to injury and lead to poor regenerative outcome. This demonstrates the powerful effect nutrient modulation can have on sensitization and recovery of a tissue from injury, and provides strong impetus for further understanding of these effects in humans. Understanding the detailed molecular mechanisms underlying the effects of nutrients on stem and tumor initiating cells may help to target desired pathways involved in tumorigenesis and regeneration using customized diets or small molecules. This may accelerate the development of therapeutic approaches to prevent or cure malignant transformation and tissue damage in patients.

CHAPTER 6

Bibliography

Aberle, H., Bauer, A., Stappert, J., Kispert, A., and Kemler, R. (1997). beta-catenin is a target for the ubiquitin-proteasome pathway. EMBO J. *16*, 3797–3804.

Anisimov, V.N., Zabezhinski, M.A., Popovich, I.G., Piskunova, T.S., Semenchenko, A.V., Tyndyk, M.L., Yurova, M.N., Rosenfeld, S.V., and Blagosklonny, M.V. (2011). Rapamycin increases lifespan and inhibits spontaneous tumorigenesis in inbred female mice. Cell Cycle Georget. Tex *10*, 4230–4236.

Aoki, R., Shoshkes-Carmel, M., Gao, N., Shin, S., May, C.L., Golson, M.L., Zahm, A.M., Ray, M., Wiser, C.L., Wright, C.V.E., et al. (2016). Foxl1-expressing mesenchymal cells constitute the intestinal stem cell niche. Cell. Mol. Gastroenterol. Hepatol. *2*, 175–188.

Asfaha, S., Hayakawa, Y., Muley, A., Stokes, S., Graham, T.A., Ericksen, R.E., Westphalen, C.B., von Burstin, J., Mastracci, T.L., Worthley, D.L., et al. (2015). Krt19(+)/Lgr5(-) Cells Are Radioresistant Cancer-Initiating Stem Cells in the Colon and Intestine. Cell Stem Cell *16*, 627–638.

Ashton, G.H., Morton, J.P., Myant, K., Phesse, T.J., Ridgway, R.A., Marsh, V., Wilkins, J.A., Athineos, D., Muncan, V., Kemp, R., et al. (2010). Focal adhesion kinase is required for intestinal regeneration and tumorigenesis downstream of Wnt/c-Myc signaling. Dev. Cell *19*, 259–269.

Azzolin, L., Panciera, T., Soligo, S., Enzo, E., Bicciato, S., Dupont, S., Bresolin, S., Frasson, C., Basso, G., Guzzardo, V., et al. (2014). YAP/TAZ incorporation in the β-catenin destruction complex orchestrates the Wnt response. Cell *158*, 157–170.

Barker, N., van Es, J.H., Kuipers, J., Kujala, P., van den Born, M., Cozijnsen, M., Haegebarth, A., Korving, J., Begthel, H., Peters, P.J., et al. (2007). Identification of stem cells in small intestine and colon by marker gene Lgr5. Nature *449*, 1003–1007.

Barker, N., Ridgway, R.A., van Es, J.H., van de Wetering, M., Begthel, H., van den Born, M., Danenberg, E., Clarke, A.R., Sansom, O.J., and Clevers, H. (2009). Crypt stem cells as the cells-of-origin of intestinal cancer. Nature *457*, 608–611.

Barry, E.R., Morikawa, T., Butler, B.L., Shrestha, K., de la Rosa, R., Yan, K.S., Fuchs, C.S., Magness, S.T., Smits, R., Ogino, S., et al. (2013). Restriction of intestinal stem cell expansion and the regenerative response by YAP. Nature *493*, 106–110.

Bernitz, J.M., Kim, H.S., MacArthur, B., Sieburg, H., and Moore, K. (2016). Hematopoietic Stem Cells Count and Remember Self-Renewal Divisions. Cell *167*, 1296–1309.e10.

Biteau, B., Hochmuth, C.E., and Jasper, H. (2011). Maintaining tissue homeostasis: dynamic control of somatic stem cell activity. Cell Stem Cell *9*, 402–411.

Blikslager, A.T., Moeser, A.J., Gookin, J.L., Jones, S.L., and Odle, J. (2007). Restoration of barrier function in injured intestinal mucosa. Physiol. Rev. *87*, 545–564.

Boffa, D.J., Luan, F., Thomas, D., Yang, H., Sharma, V.K., Lagman, M., and Suthanthiran, M. (2004). Rapamycin inhibits the growth and metastatic progression of non-small cell lung cancer. Clin. Cancer Res. Off. J. Am. Assoc. Cancer Res. *10*, 293–300.

Bossuyt, W., Chen, C.-L., Chen, Q., Sudol, M., McNeill, H., Pan, D., Kopp, A., and Halder, G. (2014). An evolutionary shift in the regulation of the Hippo pathway between mice and flies. Oncogene *33*, 1218–1228.

Breault, D.T., Min, I.M., Carlone, D.L., Farilla, L.G., Ambruzs, D.M., Henderson, D.E., Algra, S., Montgomery, R.K., Wagers, A.J., and Hole, N. (2008). Generation of mTert-GFP mice as a model to identify and study tissue progenitor cells. Proc. Natl. Acad. Sci. U. S. A. *105*, 10420–10425.

Buczacki, S.J.A., Zecchini, H.I., Nicholson, A.M., Russell, R., Vermeulen, L., Kemp, R., and Winton, D.J. (2013). Intestinal label-retaining cells are secretory precursors expressing Lgr5. Nature *495*, 65–69.

Cai, J., Zhang, N., Zheng, Y., de Wilde, R.F., Maitra, A., and Pan, D. (2010). The Hippo signaling pathway restricts the oncogenic potential of an intestinal regeneration program. Genes Dev. *24*, 2383–2388.

Cairns, J. (1975). Mutation selection and the natural history of cancer. Nature *255*, 197–200.

Cappuzzo, F., Finocchiaro, G., Rossi, E., Jänne, P.A., Carnaghi, C., Calandri, C., Bencardino, K., Ligorio, C., Ciardiello, F., Pressiani, T., et al. (2008). EGFR FISH assay predicts for response to cetuximab in chemotherapy refractory colorectal cancer patients. Ann. Oncol. Off. J. Eur. Soc. Med. Oncol. *19*, 717–723.

Carneiro-Filho, B.A., Lima, I.P.F., Araujo, D.H., Cavalcante, M.C., Carvalho, G.H.P., Brito, G. a. C., Lima, V., Monteiro, S.M.N., Santos, F.N., Ribeiro, R.A., et al. (2004). Intestinal barrier function and secretion in methotrexate-induced rat intestinal mucositis. Dig. Dis. Sci. *49*, 65–72.

Cerletti, M., Jang, Y.C., Finley, L.W.S., Haigis, M.C., and Wagers, A.J. (2012). Short-term calorie restriction enhances skeletal muscle stem cell function. Cell Stem Cell *10*, 515–519.

Ch'ang, H.-J., Maj, J.G., Paris, F., Xing, H.R., Zhang, J., Truman, J.-P., Cardon-Cardo, C., Haimovitz-Friedman, A., Kolesnick, R., and Fuks, Z. (2005). ATM regulates target switching to escalating doses of radiation in the intestines. Nat. Med. *11*, 484–490.

Chen, J., Astle, C.M., and Harrison, D.E. (2003). Hematopoietic senescence is postponed and hematopoietic stem cell function is enhanced by dietary restriction. Exp. Hematol. *31*, 1097–1103.

Cheng, H., and Leblond, C.P. (1974). Origin, differentiation and renewal of the four main epithelial cell types in the mouse small intestine. V. Unitarian Theory of the origin of the four epithelial cell types. Am. J. Anat. *141*, 537–561.

Cheung, T.H., and Rando, T.A. (2013). Molecular regulation of stem cell quiescence. Nat. Rev. Mol. Cell Biol. *14*, 329–340.

Clevers, H., and Nusse, R. (2012). Wnt/β-catenin signaling and disease. Cell *149*, 1192–1205.

Colman, R.J., Anderson, R.M., Johnson, S.C., Kastman, E.K., Kosmatka, K.J., Beasley, T.M., Allison, D.B., Cruzen, C., Simmons, H.A., Kemnitz, J.W., et al. (2009). Caloric restriction delays disease onset and mortality in rhesus monkeys. Science *325*, 201–204.

Crist, C.G., Montarras, D., and Buckingham, M. (2012). Muscle satellite cells are primed for myogenesis but maintain quiescence with sequestration of Myf5 mRNA targeted by microRNA-31 in mRNP granules. Cell Stem Cell *11*, 118–126.

De Lorenzo, M.S., Baljinnyam, E., Vatner, D.E., Abarzúa, P., Vatner, S.F., and Rabson, A.B. (2011). Caloric restriction reduces growth of mammary tumors and metastases. Carcinogenesis *32*, 1381–1387.

Dibble, C.C., and Manning, B.D. (2013). Signal integration by mTORC1 coordinates nutrient input with biosynthetic output. Nat. Cell Biol. *15*, 555–564.

Durand, A., Donahue, B., Peignon, G., Letourneur, F., Cagnard, N., Slomianny, C., Perret, C., Shroyer, N.F., and Romagnolo, B. (2012). Functional intestinal stem cells after Paneth cell ablation induced by the loss of transcription factor Math1 (Atoh1). Proc. Natl. Acad. Sci. U. S. A. *109*, 8965–8970.

Ertl, R.P., Chen, J., Astle, C.M., Duffy, T.M., and Harrison, D.E. (2008). Effects of dietary restriction on hematopoietic stem-cell aging are genetically regulated. Blood *111*, 1709–1716.

van Es, J.H., van Gijn, M.E., Riccio, O., van den Born, M., Vooijs, M., Begthel, H., Cozijnsen, M., Robine, S., Winton, D.J., Radtke, F., et al. (2005). Notch/gamma-secretase inhibition turns proliferative cells in intestinal crypts and adenomas into goblet cells. Nature *435*, 959–963.

van Es, J.H., de Geest, N., van de Born, M., Clevers, H., and Hassan, B.A. (2010). Intestinal stem cells lacking the Math1 tumour suppressor are refractory to Notch inhibitors. Nat. Commun. *1*, 18.

van Es, J.H., Sato, T., van de Wetering, M., Lyubimova, A., Nee, A.N.Y., Gregorieff, A., Sasaki, N., Zeinstra, L., van den Born, M., Korving, J., et al. (2012a). Dll1+ secretory progenitor cells revert to stem cells upon crypt damage. Nat. Cell Biol. *14*, 1099–1104.

van Es, J.H., Haegebarth, A., Kujala, P., Itzkovitz, S., Koo, B.-K., Boj, S.F., Korving, J., van den Born, M., van Oudenaarden, A., Robine, S., et al. (2012b). A critical role for the Wnt effector Tcf4 in adult intestinal homeostatic self-renewal. Mol. Cell. Biol. *32*, 1918–1927.

Faller, W.J., Jackson, T.J., Knight, J.R.P., Ridgway, R.A., Jamieson, T., Karim, S.A., Jones, C., Radulescu, S., Huels, D.J., Myant, K.B., et al. (2015). mTORC1-mediated translational elongation limits intestinal tumour initiation and growth. Nature *517*, 497–500.

Farin, H.F., Van Es, J.H., and Clevers, H. (2012). Redundant sources of Wnt regulate intestinal stem cells and promote formation of Paneth cells. Gastroenterology *143*, 1518–1529.e7.

Fischer, M., Yen, W.-C., Kapoun, A.M., Wang, M., O'Young, G., Lewicki, J., Gurney, A., and Hoey, T. (2011). Anti-DLL4 inhibits growth and reduces tumor-initiating cell frequency in colorectal tumors with oncogenic KRAS mutations. Cancer Res. *71*, 1520–1525.

Fox, H.L., Pham, P.T., Kimball, S.R., Jefferson, L.S., and Lynch, C.J. (1998). Amino acid effects on translational repressor 4E-BP1 are mediated primarily by L-leucine in isolated adipocytes. Am. J. Physiol. *275*, C1232-1238.

Fre, S., Huyghe, M., Mourikis, P., Robine, S., Louvard, D., and Artavanis-Tsakonas, S. (2005). Notch signals control the fate of immature progenitor cells in the intestine. Nature *435*, 964–968.

Fujishita, T., Aoki, K., Lane, H.A., Aoki, M., and Taketo, M.M. (2008). Inhibition of the mTORC1 pathway suppresses intestinal polyp formation and reduces mortality in ApcDelta716 mice. Proc. Natl. Acad. Sci. U. S. A. *105*, 13544–13549.

Fukada, S., Uezumi, A., Ikemoto, M., Masuda, S., Segawa, M., Tanimura, N., Yamamoto, H., Miyagoe-Suzuki, Y., and Takeda, S. 'ichi (2007). Molecular signature of quiescent satellite cells in adult skeletal muscle. Stem Cells Dayt. Ohio *25*, 2448–2459.

Greer, E.L., and Brunet, A. (2005). FOXO transcription factors at the interface between longevity and tumor suppression. Oncogene *24*, 7410–7425.

Gregorieff, A., Pinto, D., Begthel, H., Destrée, O., Kielman, M., and Clevers, H. (2005). Expression pattern of Wnt signaling components in the adult intestine. Gastroenterology *129*, 626–638.

Grootjans, J., Lenaerts, K., Derikx, J.P.M., Matthijsen, R.A., de Bruïne, A.P., van Bijnen, A.A., van Dam, R.M., Dejong, C.H.C., and Buurman, W.A. (2010). Human intestinal ischemia-reperfusion-induced inflammation characterized: experiences from a new translational model. Am. J. Pathol. *176*, 2283–2291.

Groszer, M. (2001). Negative Regulation of Neural Stem/Progenitor Cell Proliferation by the Pten Tumor Suppressor Gene in Vivo. Science *294*, 2186–2189.

Guarente, L. (2005). Calorie restriction and SIR2 genes--towards a mechanism. Mech. Ageing Dev. *126*, 923–928.

Guba, M., von Breitenbuch, P., Steinbauer, M., Koehl, G., Flegel, S., Hornung, M., Bruns, C.J., Zuelke, C., Farkas, S., Anthuber, M., et al. (2002). Rapamycin inhibits primary and metastatic

tumor growth by antiangiogenesis: involvement of vascular endothelial growth factor. Nat. Med. *8*, 128–135.

Gulhati, P., Cai, Q., Li, J., Liu, J., Rychahou, P.G., Qiu, S., Lee, E.Y., Silva, S.R., Bowen, K.A., Gao, T., et al. (2009). Targeted inhibition of mammalian target of rapamycin signaling inhibits tumorigenesis of colorectal cancer. Clin. Cancer Res. Off. J. Am. Assoc. Cancer Res. *15*, 7207–7216.

Hanahan, D., and Weinberg, R. (2011). Hallmarks of Cancer: The Next Generation. Cell *144*, 646–674.

Haramis, A.-P.G., Begthel, H., van den Born, M., van Es, J., Jonkheer, S., Offerhaus, G.J.A., and Clevers, H. (2004). De novo crypt formation and juvenile polyposis on BMP inhibition in mouse intestine. Science *303*, 1684–1686.

Hardwick, J.C., Kodach, L.L., Offerhaus, G.J., and van den Brink, G.R. (2008). Bone morphogenetic protein signalling in colorectal cancer. Nat. Rev. Cancer *8*, 806–812.

Harrison, D.E., Strong, R., Sharp, Z.D., Nelson, J.F., Astle, C.M., Flurkey, K., Nadon, N.L., Wilkinson, J.E., Frenkel, K., Carter, C.S., et al. (2009). Rapamycin fed late in life extends lifespan in genetically heterogeneous mice. Nature.

Haug, J.S., He, X.C., Grindley, J.C., Wunderlich, J.P., Gaudenz, K., Ross, J.T., Paulson, A., Wagner, K.P., Xie, Y., Zhu, R., et al. (2008). N-cadherin expression level distinguishes reserved versus primed states of hematopoietic stem cells. Cell Stem Cell *2*, 367–379.

He, X.C., Zhang, J., Tong, W.-G., Tawfik, O., Ross, J., Scoville, D.H., Tian, Q., Zeng, X., He, X., Wiedemann, L.M., et al. (2004). BMP signaling inhibits intestinal stem cell self-renewal through suppression of Wnt-beta-catenin signaling. Nat. Genet. *36*, 1117–1121.

Hoey, T., Yen, W.-C., Axelrod, F., Basi, J., Donigian, L., Dylla, S., Fitch-Bruhns, M., Lazetic, S., Park, I.-K., Sato, A., et al. (2009). DLL4 blockade inhibits tumor growth and reduces tumor-initiating cell frequency. Cell Stem Cell *5*, 168–177.

Hope, K.J., Cellot, S., Ting, S.B., MacRae, T., Mayotte, N., Iscove, N.N., and Sauvageau, G. (2010). An RNAi screen identifies Msi2 and Prox1 as having opposite roles in the regulation of hematopoietic stem cell activity. Cell Stem Cell *7*, 101–113.

Houthoofd, K., and Vanfleteren, J.R. (2006). The longevity effect of dietary restriction in Caenorhabditis elegans. Exp. Gerontol. *41*, 1026–1031.

Howe, J.R., Roth, S., Ringold, J.C., Summers, R.W., Järvinen, H.J., Sistonen, P., Tomlinson, I.P., Houlston, R.S., Bevan, S., Mitros, F.A., et al. (1998). Mutations in the SMAD4/DPC4 gene in juvenile polyposis. Science *280*, 1086–1088.

Howe, J.R., Bair, J.L., Sayed, M.G., Anderson, M.E., Mitros, F.A., Petersen, G.M., Velculescu, V.E., Traverso, G., and Vogelstein, B. (2001). Germline mutations of the gene encoding bone morphogenetic protein receptor 1A in juvenile polyposis. Nat. Genet. *28*, 184–187.

Hüttmann, A., Liu, S.L., Boyd, A.W., and Li, C.L. (2001). Functional heterogeneity within rhodamine123(lo) Hoechst33342(lo/sp) primitive hemopoietic stem cells revealed by pyronin Y. Exp. Hematol. *29*, 1109–1116.

Igarashi, M., and Guarente, L. (2016). mTORC1 and SIRT1 Cooperate to Foster Expansion of Gut Adult Stem Cells during Calorie Restriction. Cell *166*, 436–450.

Inoki, K., Ouyang, H., Zhu, T., Lindvall, C., Wang, Y., Zhang, X., Yang, Q., Bennett, C., Harada, Y., Stankunas, K., et al. (2006). TSC2 Integrates Wnt and Energy Signals via a Coordinated Phosphorylation by AMPK and GSK3 to Regulate Cell Growth. Cell *126*, 955–968.

Ito, T., Kwon, H.Y., Zimdahl, B., Congdon, K.L., Blum, J., Lento, W.E., Zhao, C., Lagoo, A., Gerrard, G., Foroni, L., et al. (2010). Regulation of myeloid leukaemia by the cell-fate determinant Musashi. Nature *466*, 765–768.

Itzkovitz, S., Lyubimova, A., Blat, I.C., Maynard, M., van Es, J., Lees, J., Jacks, T., Clevers, H., and van Oudenaarden, A. (2011). Single-molecule transcript counting of stem-cell markers in the mouse intestine. Nat. Cell Biol. *14*, 106–114.

Jensen, J., Pedersen, E.E., Galante, P., Hald, J., Heller, R.S., Ishibashi, M., Kageyama, R., Guillemot, F., Serup, P., and Madsen, O.D. (2000). Control of endodermal endocrine development by Hes-1. Nat. Genet. *24*, 36–44.

Kabiri, Z., Greicius, G., Madan, B., Biechele, S., Zhong, Z., Zaribafzadeh, H., Edison, null, Aliyev, J., Wu, Y., Bunte, R., et al. (2014a). Stroma provides an intestinal stem cell niche in the absence of epithelial Wnts. Dev. Camb. Engl. *141*, 2206–2215.

Kabiri, Z., Greicius, G., Madan, B., Biechele, S., Zhong, Z., Zaribafzadeh, H., Edison, null, Aliyev, J., Wu, Y., Bunte, R., et al. (2014b). Stroma provides an intestinal stem cell niche in the absence of epithelial Wnts. Dev. Camb. Engl. *141*, 2206–2215.

Kalaany, N.Y., and Sabatini, D.M. (2009). Tumours with PI3K activation are resistant to dietary restriction. Nature *458*, 725–731.

Kalaitzidis, D., Sykes, S.M., Wang, Z., Punt, N., Tang, Y., Ragu, C., Sinha, A.U., Lane, S.W., Souza, A.L., Clish, C.B., et al. (2012). mTOR complex 1 plays critical roles in hematopoiesis and Pten-loss-evoked leukemogenesis. Cell Stem Cell *11*, 429–439.

Katoh, M., and Katoh, M. (2007). Notch signaling in gastrointestinal tract (review). Int. J. Oncol. *30*, 247–251.

Katz, Y., Li, F., Lambert, N.J., Sokol, E.S., Tam, W.-L., Cheng, A.W., Airoldi, E.M., Lengner, C.J., Gupta, P.B., Yu, Z., et al. (2014). Musashi proteins are post-transcriptional regulators of the epithelial-luminal cell state. eLife *3*, e03915.

Keefe, D.M., Brealey, J., Goland, G.J., and Cummins, A.G. (2000). Chemotherapy for cancer causes apoptosis that precedes hypoplasia in crypts of the small intestine in humans. Gut *47*, 632–637.

Kharas, M.G., Lengner, C.J., Al-Shahrour, F., Bullinger, L., Ball, B., Zaidi, S., Morgan, K., Tam, W., Paktinat, M., Okabe, R., et al. (2010). Musashi-2 regulates normal hematopoiesis and promotes aggressive myeloid leukemia. Nat. Med. *16*, 903–908.

Kiel, M.J., He, S., Ashkenazi, R., Gentry, S.N., Teta, M., Kushner, J.A., Jackson, T.L., and Morrison, S.J. (2007). Haematopoietic stem cells do not asymmetrically segregate chromosomes or retain BrdU. Nature *449*, 238–242.

Kim, T.-H., Escudero, S., and Shivdasani, R.A. (2012). Intact function of Lgr5 receptor-expressing intestinal stem cells in the absence of Paneth cells. Proc. Natl. Acad. Sci. U. S. A. *109*, 3932–3937.

Korinek, V., Barker, N., Moerer, P., van Donselaar, E., Huls, G., Peters, P.J., and Clevers, H. (1998). Depletion of epithelial stem-cell compartments in the small intestine of mice lacking Tcf-4. Nat. Genet. *19*, 379–383.

Kostetskii, I., Li, J., Xiong, Y., Zhou, R., Ferrari, V.A., Patel, V.V., Molkentin, J.D., and Radice, G.L. (2005). Induced deletion of the N-cadherin gene in the heart leads to dissolution of the intercalated disc structure. Circ. Res. *96*, 346–354.

Kuhnert, F., Davis, C.R., Wang, H.-T., Chu, P., Lee, M., Yuan, J., Nusse, R., and Kuo, C.J. (2004). Essential requirement for Wnt signaling in proliferation of adult small intestine and colon revealed by adenoviral expression of Dickkopf-1. Proc. Natl. Acad. Sci. U. S. A. *101*, 266–271.

Kwiatkowski, D.J., Zhang, H., Bandura, J.L., Heiberger, K.M., Glogauer, M., el-Hashemite, N., and Onda, H. (2002). A mouse model of TSC1 reveals sex-dependent lethality from liver hemangiomas, and up-regulation of p70S6 kinase activity in Tsc1 null cells. Hum. Mol. Genet. *11*, 525–534.

Kwong, L.N., and Dove, W.F. (2009). APC and its modifiers in colon cancer. Adv. Exp. Med. Biol. *656*, 85–106.

Laplante, M., and Sabatini, D.M. (2009). mTOR signaling at a glance. J. Cell Sci. *122*, 3589–3594.

Lee, C., Raffaghello, L., Brandhorst, S., Safdie, F.M., Bianchi, G., Martin-Montalvo, A., Pistoia, V., Wei, M., Hwang, S., Merlino, A., et al. (2012). Fasting Cycles Retard Growth of Tumors and Sensitize a Range of Cancer Cell Types to Chemotherapy. Sci. Transl. Med. *4*, 124ra27-124ra27.

Lee, K.-P., Lee, J.-H., Kim, T.-S., Kim, T.-H., Park, H.-D., Byun, J.-S., Kim, M.-C., Jeong, W.-I., Calvisi, D.F., Kim, J.-M., et al. (2010). The Hippo-Salvador pathway restrains hepatic oval cell proliferation, liver size, and liver tumorigenesis. Proc. Natl. Acad. Sci. U. S. A. *107*, 8248–8253.

Lei, Q.-Y., Zhang, H., Zhao, B., Zha, Z.-Y., Bai, F., Pei, X.-H., Zhao, S., Xiong, Y., and Guan, K.-L. (2008). TAZ promotes cell proliferation and epithelial-mesenchymal transition and is inhibited by the hippo pathway. Mol. Cell. Biol. *28*, 2426–2436.

Li, L., and Clevers, H. (2010). Coexistence of quiescent and active adult stem cells in mammals. Science *327*, 542–545.

Li, N., Yousefi, M., Nakauka-Ddamba, A., Jain, R., Tobias, J., Epstein, J.A., Jensen, S.T., and Lengner, C.J. (2014). Single-cell analysis of proxy reporter allele-marked epithelial cells establishes intestinal stem cell hierarchy. Stem Cell Rep. *3*, 876–891.

Li, N., Yousefi, M., Nakauka-Ddamba, A., Li, F., Vandivier, L., Parada, K., Woo, D.-H., Wang, S., Naqvi, A.S., Rao, S., et al. (2015). The Msi Family of RNA-Binding Proteins Function Redundantly as Intestinal Oncoproteins. Cell Rep. *13*, 2440–2455.

Li, N., Yousefi, M., Nakauka-Ddamba, A., Tobias, J.W., Jensen, S.T., Morrisey, E.E., and Lengner, C.J. (2016a). Heterogeneity in readouts of canonical wnt pathway activity within intestinal crypts. Dev. Dyn. Off. Publ. Am. Assoc. Anat. *245*, 822–833.

Li, N., Nakauka-Ddamba, A., Tobias, J., Jensen, S.T., and Lengner, C.J. (2016b). Mouse Label-Retaining Cells Are Molecularly and Functionally Distinct From Reserve Intestinal Stem Cells. Gastroenterology *151*, 298–310.e7.

Li, N., Nakauka-Ddamba, A., Tobias, J., Jensen, S.T., and Lengner, C.J. (2016c). Mouse Label-Retaining Cells Are Molecularly and Functionally Distinct From Reserve Intestinal Stem Cells. Gastroenterology *151*, 298–310.e7.

Li, V.S.W., Ng, S.S., Boersema, P.J., Low, T.Y., Karthaus, W.R., Gerlach, J.P., Mohammed, S., Heck, A.J.R., Maurice, M.M., Mahmoudi, T., et al. (2012). Wnt signaling through inhibition of β-catenin degradation in an intact Axin1 complex. Cell *149*, 1245–1256.

Liu, S.K., Bham, S.A.S., Fokas, E., Beech, J., Im, J., Cho, S., Harris, A.L., and Muschel, R.J. (2011). Delta-like ligand 4-notch blockade and tumor radiation response. J. Natl. Cancer Inst. *103*, 1778–1798.

Logeat, F., Bessia, C., Brou, C., LeBail, O., Jarriault, S., Seidah, N.G., and Israël, A. (1998). The Notch1 receptor is cleaved constitutively by a furin-like convertase. Proc. Natl. Acad. Sci. U. S. A. *95*, 8108–8112.

Ma, B., Chen, Y., Chen, L., Cheng, H., Mu, C., Li, J., Gao, R., Zhou, C., Cao, L., Liu, J., et al. (2015). Hypoxia regulates Hippo signalling through the SIAH2 ubiquitin E3 ligase. Nat. Cell Biol. *17*, 95–103.

Mair, W., and Dillin, A. (2008). Aging and survival: the genetics of life span extension by dietary restriction. Annu. Rev. Biochem. *77*, 727–754.

Maria Cambuli, F., Rezza, A., Nadjar, J., and Plateroti, M. (2013). Brief report: musashi1-eGFP mice, a new tool for differential isolation of the intestinal stem cell populations. Stem Cells Dayt. Ohio *31*, 2273–2278.

el Marjou, F., Janssen, K.-P., Chang, B.H.-J., Li, M., Hindie, V., Chan, L., Louvard, D., Chambon, P., Metzger, D., and Robine, S. (2004). Tissue-specific and inducible Cre-mediated recombination in the gut epithelium. Genes. N. Y. N 2000 *39*, 186–193.

Markowitz, S., Wang, J., Myeroff, L., Parsons, R., Sun, L., Lutterbaugh, J., Fan, R.S., Zborowska, E., Kinzler, K.W., and Vogelstein, B. (1995). Inactivation of the type II TGF-beta receptor in colon cancer cells with microsatellite instability. Science *268*, 1336–1338.

McCay, C.M., Crowell, M.F., and Maynard, L.A. (1989). The effect of retarded growth upon the length of life span and upon the ultimate body size. 1935. Nutr. Burbank Los Angel. Cty. Calif *5*, 155–171; discussion 172.

Melichar, B., and Zezulová, M. (2011). The significance of altered gastrointestinal permeability in cancer patients. Curr. Opin. Support. Palliat. Care *5*, 47–54.

Meng, Z., Moroishi, T., and Guan, K.-L. (2016). Mechanisms of Hippo pathway regulation. Genes Dev. *30*, 1–17.

Metcalfe, C., Kljavin, N.M., Ybarra, R., and de Sauvage, F.J. (2014). Lgr5+ stem cells are indispensable for radiation-induced intestinal regeneration. Cell Stem Cell *14*, 149–159.

Michels, K.B., and Ekbom, A. (2004). Caloric restriction and incidence of breast cancer. JAMA *291*, 1226–1230.

Milano, J., McKay, J., Dagenais, C., Foster-Brown, L., Pognan, F., Gadient, R., Jacobs, R.T., Zacco, A., Greenberg, B., and Ciaccio, P.J. (2004). Modulation of notch processing by gamma-secretase inhibitors causes intestinal goblet cell metaplasia and induction of genes known to specify gut secretory lineage differentiation. Toxicol. Sci. Off. J. Soc. Toxicol. *82*, 341–358.

Montgomery, R.K., Carlone, D.L., Richmond, C.A., Farilla, L., Kranendonk, M.E.G., Henderson, D.E., Baffour-Awuah, N.Y., Ambruzs, D.M., Fogli, L.K., Algra, S., et al. (2011). Mouse telomerase reverse transcriptase (mTert) expression marks slowly cycling intestinal stem cells. Proc. Natl. Acad. Sci. U. S. A. *108*, 179–184.

Moore, K.A., and Lemischka, I.R. (2006). Stem cells and their niches. Science *311*, 1880–1885.

Morley, S.J., and Traugh, J.A. (1990). Differential stimulation of phosphorylation of initiation factors eIF-4F, eIF-4B, eIF-3, and ribosomal protein S6 by insulin and phorbol esters. J. Biol. Chem. *265*, 10611–10616.

Nejdfors, P., Ekelund, M., Weström, B.R., Willén, R., and Jeppsson, B. (2000). Intestinal permeability in humans is increased after radiation therapy. Dis. Colon Rectum *43*, 1582-1587-1588.

Noah, T.K., and Shroyer, N.F. (2013). Notch in the intestine: regulation of homeostasis and pathogenesis. Annu. Rev. Physiol. *75*, 263–288.

Nogueira, V., Park, Y., Chen, C.-C., Xu, P.-Z., Chen, M.-L., Tonic, I., Unterman, T., and Hay, N. (2008). Akt Determines Replicative Senescence and Oxidative or Oncogenic Premature Senescence and Sensitizes Cells to Oxidative Apoptosis. Cancer Cell *14*, 458–470.

Orford, K.W., and Scadden, D.T. (2008). Deconstructing stem cell self-renewal: genetic insights into cell-cycle regulation. Nat. Rev. Genet. *9*, 115–128.

Park, S.-M., Deering, R.P., Lu, Y., Tivnan, P., Lianoglou, S., Al-Shahrour, F., Ebert, B.L., Hacohen, N., Leslie, C., Daley, G.Q., et al. (2014). Musashi-2 controls cell fate, lineage bias, and TGF-β signaling in HSCs. J. Exp. Med. *211*, 71–87.

Pazhanisamy, S.K. (2009). Stem cells, DNA damage, ageing and cancer. Hematol. Oncol. Stem Cell Ther. *2*, 375–384.

Phoenix, K.N., Vumbaca, F., Fox, M.M., Evans, R., and Claffey, K.P. (2010). Dietary energy availability affects primary and metastatic breast cancer and metformin efficacy. Breast Cancer Res. Treat. *123*, 333–344.

Pietras, E.M., Warr, M.R., and Passegué, E. (2011). Cell cycle regulation in hematopoietic stem cells. J. Cell Biol. *195*, 709–720.

Potten, C.S. (2004). Radiation, the ideal cytotoxic agent for studying the cell biology of tissues such as the small intestine. Radiat. Res. *161*, 123–136.

Potten, C.S., Hume, W.J., Reid, P., and Cairns, J. (1978). The segregation of DNA in epithelial stem cells. Cell *15*, 899–906.

Potten, C.S., Owen, G., and Booth, D. (2002). Intestinal stem cells protect their genome by selective segregation of template DNA strands. J. Cell Sci. *115*, 2381–2388.

Potten, C.S., Booth, C., Tudor, G.L., Booth, D., Brady, G., Hurley, P., Ashton, G., Clarke, R., Sakakibara, S., and Okano, H. (2003). Identification of a putative intestinal stem cell and early lineage marker; musashi-1. Differ. Res. Biol. Divers. *71*, 28–41.

Powell, A.E., Wang, Y., Li, Y., Poulin, E.J., Means, A.L., Washington, M.K., Higginbotham, J.N., Juchheim, A., Prasad, N., Levy, S.E., et al. (2012). The pan-ErbB negative regulator Lrig1 is an intestinal stem cell marker that functions as a tumor suppressor. Cell *149*, 146–158.

Powers, T., and Walter, P. (1999). Regulation of ribosome biogenesis by the rapamycin-sensitive TOR-signaling pathway in Saccharomyces cerevisiae. Mol. Biol. Cell *10*, 987–1000.

Raffaghello, L., Lee, C., Safdie, F.M., Wei, M., Madia, F., Bianchi, G., and Longo, V.D. (2008). Starvation-dependent differential stress resistance protects normal but not cancer cells against high-dose chemotherapy. Proc. Natl. Acad. Sci. *105*, 8215–8220.

Raffaghello, L., Safdie, F., Bianchi, G., Dorff, T., Fontana, L., and Longo, V.D. (2010). Fasting and differential chemotherapy protection in patients. Cell Cycle *9*, 4474–4476.

Riccio, O., van Gijn, M.E., Bezdek, A.C., Pellegrinet, L., van Es, J.H., Zimber-Strobl, U., Strobl, L.J., Honjo, T., Clevers, H., and Radtke, F. (2008). Loss of intestinal crypt progenitor cells owing to inactivation of both Notch1 and Notch2 is accompanied by derepression of CDK inhibitors p27Kip1 and p57Kip2. EMBO Rep. *9*, 377–383.

Richmond, C.A., Shah, M.S., Deary, L.T., Trotier, D.C., Thomas, H., Ambruzs, D.M., Jiang, L., Whiles, B.B., Rickner, H.D., Montgomery, R.K., et al. (2015). Dormant Intestinal Stem Cells Are Regulated by PTEN and Nutritional Status. Cell Rep. *13*, 2403–2411.

Roche, K.C., Gracz, A.D., Liu, X.F., Newton, V., Akiyama, H., and Magness, S.T. (2015). SOX9 maintains reserve stem cells and preserves radioresistance in mouse small intestine. Gastroenterology *149*, 1553–1563.e10.

Rodgers, J.T., King, K.Y., Brett, J.O., Cromie, M.J., Charville, G.W., Maguire, K.K., Brunson, C., Mastey, N., Liu, L., Tsai, C.-R., et al. (2014). mTORC1 controls the adaptive transition of quiescent stem cells from G0 to G(Alert). Nature *510*, 393–396.

Roskoski, R. (2014). The ErbB/HER family of protein-tyrosine kinases and cancer. Pharmacol. Res. *79*, 34–74.

Rossi, D.J., Jamieson, C.H.M., and Weissman, I.L. (2008). Stems cells and the pathways to aging and cancer. Cell *132*, 681–696.

Roth, S., Franken, P., Sacchetti, A., Kremer, A., Anderson, K., Sansom, O., and Fodde, R. (2012). Paneth cells in intestinal homeostasis and tissue injury. PloS One *7*, e38965.

Russo, F., Linsalata, M., Clemente, C., D'Attoma, B., Orlando, A., Campanella, G., Giotta, F., and Riezzo, G. (2013). The effects of fluorouracil, epirubicin, and cyclophosphamide (FEC60) on the intestinal barrier function and gut peptides in breast cancer patients: an observational study. BMC Cancer *13*, 56.

Safdie, F.M., Dorff, T., Quinn, D., Fontana, L., Wei, M., Lee, C., Cohen, P., and Longo, V.D. (2009). Fasting and cancer treatment in humans: A case series report. Aging *1*, 988–1007.

Sakakibara, S., Nakamura, Y., Yoshida, T., Shibata, S., Koike, M., Takano, H., Ueda, S., Uchiyama, Y., Noda, T., and Okano, H. (2002). RNA-binding protein Musashi family: roles for CNS stem cells and a subpopulation of ependymal cells revealed by targeted disruption and antisense ablation. Proc. Natl. Acad. Sci. U. S. A. *99*, 15194–15199.

Saleh, A., Simone, B., Palazzo, J., Savage, J.E., Sano, Y., Dan, T., Jin, L., Champ, C., Zhao, S., Lim, M., et al. (2013). Caloric restriction augments radiation efficacy in breast cancer. Cell Cycle *12*, 1955–1963.

Samuels, Y., and Waldman, T. (2010). Oncogenic mutations of PIK3CA in human cancers. Curr. Top. Microbiol. Immunol. *347*, 21–41.

Samuels, Y., Wang, Z., Bardelli, A., Silliman, N., Ptak, J., Szabo, S., Yan, H., Gazdar, A., Powell, S.M., Riggins, G.J., et al. (2004). High frequency of mutations of the PIK3CA gene in human cancers. Science *304*, 554.

San Roman, A.K., Jayewickreme, C.D., Murtaugh, L.C., and Shivdasani, R.A. (2014). Wnt secretion from epithelial cells and subepithelial myofibroblasts is not required in the mouse intestinal stem cell niche in vivo. Stem Cell Rep. *2*, 127–134.

Sangiorgi, E., and Capecchi, M.R. (2008). Bmi1 is expressed in vivo in intestinal stem cells. Nat. Genet. *40*, 915–920.

Sansom, O.J., Reed, K.R., Hayes, A.J., Ireland, H., Brinkmann, H., Newton, I.P., Batlle, E., Simon-Assmann, P., Clevers, H., Nathke, I.S., et al. (2004). Loss of Apc in vivo immediately perturbs Wnt signaling, differentiation, and migration. Genes Dev. *18*, 1385–1390.

Sato, T., Vries, R.G., Snippert, H.J., van de Wetering, M., Barker, N., Stange, D.E., van Es, J.H., Abo, A., Kujala, P., Peters, P.J., et al. (2009). Single Lgr5 stem cells build crypt-villus structures in vitro without a mesenchymal niche. Nature *459*, 262–265.

Sato, T., van Es, J.H., Snippert, H.J., Stange, D.E., Vries, R.G., van den Born, M., Barker, N., Shroyer, N.F., van de Wetering, M., and Clevers, H. (2011). Paneth cells constitute the niche for Lgr5 stem cells in intestinal crypts. Nature *469*, 415–418.

Schröder, N., and Gossler, A. (2002). Expression of Notch pathway components in fetal and adult mouse small intestine. Gene Expr. Patterns GEP *2*, 247–250.

Seiler, K.M., Schenhals, E.L., von Furstenberg, R.J., Allena, B.K., Smith, B.J., Scaria, D., Bresler, M.N., Dekaney, C.M., and Henning, S.J. (2015). Tissue underlying the intestinal epithelium elicits proliferation of intestinal stem cells following cytotoxic damage. Cell Tissue Res. *361*, 427–438.

Sengupta, S., Peterson, T.R., Laplante, M., Oh, S., and Sabatini, D.M. (2010). mTORC1 controls fasting-induced ketogenesis and its modulation by ageing. Nature *468*, 1100–1104.

Shah, S.C., Colombel, J.-F., Sands, B.E., and Narula, N. (2016). Mucosal Healing Is Associated With Improved Long-term Outcomes of Patients With Ulcerative Colitis: A Systematic Review and

Meta-analysis. Clin. Gastroenterol. Hepatol. Off. Clin. Pract. J. Am. Gastroenterol. Assoc. *14*, 1245–1255.e8.

Shao, D., Zhai, P., Del Re, D.P., Sciarretta, S., Yabuta, N., Nojima, H., Lim, D.-S., Pan, D., and Sadoshima, J. (2014). A functional interaction between Hippo-YAP signalling and FoxO1 mediates the oxidative stress response. Nat. Commun. *5*, 3315.

Shen, Z., and Stanger, B.Z. (2015). YAP regulates S-phase entry in endothelial cells. PloS One *10*, e0117522.

Shroyer, N.F., Helmrath, M.A., Wang, V.Y.-C., Antalffy, B., Henning, S.J., and Zoghbi, H.Y. (2007). Intestine-specific ablation of mouse atonal homolog 1 (Math1) reveals a role in cellular homeostasis. Gastroenterology *132*, 2478–2488.

Snippert, H.J., Schepers, A.G., van Es, J.H., Simons, B.D., and Clevers, H. (2014). Biased competition between Lgr5 intestinal stem cells driven by oncogenic mutation induces clonal expansion. EMBO Rep. *15*, 62–69.

Stamos, J.L., Chu, M.L.-H., Enos, M.D., Shah, N., and Weis, W.I. (2014). Structural basis of GSK-3 inhibition by N-terminal phosphorylation and by the Wnt receptor LRP6. eLife *3*, e01998.

Stanger, B.Z., Datar, R., Murtaugh, L.C., and Melton, D.A. (2005). Direct regulation of intestinal fate by Notch. Proc. Natl. Acad. Sci. U. S. A. *102*, 12443–12448.

Sun, J., Ramos, A., Chapman, B., Johnnidis, J.B., Le, L., Ho, Y.-J., Klein, A., Hofmann, O., and Camargo, F.D. (2014). Clonal dynamics of native haematopoiesis. Nature *514*, 322–327.

Takeda, N., Jain, R., LeBoeuf, M.R., Wang, Q., Lu, M.M., and Epstein, J.A. (2011). Interconversion between intestinal stem cell populations in distinct niches. Science *334*, 1420–1424.

Tao, S., Tang, D., Morita, Y., Sperka, T., Omrani, O., Lechel, A., Sakk, V., Kraus, J., Kestler, H.A., Kühl, M., et al. (2015). Wnt activity and basal niche position sensitize intestinal stem and progenitor cells to DNA damage. EMBO J. *34*, 624–640.

Tetteh, P.W., Basak, O., Farin, H.F., Wiebrands, K., Kretzschmar, K., Begthel, H., van den Born, M., Korving, J., de Sauvage, F., van Es, J.H., et al. (2016). Replacement of Lost Lgr5-Positive Stem Cells through Plasticity of Their Enterocyte-Lineage Daughters. Cell Stem Cell *18*, 203–213.

Tian, H., Biehs, B., Warming, S., Leong, K.G., Rangell, L., Klein, O.D., and de Sauvage, F.J. (2011). A reserve stem cell population in small intestine renders Lgr5-positive cells dispensable. Nature *478*, 255–259.

Tinkum, K.L., Stemler, K.M., White, L.S., Loza, A.J., Jeter-Jones, S., Michalski, B.M., Kuzmicki, C., Pless, R., Stappenbeck, T.S., Piwnica-Worms, D., et al. (2015). Fasting protects mice from lethal DNA damage by promoting small intestinal epithelial stem cell survival. Proc. Natl. Acad. Sci. U. S. A. *112*, E7148-7154.

Ueo, T., Imayoshi, I., Kobayashi, T., Ohtsuka, T., Seno, H., Nakase, H., Chiba, T., and Kageyama, R. (2012). The role of Hes genes in intestinal development, homeostasis and tumor formation. Dev. Camb. Engl. *139*, 1071–1082.

Valvezan, A.J., Zhang, F., Diehl, J.A., and Klein, P.S. (2012). Adenomatous Polyposis Coli (APC) Regulates Multiple Signaling Pathways by Enhancing Glycogen Synthase Kinase-3 (GSK-3) Activity. J. Biol. Chem. *287*, 3823–3832.

Valvezan, A.J., Huang, J., Lengner, C.J., Pack, M., and Klein, P.S. (2014). Oncogenic mutations in adenomatous polyposis coli (Apc) activate mechanistic target of rapamycin complex 1 (mTORC1) in mice and zebrafish. Dis. Model. Mech. *7*, 63–71.

VanDussen, K.L., Carulli, A.J., Keeley, T.M., Patel, S.R., Puthoff, B.J., Magness, S.T., Tran, I.T., Maillard, I., Siebel, C., Kolterud, Å., et al. (2012). Notch signaling modulates proliferation and differentiation of intestinal crypt base columnar stem cells. Dev. Camb. Engl. *139*, 488–497.

Vazquez, F., and Devreotes, P. (2006). Regulation of PTEN function as a PIP3 gatekeeper through membrane interaction. Cell Cycle Georget. Tex *5*, 1523–1527.

Venkatraman, A., He, X.C., Thorvaldsen, J.L., Sugimura, R., Perry, J.M., Tao, F., Zhao, M., Christenson, M.K., Sanchez, R., Yu, J.Y., et al. (2013). Maternal imprinting at the H19-Igf2 locus maintains adult haematopoietic stem cell quiescence. Nature *500*, 345–349.

Vermeulen, L., Morrissey, E., van der Heijden, M., Nicholson, A.M., Sottoriva, A., Buczacki, S., Kemp, R., Tavaré, S., and Winton, D.J. (2013). Defining stem cell dynamics in models of intestinal tumor initiation. Science *342*, 995–998.

Voehringer, D., Liang, H.-E., and Locksley, R.M. (2008). Homeostasis and effector function of lymphopenia-induced “memory-like” T cells in constitutively T cell-depleted mice. J. Immunol. Baltim. Md 1950 *180*, 4742–4753.

Vogelstein, B., Fearon, E.R., Hamilton, S.R., Kern, S.E., Preisinger, A.C., Leppert, M., Nakamura, Y., White, R., Smits, A.M., and Bos, J.L. (1988). Genetic alterations during colorectal-tumor development. N. Engl. J. Med. *319*, 525–532.

Vogelstein, B., Papadopoulos, N., Velculescu, V.E., Zhou, S., Diaz, L.A., and Kinzler, K.W. (2013). Cancer genome landscapes. Science *339*, 1546–1558.

Vooijs, M., Ong, C.-T., Hadland, B., Huppert, S., Liu, Z., Korving, J., van den Born, M., Stappenbeck, T., Wu, Y., Clevers, H., et al. (2007). Mapping the consequence of Notch1 proteolysis in vivo with NIP-CRE. Dev. Camb. Engl. *134*, 535–544.

Wang, S., Li, N., Yousefi, M., Nakauka-Ddamba, A., Li, F., Parada, K., Rao, S., Minuesa, G., Katz, Y., Gregory, B.D., et al. (2015). Transformation of the intestinal epithelium by the MSI2 RNA-binding protein. Nat. Commun. *6*, 6517.

Weissman, I.L. (2000). Stem cells: units of development, units of regeneration, and units in evolution. Cell *100*, 157–168.

Weissman, I.L., Anderson, D.J., and Gage, F. (2001). Stem and progenitor cells: origins, phenotypes, lineage commitments, and transdifferentiations. Annu. Rev. Cell Dev. Biol. *17*, 387–403.

Wilson, A., Laurenti, E., Oser, G., van der Wath, R.C., Blanco-Bose, W., Jaworski, M., Offner, S., Dunant, C.F., Eshkind, L., Bockamp, E., et al. (2008). Hematopoietic stem cells reversibly switch from dormancy to self-renewal during homeostasis and repair. Cell *135*, 1118–1129.

Wong, V.W.Y., Stange, D.E., Page, M.E., Buczacki, S., Wabik, A., Itami, S., van de Wetering, M., Poulsom, R., Wright, N.A., Trotter, M.W.B., et al. (2012). Lrig1 controls intestinal stem-cell homeostasis by negative regulation of ErbB signalling. Nat. Cell Biol. *14*, 401–408.

Wu, H., Wei, L., Fan, F., Ji, S., Zhang, S., Geng, J., Hong, L., Fan, X., Chen, Q., Tian, J., et al. (2015). Integration of Hippo signalling and the unfolded protein response to restrain liver overgrowth and tumorigenesis. Nat. Commun. *6*, 6239.

Yan, K.S., Chia, L.A., Li, X., Ootani, A., Su, J., Lee, J.Y., Su, N., Luo, Y., Heilshorn, S.C., Amieva, M.R., et al. (2012). The intestinal stem cell markers Bmi1 and Lgr5 identify two functionally distinct populations. Proc. Natl. Acad. Sci. U. S. A. *109*, 466–471.

Yilmaz, Ö.H., Valdez, R., Theisen, B.K., Guo, W., Ferguson, D.O., Wu, H., and Morrison, S.J. (2006). Pten dependence distinguishes haematopoietic stem cells from leukaemia-initiating cells. Nature *441*, 475–482.

Yilmaz, Ö.H., Katajisto, P., Lamming, D.W., Gültekin, Y., Bauer-Rowe, K.E., Sengupta, S., Birsoy, K., Dursun, A., Yilmaz, V.O., Selig, M., et al. (2012). mTORC1 in the Paneth cell niche couples intestinal stem-cell function to calorie intake. Nature *486*, 490–495.

Yimlamai, D., Christodoulou, C., Galli, G.G., Yanger, K., Pepe-Mooney, B., Gurung, B., Shrestha, K., Cahan, P., Stanger, B.Z., and Camargo, F.D. (2014). Hippo pathway activity influences liver cell fate. Cell *157*, 1324–1338.

Yousefi, M., Li, N., Nakauka-Ddamba, A., Wang, S., Davidow, K., Schoenberger, J., Yu, Z., Jensen, S.T., Kharas, M.G., and Lengner, C.J. (2016). Msi RNA-binding proteins control reserve intestinal stem cell quiescence. J. Cell Biol. *215*, 401–413.

Yousefi, M., Berry, C., Li, N., Schoenberger, J., Simeonov, K., Nakauka-Ddamba, A., Cedeno, R.J., and Lengner, C.J. (2017). Calorie restriction governs intestinal epithelial regeneration through cell autonomous regulation of mTORC1 in reserve stem cells. Consid.

Yu, F.-X., and Guan, K.-L. (2013). The Hippo pathway: regulators and regulations. Genes Dev. *27*, 355–371.

Zhao, B., Wei, X., Li, W., Udan, R.S., Yang, Q., Kim, J., Xie, J., Ikenoue, T., Yu, J., Li, L., et al. (2007). Inactivation of YAP oncoprotein by the Hippo pathway is involved in cell contact inhibition and tissue growth control. Genes Dev. *21*, 2747–2761.

Zhao, B., Ye, X., Yu, J., Li, L., Li, W., Li, S., Yu, J., Lin, J.D., Wang, C.-Y., Chinnaiyan, A.M., et al. (2008). TEAD mediates YAP-dependent gene induction and growth control. Genes Dev. *22*, 1962–1971.

Zhao, B., Li, L., Tumaneng, K., Wang, C.-Y., and Guan, K.-L. (2010). A coordinated phosphorylation by Lats and CK1 regulates YAP stability through SCF?-TRCP. Genes Dev. *24*, 72–85.

Zhou, D., Zhang, Y., Wu, H., Barry, E., Yin, Y., Lawrence, E., Dawson, D., Willis, J.E., Markowitz, S.D., Camargo, F.D., et al. (2011). Mst1 and Mst2 protein kinases restrain intestinal stem cell proliferation and colonic tumorigenesis by inhibition of Yes-associated protein (Yap) overabundance. Proc. Natl. Acad. Sci. U. S. A. *108*, E1312-1320.

Zoncu, R., Efeyan, A., and Sabatini, D.M. (2011). mTOR: from growth signal integration to cancer, diabetes and ageing. Nat. Rev. Mol. Cell Biol. *12*, 21–35.